Analysis of genes implicated in Alzheimer's disease pathogenesis using *Danio Rerio* as a model organism

Morgan Newman

Supervised by Michael Lardelli and Simon Koblar



Submitted for partial fulfilment for the degree of Doctor of Philosophy (PhD)

Discipline of Genetics

School of Molecular and Biomedical Science

The University of Adelaide University SA

AUSTRALIA

August 2008

Declaration

This work contains no material which has been accepted fro the award of any other degree or diploma in any university or other tertiary institution and, to the best of my knowledge and belief, contains no material previously published or written by another person, except where due reference has been given in the text.

I give consent to this copy of my thesis when deposited in the university Library, being made available for loan and photocopying, subject to the provisions of the Copyright Act 1968. The author acknowledges that copyright of published works contained within this thesis (as listed below) resides with the copyright holders of those works.

Signed

…….Date……

Contents

List of Publications **3**

Acknowledgements **4**

Abstract **5**

CHAPTER I **7**

INTRODUCTION 7
REVIEW PAPER I 7
I.2 RECENT DEVELOPMENTS TOWARDS PSEN'S FUNCTION IN ALZHEIMER'S DISEASE 9
I.3 THE CELL CYCLE HYPOTHESIS FOR ALZHEIMER'S DISEASE PATHOGENESIS 10
I.4 THE FUNCTION OF CYCLIN G1 12
I.5 AIMS OF THE PHD RESEARCH PROJECT 13
I.6 SUMMARY OF PAPERS II-IV AND LINKS BETWEEN THEM 14

CHAPTER II **17**

RESEARCH PAPER II 17

CHAPTER III **22**

RESEARCH PAPER III 22

CHAPTER IV **25**

RESEARCH PAPER IV 25

Significance of The PhD Research Project and Future Directions **27**

REFERENCES **28**

List of Publications

Alzheimer Disease: Amyloidogenesis, the presenilins and animal models. Review paper.

Morgan Newman, Ian Musgrave and Michael Lardelli

Biochimica et Biophysica Acta 1772 (2007) 285-297.

Interference with splicing of Presenilin transcripts has potent dominant negative effects on Presenilin activity.

Svanhild Nornes, Morgan Newman, Giuseppe Verdile, Simon Wells, Cristi L. Stoick-Cooper, Ben Tucker, Inna Frederich-Sleptsova, Ralph Martins and Michael Lardelli

Human Molecular Genetics, 2008, Vol17, No3 402-4122.2.

Altering presenilin gene activity in zebrafish embryos causes changes in expression of genes with proposed functions in Alzheimer Disease pathogenesis.

Morgan Newman, Ben Tucker, Svanhild Nornes and Michael Lardelli

Journal of Alzhiemer's Disease, 2008, Accepted Manuscript.

Acknowledgements

I would like to give my thanks and appreciation to:

Michael, for excellent supervision and guidance.

Svanhild, for always being there with support, assistance and advice.

Members of the zebrafish community, especially Simon, Ben, Martin, Tanya, Amanda and Jason for their advice on everything 'fishy'.

Past and present members of the Genetics discipline for their support and advice over the last few years.

My fantastic family for all their love and support during this time especially MUM!!!

Finally, my awesome friends for providing timely distractions and listening to me.

Without these people (science related or not), none of this would have been possible.

Abstract

Alzheimer's disease (AD) is the most prevalent form of dementia. There is considerable evidence that AD is caused by accumulating amyloid beta peptides in the brain, as a result of amyloid precursor protein (APP) cleavage by secretase enzymes. The presenilin proteins are central to the gamma-secretase cleavage of the intramembrane domain of APP. Aberrant splicing and point mutations in the human presenilin genes, *PSEN1* and *PSEN2*, have been linked to familial forms of AD, through aberrant APP cleavage resulting in irregular amyloid beta formation. Paper 1 gives a review of the literature on AD research and how animal models are used to elucidate mechanisms of AD pathogenesis. The zebrafish model is used in this thesis to investigate genes with potential relevance to AD initiation and pathogenesis. Paper 2 demonstrates that low-level aberrant splicing of exon 8 in *psen1* transcripts in zebrafish embryos produces potent dominant negative effects that increased *psen1* transcription, cause a dramatic hydrocephalus phenotype, decreased pigmentation and other developmental defects. Similar effects are also observed after low-level interference with splicing of exon 8 in *psen2* transcripts. In paper 3, a microarray analysis was performed to analyse global gene expression changes to illuminate the molecular aetiology of the phenotypic effects described in paper 2. Of the 100 genes that showed greatest dysregulation after *psen1* or *psen2* manipulation, 12 genes were common to both treatments. Five of these have known function and showed increased expression. C*yclin* G1 (*ccng1)* was of particular interest as the human CCNG1 protein shows increased immunoreactivity in the cytoplasm of neurons in human AD brains. Phylogenetic and conserved synteny analysis confirmed the orthology of zebrafish *ccng1* with human *CCNG1*. Expression of zebrafish *ccng1* in developing embryos at 24 hours post fertilization (hpf) was

observed in the eye, tectum and somites. Decreased Ccng1 expression does not lead to any developmental defects and also cannot rescue the hydrocephalus or pigmentation phenotypes of embryos with aberrant splicing of *psen1* exon 8. An analysis of zebrafish *ccng1* function in paper 4 (thesis chapter in the form of a manuscript) indicates that truncation of Ccng1 appears to cause developmental defects in the brain, notochord and somites, however, it does not decrease the level of normal *ccng1* transcript. The *CCNG1* paralogue, *Cyclin G2*, (*CCNG2),* is also expressed in zebrafiish (*ccng2*). Decreasing the expression of Ccng2 results in similar effects on embryo development as truncating Ccng1. Therefore, the truncated forms of Ccng1 potentially interfere with Ccng2 function in a dominant negative manner.

CHAPTER I

Introduction

Review Paper I

Alzheimer Disease: Amyloidogenesis, the presenilins and animal models.

Morgan Newman[1], Ian Musgrave[2] and Michael Lardelli[1]

[1]Discipline of Genetics, School of Molecular and Biomedical Science, The University of Adelaide, Adelaide, SA 5005, Australia

[2]Department of Clinical and Experimental Pharmacology, The University of Adelaide, Adelaide, SA 5005, Australia

Biochimica et Biophysica Acta, 1772 (2007), 285-297

STATEMENT OF AUTHORSHIP

Alzheimer Disease: Amyloidogenesis, the presenlins and animal models. Review paper.

Biochimica et Biophysica Acta 1772 (2007) 285-297

Morgan Newman (Candidate)

Wrote manuscript and acted as corresponding author.

Certification that the statement of contribution is accurate

Signed

…….Date……

Ian Musgrave (co-author)

Contributed to section 2.4 Alternative initiating mechanisms for the amyloid cascade hypothesis and composed figure 1.

Certification that the statement of contribution is accurate and permission is given for the inclusion of the paper in the thesis

Signed

…….Date……

Michael Lardelli (co-author)

Supervised development of work.

Certification that the statement of contribution is accurate and permission is given for the inclusion of the paper in the thesis

Signed

……..Date……

Available online at www.sciencedirect.com
ScienceDirect
Biochimica et Biophysica Acta 1772 (2007) 285–297
Biochimica et Biophysica Acta BBA
www.elsevier.com/locate/bbadis

Review

Alzheimer disease: Amyloidogenesis, the presenilins and animal models

M. Newman [a,*], F.I. Musgrave [b], M. Lardelli [a]

[a] Discipline of Genetics, School of Molecular and Biomedical Science, The University of Adelaide, Adelaide, SA 5005, Australia
[b] Department of Clinical and Experimental Pharmacology, The University of Adelaide, Adelaide, SA 5005, Australia

Received 6 September 2006; received in revised form 6 November 2006; accepted 5 December 2006
Available online 8 December 2006

Abstract

Alzheimer's disease is the most prevalent form of dementia. Neuropathogenesis is proposed to be a result of the accumulation of amyloid beta peptides in the brain together with oxidative stress mechanisms and neuroinflammation. The presenilin proteins are central to the gamma-secretase cleavage of the amyloid prescursor protein (APP), releasing the amyloid beta peptide. Point mutations in the presenilin genes lead to cases of familial Alzheimer's disease by increasing APP cleavage resulting in excess amyloid beta formation. This review discusses the molecular mechanism of Alzheimer's disease with a focus on the presenilin genes. Alternative splicing of transcripts from these genes and how these may function in several disease states is discussed. There is an emphasis on the importance of animal models in elucidating the molecular mechanisms behind the development of Alzheimer's disease and how the zebrafish, *Danio rerio*, can be used as a model organism for analysis of presenilin function and Alzheimer's disease pathogenesis.
© 2006 Elsevier B.V. All rights reserved.

Keywords: Alzheimer's disease; Amyloid-beta; Animal models; Oxidative stress; Presenilin; Zebrafish

1. Introduction

Alzheimer's disease (AD) is the most prevalent form of dementia affecting more than 20 million people worldwide [1,2]. Furthermore, as a consequence of the worlds aging population, the prevalence of AD is expected to increase [1]. This highlights the importance of research investigating the mechanisms behind the development of the disease. Apart from the recognisable behavioural differences, it is difficult to positively diagnose someone with Alzheimer's during the early stages of the disease [1]. However the AD brain shows a consistent pathology amongst patients, with amyloid aggregates and neurofibrillary tangles evident in the AD brain. Intense research has identified genes involved in the development of these pathologies, namely the amyloid precursor protein and the presenilins. The increasing knowledge on AD pathogenesis has revealed the complex nature of this disease and highlights the need to elucidate the molecular mechanisms involved. This review discusses the current knowledge of the molecular mechanisms of Alzheimer Disease, focusing on amyloidogenesis, the role of the presenilin genes and the importance of animal models to further elucidate the mechanisms behind the development of the disease.

The most common form of AD in the population (approximately 90%) occurs sporadically and is late in onset, usually occurring after 65 years of age [1,2]. Familial Alzheimer's disease (FAD), only accounts for approximately 10% of cases and symptoms usually occur before the age of 65 [1]. The mode of inheritance of AD differs for each type. The majority of FAD and sporadic AD cases have a complex inheritance, while only 10% of FAD cases are inherited in an autosomal dominant pattern [3]. In affected individuals the disease causes a progressive and permanent decline in memory and cognitive abilities. The first cognitive area affected is episodic memory [4]. During disease progression, attention, executive functions, semantic memory, language and spatial orientation all begin to deteriorate [5]. However the molecular, cellular and pathological triggers for the onset of the cognitive deterioration are poorly understood.

* Corresponding author.
E-mail addresses: morgan.newman@adelaide.edu.au (M. Newman), ian.musgrave@adelaide.edu.au (F.I. Musgrave), michael.lardelli@adelaide.edu.au (M. Lardelli).

0925-4439/$ - see front matter © 2006 Elsevier B.V. All rights reserved.
doi:10.1016/j.bbadis.2006.12.001

2. The pathogenesis and genetics of Alzheimer's disease

Alzheimer's disease was originally recognised by Alois Alzheimer in 1907 as a separate form of dementia. Since this original observation the two main histological features of amyloid plaques and neurofibrillary tangles (NFT) have been described in the AD brain [6]. These features are found to be present in the temporal neocortex and hippocampal regions of the AD brain [7]. The hippocampus resides in the cerebral cortex of the forebrain and is thought to be involved in memory storage. Amyloid plaques and NFTs result from an aberration in deposition of the amyloid beta peptide (Aβ peptide) and the hyperphosphorylated tau protein respectively and these depositions lead to neuronal loss and neurotoxicity in the AD affected brain [8]. Accumulation of Aβ peptides may be the key event in pathogenesis of AD. The exact mechanism by which Aβ peptide deposition induces neurotoxicity is unclear, but it appears the oxidative stress plays an important role. Oxidative stress is extensive in AD [9,10] and Aβ peptides stimulate oxidative stress by both direct and indirect mechanisms. Aβ peptides by themselves may act as enzymes [11], as they are capable of directly producing hydrogen peroxide and generating free radicals through metal ion reduction [12,13]. As well, Aβ peptide can bind to mitochondrial proteins resulting in the generation of free radicals [14]. Furthermore, Aβ peptides generate oxidative stress via neuroinflammation. Considerable evidence has supported that neuroinflammation is associated with AD pathology [15]. The death of neurons observed in AD is partly attributed to the activation of two major brain cell types, astrocytes and microglia that participate in the immune/inflammatory response to Aβ deposition. However, these cells can have both neuroprotective and neurodegenerative functions. For example, astrocytes cluster at sites of amyloid deposition and are thought to be involved in the clearance of plaques, evident through their ability to degrade amyloid beta deposits *in vitro* and *in situ* [16]. Both astrocytes and microglia release pro-inflammatory molecules upon activation, in particular, astrocytes can be activated by amyloid beta deposits to produce reactive oxygen species, as well as chemokines, cytokines, that lead to neuronal cell death [17]. Aβ peptides also induce the expression of nitric oxide synthase in microglia and the release of reactive nitric oxide which results in the loss of selected neuron populations [18]. Furthermore, Aβ peptides stimulate microglial cells to release a neurotoxin, quinolinic acid [19], which may also play a role in neurotoxicity.

2.1. The amyloid cascade hypothesis

The amyloid beta hypothesis predicts that an aberration in the proteolytic processing of the amyloid precursor protein (APP) leads to the increased production of Aβ peptides, this in turn leads to the accumulation of Aβ, a primary event in the pathogenesis of AD [1]. The accumulated Aβ eventually deposits into amyloid plaques present in the AD brain parenchyma. Together with the secondary events of microglial and astrocyte activation and NFT formation there is widespread neuronal dysfunction and selective neuronal loss. Currently, this hypothesis is being referred to as the Aβ cascade hypothesis, where increased production and possibly decreased clearance of Aβ peptides leads to an accumulation of these peptides and the subsequent pathogenesis observed in AD.

APP is a ubiquitously expressed type I integral membrane glycoprotein with various major isoforms. The largest of the APP alternate transcripts comprises an alternatively spliced exon at residue 289 which contains a serine protease inhibitor of the Kunitz type (KPI) [20]. APP resides on chromosome 21 and Down's syndrome cases (caused by an extra copy of 21) have been shown to develop early onset dementia. This observation, in conjunction with other studies lead to the discovery of the first reported partial amino acid sequence of Aβ in 1984 [21]. APP is expressed abundantly in a variety of tissues and processing of APP is a normal event in nearly all neural and non-neural cells throughout the body. Proteolytic processing of APP that releases the Aβ fragment is a result of cleavage events by secretase proteins. APP processing by the secretase proteins occurs in two distinct pathways, the non-amyloidogenic and amyloidogenic pathways. Soluble APP is cleaved by α-secretase and β-secretase to release the soluble α-APP and β-APP, respectively, into the extracellular matrix [22]. In the non-amyloidogenic pathway, γ-secretase cleavage of the remaining C-terminal fragment (CTF) releases the p3 fragment, while in the amyloidogenic pathway this cleavage releases the Aβ peptide (Fig. 2). The cleavage by γ-secretase is a heterogenous event that releases Aβ peptides of different sizes, with Aβ-40 and Aβ-42 being the most common forms. Aβ-40 and Aβ-42 are both toxic peptides, however the Aβ-42 isoform is insoluble and more capable of aggregating into amyloid plaques. Upon accumulation of Aβ-42 there is a resulting neuronal cytotoxicity that induces neuropathological events leading to neurodegeneration of the brain [23]. More specifically, Aβ-42 can aggregate into two different conformation states. There is the non-β sheet, non-fibrillar state and the β sheet fibrillar state which is cytotoxic and eventually deposits into plaques [24]. Aβ-42 exists initially as a monomer, during oligomerisation the monomers further oligomerise into larger forms such as large oligomers, protofibrils and fibrils. During oligomerisation there are conformational changes occurring in these elements that transform them into a β sheet fibrillar state [23]. The Aβ oligomeric intermediates (oligomers, protofibrils) and the mature fibrils are all neurotoxic, and it has been demonstrated that the oligomers and protofibrils are actually more neurotoxic than the mature fibrils or amyloid plaques [25].

2.2. Genes implicated in Alzheimer's disease

Three genes that have been implicated in AD pathogenesis are APP, presenilin 1 (PS1) or presenilin 2 (PS2), as mutations in these genes have been identified in cases of familial AD [26]. PS1 is central to the γ-secretase complex of proteins that cleave Notch and APP [27]. It is the presenilin-mediated cleavage of APP that results in the release of various lengths of the Aβ peptide. The pathological characteristics of FAD and the sporadic form of AD are proposed to be similar; therefore somatic changes in APP, PS1 or PS2 may potentially have a role

in sporadic cases of AD. Along with causative mutations in PS1, PS2 and APP, the apolipoprotein (APOE) gene has been identified as a major genetic risk factor for sporadic AD. E4 is an isoform of APOE and carriers of the E4 allele are at a higher risk of developing AD, with homozygotes usually developing AD earlier than heterozygotes [28]. However the presence of the APOE4 allele, has not been found to be necessary or sufficient for the development of the disease [28].

The gene encoding APP was the first to be identified has having an association with FAD. Currently there are 27 mutations in the APP gene that have been described in families with AD and these mutations are clustered around the Aβ sequence on APP [29]. Mutations in PS1, PS2 and APP account for approximately 50% of Familial AD cases and there is almost 100% penetrance of the mutated gene product that leads to AD development [29]. Worldwide studies on FAD cases have uncovered 157 and 10 pathogenic mutations in the PS1 and PS2 genes respectively (http://www.molgen.ua.ac.be/ADMutations/)[30]. The presenilin section of this review discusses presenilin associated FAD mutations in more depth.

In vitro and *in vivo* models of familial AD mutations have demonstrated an enhancement of APP proteolytic processing through aberrations of the γ-secretase complex [31,32]. These alterations generally increase the production of Aβ-42 or decrease the production of Aβ-40, which results in changes to the Aβ-40/Aβ-42 ratio, an important aspect of AD [33,34]. A shift in APP processing to release the longer Aβ-42 isoform leads to Aβ fibril formation [32,35]. These mutations usually have a familial inheritance pattern. For example, a mutation in APP identified in a Swedish family alters two amino acids that precede the Aβ amino terminus and results in enhanced β-secretase cleavage, causing an increase in Aβ production [36]. Aβ peptides with the Flemish mutation assemble into fibrils and protofibrils at a slower rate compared to wild type [37], while in the Dutch mutant, Aβ protofibrils and fibrils are formed at a much faster rate than wild type [38]. Theuns et al. [33] have to date reported the furthermost C-terminal APP K724N mutation. *In vitro* expression analysis of this mutation displayed an increase in Aβ-42 and decrease in Aβ-40 levels, which increased the Aβ-40/Aβ-42 ratio three-fold [33]. Even though these mutations are located on adjacent codons on APP, they produce different pathological characteristics in the patient population.

2.3. Linking oxidative stress with Alzheimer's disease

Oxidative stress is associated with a wide range of disease states including cancer, diabetes and neurodegenerative disorders such as AD. Oxidative stress results from a disturbance in the balance of antioxidants and reactive oxygen species (ROS) generated within the body, resulting in an excess of ROS. This leads to the destruction of both neuronal and vascular cells [11]. Oxidative stress disturbs the normal functioning of cells through cell membrane lipid destruction and cleavage of DNA [39]. Whether oxidative stress is involved at the onset of AD is still unclear. However it is thought to play a significant role during disease progression, particularly in cellular and tissue damage that occurs throughout AD. As noted above, oxidative stress is extensive in AD. It has also been suggested that there is a close correlation between oxidative stress and Aβ deposition, evident through mouse brain Aβ deposits co-localising with a variety of oxidative stress markers [40]. Aβ is proposed to be a metalloenzyme that is capable of generating hydrogen peroxide through its superoxide dismutase activity [11]. Hydrogen peroxide is capable of being further transformed to the reactive hydroxyl radical in the presence of transition metals, following this transformation lipid peroxidation reactions bring about oxidative damage, leading to oxidative toxicity in neurons [11]. It has been further suggested that oxidative stress may actually promote the amyloidogenic pathway [11], the resulting increase in Aβ can in turn generate more hydrogen peroxide leading to further oxidative damage in neurons and vascular cells. A cyclic pathway of excess Aβ promoting oxidative damage which promotes further Aβ production would result in heightened neurotoxicity and subsequently enhance the development of AD [11]. As discussed above, Aβ can produce oxidative damage by stimulating neuroinflammation, as well as generating ROS as a result of binding to mitochondrial proteins. Furthermore, intermediate amyloid aggregates can interact with cell membranes, where they form non-specific ion channels, with the resultant increases in intracellular calcium triggering the production of ROS [41]. Thus there is a strong link between Aβ, oxidative stress and AD (see Fig. 1).

2.4. Alternative initiating mechanisms for the amyloid cascade hypothesis

Apart from the identified FAD point mutations there is evidence that other neurochemical factors may initiate the deposition of Aβ in FAD or sporadic AD. The following are

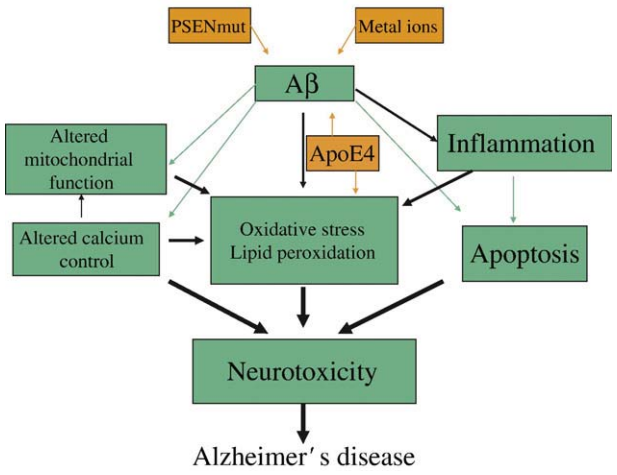


Fig. 1. Amyloid ß-protein (Aß) can accumulate through over production (e.g., presenillin mutation [PSENmut]) or reduced removal (e.g., APOE4). Oligomerization of Aß results in production of oxidative stress by itself (which can be augmented by heavy metals), of via induction of several other interacting mechanisms.

some of the current alternate mechanisms that possibly contribute to or initiate the development of neuropathological features of AD.

2.4.1. The role of vascular dysfunction and risk factors for AD pathogenesis

Cardiovascular disease and type 2 diabetes are risk factors for AD. Vascular risk factors such as hypertension and hypercholesterolemia are proposed to promote the production of Aβ [42,43], while being overweight or obese is also now associated with AD [44,45]. Vascular risk factors appear to be exacerbated by the inheritance of the E4 allele of the APOE gene, thus the presence of this allele increases the risk of developing both vascular dysfunction and AD [43]. A recent study by Balakrishnan et al. [46] investigated whether being overweight or obese contributes to AD development by modulating Aβ levels. In their study of 18 adults they found a correlation between the direct measures of obesity and plasma levels of Aβ-42 [46]. This is the first study to suggest that being overweight and obese is a risk factor for developing AD by increasing plasma levels of Aβ-42.

Recent findings have also suggested that neurovascular dysfunction is an important feature of chronic neurodegeneration in AD [47]. The neurovascular hypothesis as suggested by Zlokovic et al. [47] proposes that there is faulty clearance of Aβ across the blood brain barrier (BBB). In one instance the faulty clearance, possibly due to aberrant angiogenesis, results in increased Aβ levels. Furthermore, another pathway could involve increased Aβ concentration in conjunction with atherosclerosis. Together, these mechanisms are proposed to cause premature aging of the cerebrovascular system [47]. Both of these cascades could initiate neurovascular uncoupling, vessel regression, brain hypoperfusion and neurovascular inflammation [47]. Flow on effects include compromise of the BBB, an ionic imbalance and metabolic poisoning in the brain interstitial fluid, finally leading to synaptic dysfunction and neuronal injury and loss, evident pathologies in AD [47].

2.4.2. Redox active metals are key mediating factors in the pathophysiology of AD

It is likely that there is a pathological interaction of Aβ with redox active metals such as zinc, copper and iron, due to these metals having a high concentration in the areas of the brain that are affected by AD, namely the cortex, hippocampus and cortical vasculature [48,49,50]. Redox active metals may play a role in oxidative stress as they influence the production of hydrogen peroxide [24] (see Fig. 1). The binding of trace levels of these metals to Aβ, promotes the catalytic production of hydrogen peroxide from oxygen through metal reduction [13]. The effect of these metals on the oxidative mechanisms of Aβ cytotoxicity is complex and not yet fully elucidated, however the effect of zinc on AD pathology may be explained by 'The Zinc Paradox' [24]. During normal physiology, zinc, copper and to a lesser extent iron interact with APP and Aβ, probably existing in a delicate balance. Perturbations in this balance may result from abnormal Aβ metabolism and synaptic zinc flooding, resulting in a change in zinc and copper metabolism leading to the formation of fibrillar Aβ. Consequently, this fibril formation triggers an inflammatory response that lowers pH and leads to a disruption of zinc homeostasis [24]. Zinc is released into the cellular environment and this triggers events that lead to oxidative stress-induced cell death [51]. Copper ions are then free to compete for zinc's binding site on Aβ and these ions can then catalyse hydrogen peroxide production by Aβ. Zinc is essential in human nutrition; however the role of cerebral zinc in AD pathology requires further elucidation. Since it has been established that zinc is elevated in cored amyloid plaques [52] and zinc flooding can lead to increased Aβ fibril formation and oxidative stress, zinc may, paradoxically, be a pathological factor for AD.

3. The presenilin proteins

In humans the *PS1* gene resides on chromosome 14 [53] and the *PS2* gene resides on chromosome 1 [54,55]. Presenilin proteins are evolutionarily conserved amongst species. Presenilins are transcribed in both the central nervous system and in non-neuronal organs. Presenilin functions within the γ-secretase complex, with the mature complex predominantly existing at the cell surface regulating the cleavage of a number of single transmembrane domain proteins [56]. Furthermore presenilin (as a part of the γ-secretase complex) is also found to reside in the membranes of the endoplasmic reticulum and Golgi apparatus [57]. *In vitro* generated point mutations in the *PS1* gene leads to an increased production of Aβ peptides [58,59,60] and there is a reduction in γ-secretase cleavage of APP in neuronal cultures derived from *PS1* deficient mice embryos [61]. These findings and more led to the conclusion that mutations in *PS1* have a gain-of-function phenotype and that PS1 is a target for anti-amyloidogenic therapy in AD. It now is well substantiated that presenilins functions in the γ-secretase cleavage of APP, however, the complete function of PS1 and PS2 has not yet been determined. PS1 and PS2 are highly homologous and share 62% amino acid identity. Upon deletion of PS1 and PS2 in the forebrain of mice, there is a severe phenotype that resembles a Notch gene knockout [62]. There are also evident biochemical alterations of neuronal atrophy, astrogliosis, caspase-3-mediated apoptosis and tau hyperphosphorylation [63]. Together these alterations demonstrate that the presenilins are essential for the ongoing maintenance of cortical structures and function in the brain [63]. Presenilins are also involved in several cell-signalling pathways with an essential function during development [64] and they regulate β-catenin stability and trafficking of membrane proteins [65,66]. Presenilin has also been implicated in calcium signalling. Tu et al. [67] recently demonstrated the presenilin holoprotein accounting for ~80% of in Ca^{2+} leakage from the ER. Interestingly it appears to be independent of its γ-secretase activity [67].

Presenilins have also been implicated in different apoptotic pathways. A partial cDNA clone encoding a portion of PS2 CTF rescued a T-cell receptor and FAS-induced apoptosis [68]. Furthermore, PS is implicated in mitochondria-dependent apoptotic cell death, through its interactions with the anti-

apoptotic proteins Bcl-2 [69] and Bcl-X_L [69,70]. Even though presenilins' involvement in apoptotic processes has been demonstrated, the actual mechanism of their apoptotic function is yet to be elucidated (Fig. 2).

The SEL-12 protein, a presenilin homologue, is expressed throughout the nematode *Caenorhabditis elegans* (*C. elegans*). Due to the almost identical function of SEL-12 and human PS1, the study of SEL-12: LacZ fusion proteins has predicted the topology of the PS1 protein to encompass eight transmembrane (TM) domains, with a hydrophilic loop between the sixth and seventh domain [71]. Other topological studies using a similar experimental design that probes for membrane topology by using the glycosylation of PS1 hybrid proteins, have suggested models of the presenilin protein ranging between 6 and 9 TM domains [72–75]. The conserved aspartate residues Asp 257 in TM6 and Asp385 in TM7, appear to contain the active site of PS1 that contributes to γ-secretase activity and the region between these two residues is critical for PS1 endoproteolysis. It has been demonstrated that mutations in either of the two aspartate residues prevent endoproteolysis of PS1 in the cytoplasmic loop, substantially reduce the production of Aβ and decrease Aβ secretion by 60% [76], while mutating an equivalent aspartate in PS2 results in undetectable levels of Aβ [77]. The major endoproteolysis site of the PS1 holoprotein has been identified as residue 298 located in the large hydrophilic loop [78].

Presenilin is translated as a full-length holoprotein which is predominantly endoproteolytically cleaved by presinilinase into the 27-kDa N-terminal (NTF) and 17-kDa CTF [79]. The site of endoproteolysis has been shown to be in the exon 9 hydrophilic loop region, since a PS1 variant lacking exon 9 did not undergo endoproteolysis [79]. Endoproteolysis appears to be the critical event that brings about PS1 stability and biological activity as antibody staining of specific sections of presenilin has indicated that there is very little full-length PS1 or PS2 protein detected in brain tissue [78]. Ratovitski et al. [80] demonstrated that presenilin NTF and CTF are significantly more stable then the full-length polypeptide in mouse cell lines expressing human presenilin. Thus, presenilin is mainly present as N- and C-terminal endoproteolytic fragments. These fragments dimerise to form the active, functional presenilin heterodimer [78]. As a consequence of the heterodimer formation the fragments are protected from the relatively rapid degradation that is evident for the holoprotein [81]. PS1 is able to form both low (100–180 kDa) and high (>250 kDa) molecular weight complexes that can contain the full length or the heterodimeric CTF and NTF fragments [81,82]. Furthermore the formation of the higher molecular weight complex appears to be required for presenilin mediated cleavage of APP and the signal receptor Notch (described in detail later). Hebert et al. [83] have proposed a hypothetical model of PS1 maturation that is in accordance with a model proposed by Haas and Steiner et al. [84]. In this model, PS1 homodimerises before the full-length protein is endoproteolytically cleaved by presinilinase. A tetramer of hetero and homodimers would then be required for the assembly and stability of the high molecular weight complex needed for γ-secretase activity [83]. Through yeast two hybrid and split-ubiquitin assays, Cervantes et al. [85] have also observed NTF: NTF and CTF: CTF dimers. Subsequently, a tetramer model of the presenilin functional complex was proposed and further analysis of the effect of FAD mutations on NTF: NTF homodimerisation displayed these mutations affecting the NTF: NTF interaction. This result implies that FAD mutations influence the assembly or possibly the stability of the functional presenilin complex.

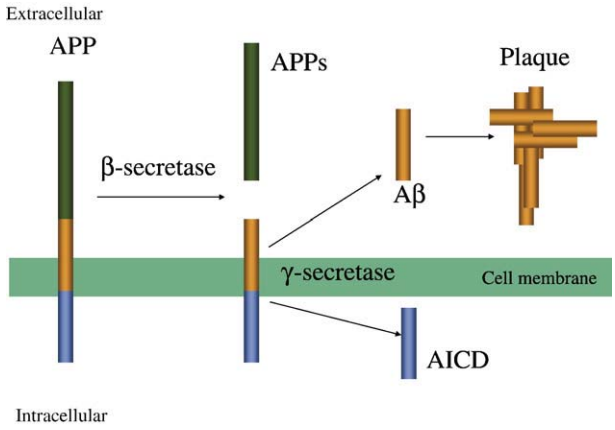


Fig. 2. Processing of APP in the amyloidogenic pathway. Cleavage of APP by secretase enzymes releases the amyloid beta peptide, excess peptides eventually deposit into amyloid plaques.

3.1. Presenilin is integral to the γ-secretase complex

γ-Secretase is a transmembrane aspartyl protease that exists as a mature complex within the plasma membrane, where it interacts with and cleaves single transmembrane receptors such as Notch and APP [56]. Prior to cleavage these substrates undergo a shedding of a large ectodomain leaving a membrane-embedded CTF. The CTF is subject to intramembrane cleavage by the γ-secretase complex, the proteolytic cleavage releases an intracellular domain that is able to modulate transcription [86].

Findings by Kimberly et al. [87] suggest that four membrane proteins comprise the γ-secretase complex and these enzymes co-assemble to form the active complex in mammalian cells. Currently it is thought that the higher molecular weight complex that PS1 forms contains the proteins nicastrin (NCT), anterior pharynx defective (APH-1) and presenilin enhancer 2 (PEN2). Through multistep affinity purification of γ-secretase, the PS, NCT, APH-1 and PEN-2 proteins were shown to co-purify as a complex [88]. Overexpression studies of APH1a, APH1b, PEN2 and NCT DNA in HEK293 cells, resulted in an increase in the production of Aβ-40 and Aβ-42, suggesting that these proteins are limiting for γ-secretase activity. Overexpression of APH-1 in S2 cells of the fruit fly *Drosophila melanogaster* results in a marked increase in the PS1 holoprotein that is further enhanced by overexpression of NCT [89]. RNAi depletion of PEN2 in S2 cells, mammalian neuronal cells and mouse neuroblastoma cells results in an accumulation of the full length PS protein, thus preventing endoproteolysis [89]. Furthermore, RNAi-mediated inactivation combinations in S2

cells of PEN2 and NCT or PEN2 and APH-1 totally abolished this accumulation [89]. Interestingly, when NCT is deleted in *C. elegans* or *Drosophila*, the resulting phenotypes are similar to the loss of PS1 or Notch [90,91]. Cleavage of APP and Notch at the γ-secretase cleavage site is also eliminated, together with a loss of PS1 endoproteolysis and maturation [90]. This is also evident in NCT null mouse embryos. These embryos have severe developmental defects and die by embryonic day 10.5 [92]. Furthermore, embryonic fibroblast cells isolated from these NCT null mice have decreased levels of APH-1, PEN-2 and PS1 fragments together with a significant accumulation of full-length PS1 [93]. Collectively, these results implicate APH-1 as acting in the stabilisation of the PS holoprotein in the complex, while PEN-2 and NCT assist the endoproteolysis of PS1, thus providing γ-secretase activity. Recently, Chen et al. [94] discovered a new member of the γ-secretase complex, a type 1 transmembrane protein named TMP21 that is a member of the p24 cargo-family. It was isolated in a high molecular weight presenilin complex and was shown to interact with all of the complex components. They demonstrated that overexpression of TMP21 had no effect on the levels of the other complex components or Aβ production, however suppression by small interfering RNAs increased the production of Aβ40 and Aβ42. Thus, through its interaction within the γ-secretase complex TMP21 appears to modulate Aβ production [94]. PS1 has homology to part of an active site of a known bacterial aspartyl protease [95].

Notch proteins are a group of large cell-surface receptors that are required for cell-fate decisions during development. Following binding to its ligand on the cell surface, Notch-1 undergoes γ-secretase cleavage at site 3 (S3) within its intracellular domain to release the Notch intracellular domain (NICD) fragment [96]. NICD then translocates to the nucleus and interacts with DNA-binding proteins to regulate transcription. Mutations in the SEL-12 protein of *C. elegans* result in an egg laying defect, indicating a loss of Notch function. Expression of human PS1 or PS2 in these mutants rescues the egg laying defect. However, in the presence of FAD point mutations there is an observed reduction in rescue [65]. Knocking out PS in *Drosophila* results in phenotypes identical to Notch null mutants [97]. Therefore, PS is required for Notch function and presenilin's function in notch signalling is conserved between humans, *C. elegans* [98] and *Drosophila*.

A diverse range of additional cell surface proteins have been identified as γ-secretase and presenilin substrates. There is little in common between these substrates except that they all posses single transmembrane domains. Deleted in colon cancer (DCC), ErbB4, Delta and p75 neurotrophin receptor (p75NTR) are γ-secretase substrates known to influence neuronal structure and function and are important for development of the nervous system. However the role of cleavage of these proteins by γ-secretase is unknown [99]. Even though it can be postulated that perturbations in the γ-secretase mediated cleavage of these proteins may affect neuronal function, currently an association of these molecules with neurodegeneration or AD development has not be established.

3.2. Presenilin mutations and alternative splicing in Alzheimer's disease

The majority of missense mutations identified in FAD occur at highly conserved sites [100] and are spread throughout the gene. The mutations identified in PS1 are spread through TM domains 1–6 and also in the N and C-terminus, while in PS2 the FAD mutations are present in TM domains 2 and 5 and a mutation identified in a sporadic case of AD is found at the N-terminus [29]. Interestingly, approximately 21% of PS1 AD associated mutations and 4 out of 10 reported PS2 mutations are found in exon 5 [64]. Therefore this region may hold some importance in regard to structure and function of presenilin within the lipid bilayer as exon 5 resides in transmembrane domain 2 of PS1 and PS2 [64]. Presenilin mutations also disturb protein interactions in the γ-secretase complex through conformation changes that affect APP processing [29] and alter the Aβ40/42 ratio either through in an increase in Aβ-42 or a decrease in Aβ-40 [33,34,60]. This is evident through a consistent overproduction of Aβ-42 peptides in brain tissue of FAD patients [29] and transgenic mice harbouring a human PS1 mutation [3]. Furthermore, cultured cells transfected with mutant PS1 or PS2 have a 1.5 to 5 fold increase in the intracellular concentration of Aβ 1–42 compared to cells with wild type PS1 or PS2 [29].

The alternative splicing of exons within a gene, results in the production of different protein isoforms. The isoforms may share or differ in function from the original protein [101]. Splice variants have been identified in PS1 and PS2. In human brain tissue of sporadic AD patients a splicing variant of PS2 (PS2V) has been detected. This variant is preferentially expressed and lacks exon 5 [101]. Due to the exclusion of exon 5 a frameshift occurs in exon 6, resulting in a PS2V containing residues Met1 to Leu119 which is encoded by the amino terminal and a further five additional residues at its carboxyl terminus [102]. In the study by Sato et al. [101] 83% of the variant positive cases had sporadic AD and in neuroblastoma cells the spliced variant was detected under hypoxic conditions. Upon antioxidant treatment, there was an inhibition of the hypoxia induced spliced variant [101]. Interestingly a study by Matsuzaki et al. [103] showed that the PS2V induced by hypoxia can be accelerated by chronic exposure to aluminium. The resulting cell death from this exposure is due to the hypoxic conditions and can be partly attributed to oxidative stress. Considering that aluminium is not a necessary metal for cell function, this result may indicate that chronic aluminium exposure is an environmental risk factor for the development of AD [103].

Kwok et al. [104] discovered an early-onset FAD case that had a novel missense mutation (L271V) present in PS1. Exon trapping analysis confirmed that this mutation results in altered exon 8 splicing and a variant neuropathology in the pedigree. Neuropathological analysis demonstrated the presence of large non-cored plaques, which indicate diffuse plaques rather then the typical neuritic amyloid plaques. Western blots of cell lysates immunoprecipitated with anti-tau or antiGSK-3β indicated that wildtype but not exon 8-deleted PS1 is able to interact directly with Tau and GSK-3β. This supports the idea

that the exon 8 region of PS1 interacts with these proteins. Since GSK-3β phosphorylates tau and initiates neuritic dystrophy, PS1 exon 8 appears to be necessary for neuritic plaque formation. Biochemical analysis indicated that this mutation increased the production of the Aβ-42 peptide [104]. A novel variant of PS1 in an AD Finnish pedigree has also presented with diffuse plaques. Through molecular analysis it was demonstrated that this variant had a deletion of exon 9 [105]. Therefore, it appears that the loss of either exon 8 or 9 results in AD with diffuse plaques lacking the dense neuritic core of Aβ, implying that this region of presenilin has some role in neuritic plaque development. The presence of diffuse rather then neuritic plaques in these cases provides further evidence that the pathogenic events of AD occur before the aggregation of Aβ into neuritic plaques.

3.3. Aberrant presenilins are implicated in other disease states

Aberrant splicing events in the PS1 gene have been observed in other neurological disorders. The presence of PS1 gene products that have deletions in the exons 4–8 region have been found in the brain of sporadic cases of frontotemporal dementia (FTD) [106]. As previously mentioned this disorder has NFTs present in the brain with no detection of amyloid plaques. Furthermore, the increased expression of the PS2V isoform detected in the brains of sporadic AD patients, has also been detected in the cortex at significantly elevated levels in some bipolar and schizophrenia cases [64] A novel mutation in PS1 (Gly183Val) was identified in a patient with a Pick type tauopathy, with the absence of Aβ plaques [107]. This mutation affects the splice signal of the sixth exon intron junction, which may result in aberrant splicing. Preliminary analysis of alternatively spliced products revealed a premature stop codon downstream of exon 5 [107]. These aberrantly spliced presenilins are toxic to normal presenilin function possibly through a loss of function or dominant negative affect. These findings implicate aberrant splicing of the presenilins in neurodegeneration together with its already documented role in development.

A casual link between neurodegenerative and cerebrovascular diseases has been consistently suggested when analysing these types of disorders, with vascular risk factors being identified has possible risk factors for AD pathogenesis [108]. Recently Rovelet-Lecrux et al. [109] demonstrated duplication of the APP locus in five families. These individuals develop early-onset AD with cerebral amyloid angiopathy (CAA). CAA is a disease where Aβ peptides deposit in the walls of small blood vessels in the brain leading to stroke, haemorrhages and dementia. Individuals with an APP duplication either present with dementia or intracerebral haemorrhages or a mixture of both phenotypes [109], thus suggesting a link between dementia (AD) and the vasculature of the brain. Missense mutations in the Notch 3 gene have been attributed to the vascular disease, cerebral autosomal dominant arteriopathy with subcortical infarcts and leukoencephalopathy (CADASIL) [110]. The common symptoms of this disorder are migraines, ischemic strokes, mood disorders and progressive cognitive impairment that results in dementia [111]. Along with dementia progression, a further link to neurodegenerative disorders is evident though recent research identifying the basis of CADASIL as being a degenerative disorder of brain vessels [108]. Interestingly, the intramembrane region of Notch 3 possibly undergoes presenilin mediated γ-secretase cleavage, similar to the cleavage events of APP in AD pathogenesis. The role of Notch in vascular integrity and the role of presenilin in Notch signalling suggest the existence of molecular commonalities between these two diseases.

3.4. Presenilin regulation of the Wnt/β-catenin signalling pathway

The armadillo homologue, β-catenin is an effector molecule in the Wnt/Wingless signalling pathway. It is a transcription factor bound at the cell membrane, where it is involved in the maintenance of the link between the cadherins and the actin cytoskeleton [112]. β-catenin is also located in the cytoplasm in a complex with GSK3-β. Phosphorylation by GSK3-β promotes the ubiquitination of β-catenin, which in turn leads to the rapid degradation of β-catenin by the proteosome [113]. However GSK3-β can be inhibited by signalling through the soluble ligand, Wnt. Inhibition by Wnt results in the accumulation of unphosphorylated β-catenin in the cytoplasm, which eventually translocates to the nucleus. In the nucleus β-catenin binds to the LEF/TCF family of transcriptional regulators that activates target genes of Wnt.

Together with its role in intramembrane proteolysis of Notch and APP [27], PS1 also regulates protein degradation of β-catenin in the Wnt signalling pathway [114,115]. Co-immunoprecipitation experiments have demonstrated that β-catenin binds to the loop domain of PS1 coded by exons 8, 9 and 10 [116]. The functional relevance of this binding has been contradictory where PS1 FAD mutations have either increased β-catenin degradation [117] or interfered with the turnover of β-catenin leading to its accumulation [118]. Using PS1 knockout fibroblasts, Soriano et al. [115] convincingly demonstrated β-catenin accumulating in the cytoplasm with activation of LEF/TCF gene transcription. This indicates that PS1 negatively regulates Wnt/β-catenin pathway [115]. This is further supported by the evident accumulation of armadillo (*Drosophila* homologue of β-catenin) in presenilin-deficient *Drosophila* embryos [114]. It has been speculated that PS1 is needed for the phosphorylation of β-catenin, however Soriano et al. [115] demonstrated an accumulation of phosphorylated β-catenin in the PS1 deficient cells. Furthermore in the presence of a proteosome inhibitor there are lowered levels of ubiquitinated β-catenin observed in PS1 deficient cells compared to wild type cells, which suggested that PS1 is possibly required for the ubiquitination of β-catenin [115]. How PS1 affects the Wnt/β-catenin pathway and furthermore how Aβ production is affected by the interaction between PS1 and β-catenin still remains to be elucidated, though it does appear that this interaction functions in multiple signals that lead to cell fate decisions [35]. The loss of Wnt signalling does appear to play a role in AD [39], evident through the neurotoxicity of Aβ aggregation in hippocampal cells being linked to an increase in

the level of GSK-3β and a subsequent loss of β-catenin. As GSK-3β mediates the phosphorylation of tau, the increase in GSK-3β due to Aβ aggregation may contribute to the formation of NFTs. Overexpression of dishevelled, a downstream transducer of Wnt signalling, inhibits GSK-3β mediated phosphorylation of tau, demonstrating a possible role in increasing neuronal protection during neurodegenerative disorders together with its role in regulating notch signalling [119].

4. Animal models of Alzheimer's disease pathogenesis

Reliable animal models are required to facilitate the understanding of neurodegenerative pathways in AD. Models should allow for the testing of compounds at various points of the pathogenetic cascade in order to search for disease modifying drugs. Furthermore, they remain an invaluable tool for identifying molecular, cellular and pathological changes that trigger the onset of cognitive decline in AD. Specifically, the *presenilin* gene is highly conserved during evolution, with orthologues in mouse, *C. elegans* and *Drosophila* [100]. *Danio rerio*, more commonly known as zebrafish, has two orthologues, zebrafish *psen1* [120] and zebrafish *psen2* [121]. Transcripts from these genes have been demonstrated in zebrafish embryos, suggesting their requirement for development [122].

Drosophila and C. elegans models have been explored to investigate aspects of AD neuropathology. Recently Crowther and colleagues [123] developed a *Drosophila* model, in which human Artic mutant Aβ production is driven in the CNS and retina. This expression results in intracellular Aβ accumulation and non-amyloid aggregates that resemble diffuse plaques. These histological changes are associated with progressive locomotor deficits and premature death, indicating that the accumulation and aggregation of Aβ is sufficient to cause aspects of Aβ pathogenesis [123]. Moreover the fly phenotype is rescued by congo red, a dye that had been previously shown to reduce Aβ aggregation *in vitro* [123]. A study by Finelli et al. [124] examined the overexpression of Aβ-42 in *Drosophila* nervous system tissues. Overexpressing Aβ-42 in the eye resulted in a rough eye phenotype that worsened with age. There was also evidence of insoluble aggregates forming in the photoreceptors. Flies overexpressing Aβ-42 in the brain had a reduced life span in comparison to control flies [124].

C. elegans possesses three orthologues of human presenilin, sel-12 [98], hop-1 [125] and spe-4 [126,127]. Complete presenilin function is evident in the SEL-12 protein as human PS1 and PS2 substitute for SEL-12 activity in *C. elegans*. Also, as previously mentioned, the structure of the SEL-12 protein was used to determine the transmembrane domains of human PS1. In 1995, Link et al. [128] generated a *C. elegans* model of Aβ molecular pathology by genetically engineering animals to express human Aβ specifically in muscle cells. These nematodes produce muscle specific Aβ deposits that are immunoreactive with monoclonal and polyclonal anti-Aβ antibodies. The transgenic nematode larvae present with progressive muscle paralysis and vacuoles, phenotypes that can be attributed to toxicity in muscle cells [128].

4.1. Mouse models of AD neuropathology

There have been numerous transgenic mice developed that model phenotypes observed in AD. Oddo et al. [129] developed a triple-transgenic model in which cDNA from human APP Swedish mutation and human P301L Tau mutation were co-microinjected into embryos from homozygous mice with a human PS1 AD knock-in mutation [129]. This method generated triple transgenic mice with the same genetic background. Further studies showed that these mice present with amyloid plaques and NFTs in AD-relevant regions of the brain. The mice also develop dysfunctions in synaptic plasticity [130] in conjunction with the early intraneuronal accumulation of Aβ. More recently, this group has demonstrated that these mice present with an impairment of long-term memory retention at 4 months of age, indicating that intraneuronal Aβ may be involved in the onset of cognitive deterioration. Feng et al. [63] in reported studies on conditional deletion of PS1 and PS2 in the adult mouse. The loss of presenilin activity in adult mice resulted in forebrain degeneration, evident through cortical shrinkage, together with enlargement of the lateral and third ventricles. These are hallmark features in the brains of AD patients with advanced disease [63]. They also uncovered a series of cellular aberrations in these mice such as neuronal atrophy, astrogliosis, apoptosis and tau hyperphosphorylation. These results implicate the presenilins in the maintenance of cortical structures and functions [63].

In addition to these recent mouse models there are approximately 20 other strains of transgenic mice based on mutations in APP. However, the majority of these, particularly the Tg2576 mouse model (harbours the Swedish APP mutation), are missing important aspects of AD pathology, namely the neurofibrillary tangles [131]. Furthermore these transgenic mice present with memory loss but are lacking the evident neurodegenerative features of AD, thus, they resemble the latent phase of AD [131]. In comparison tau expressing transgenic mice develop neurofibrillary tangles, have evident neuronal loss and also present with other aspects of AD associated neurodegeneration [131]. In one particular line of tau transgenic mice containing the R406W tau mutation, aged transgenic mice present with memory impairment, without any obvious sensorimotor deficits [132]. Evidently there is a need to develop a model that mimics all aspects of the pathogenic cascade, from the triggering mechanisms of AD, to the latent phase of the disease.

4.2. The use of zebrafish to model Alzheimer's disease pathology

The zebrafish is an effective and simple model organism for studies of development and disease processes in the nervous system [133]. Developmental features of early embryonic patterning, early development of the nervous system and particular cell fates have been characterised in the zebrafish. The zebrafish as a vertebrate is more closely related to humans than invertebrate models such as yeast, worms or flies. The zebrafish is an advantageous model for genetic studies as it is

genetically malleable by injection of morpholino antisense oligonucleotides (MO), mRNA or transgenes. With these technologies it is possible to make both subtle and drastic changes in gene expression and observe the affects in the developing transparent embryo. MOs can be designed to block translation of a particular gene or to block the splicing of particular exons into transcripts. Overexpression studies can also be performed by injecting sense mRNA of a gene. For both MO and mRNA injection, the phenotypic affects on embryonic development usually only persist during embryogenesis (i.e. 2 days). Transgenic zebrafish can also be developed by using efficient vectors such as the sleeping beauty transposase system to insert genes under the control of tissue specific promoters. Furthermore, conditionally expressed transgenics can be generated using heatshock promoters and the Cre/loxP and GAL4-UAS systems for the analysis of gene function in specific tissues at specific times [134].

Zebrafish embryos are a valuable system in which to study presenilin function. Orthologues of *PS1* and *PS2* have been identified in zebrafish (*psen1* and *psen2*). Sequence alignment of zebrafish and human presenilin protein sequences displays these primary structures as being highly conserved, though there are highly variable regions at the N-terminus and the C-terminal half of the cytoplasmic loop domains. Transcripts from zebrafish *psen1* are ubiquitously expressed from fertilisation in the zebrafish. This implies that zebrafish *psen1* has an essential function throughout embryonic development [120]. Similar to full-length human *PSEN1*, zebrafish *psen1* cDNA stably transfected in HEK 293 cells, is rapidly turned over with very little being turned into stable CTFs [120]. However, *in vivo* the CTF concentration of zebrafish psen1 steadily increases during embryogenesis to 24 h post fertilisation (hpf), suggesting developmental regulation [122]. Zebrafish *psen2* mRNA is present from fertilisation but protein expression has only been detected from the onset of gastrulation (6 hpf).

Pen-2 is a critical member of the γ-secretase complex. It is thought to facilitate the endoproteolysis of PS1 [135], thus conferring γ-secretase activity. Both zebrafish Pen-2 and zebrafish Aph-1 (another member of the γ-secretase complex) are present from fertilisation similar to psen1. At 12 hpf both genes are ubiquitously expressed in the embryo and by 24 hpf they are expressed predominantly in the brain [136]. Injection of MO blocking Pen-2 translation led to a reduction in islet-1 positive neurons along the spinal cord, a reduction in Notch signalling, an impairment of somitogenesis and induced apoptosis throughout the whole fish [136]. The loss of islet-1 positive neurons in the spinal cord and the increase in apoptosis could be rescued by a concurrent knockdown of p53, implying that loss of Pen-2 induces a p53-dependent apoptotic pathway [136]. The p53-dependant apoptotic pathway contributes to neuronal loss, therefore Pen-2 may have a protective function against apoptosis and promote neuronal survival *in vivo*.

By modulating presenilin expression, it is possible to elucidate its function and regulation in zebrafish. DAPT is a known γ-secretase inhibitor that reduces Aβ peptide levels in the brain [137]. DAPT treatment impairs Notch processing through an interference of presenilin function [138] resulting in severe side affects of γ-secretase inhibitors on Notch dependent cell fate decisions [138]. Treatment of embryos with DAPT affects somitogenesis and neurogenesis by 24 hpf [138]. This phenotype is indistinguishable from Notch signalling deficiencies and can be rescued by injection of mRNA encoding the NICD fragment of zebrafish Notch1. Injection of MOs that block *psen1* transcript translation, leads to disruption of somite formation consistent with partial loss of Notch signalling in the presomitic mesoderm [122]. There is a disruption of myoD expression, a phenotype that is similar in mice lacking PS1 activity. Such mice have a milder phenotype than Notch1 null mutant mice and this has been attributed to the redundant activity of mouse PS2 [139]. However, PS2 knockout alone does not produce a notch phenotype [139]. The possible redundancy between mouse PS1 and PS2 in notch signalling is not reflected in the activity of zebrafish psen1 and psen2. Overexpression of zebrafish *psen2* by microinjection of *psen2* mRNA does not appear to regulate transcription of *psen1* in early zebrafish embryos (12 hpf) [122]. In contrast to observations in mouse cell culture [140], overexpression of *PS2* also does not alter the level of endogenous PS1 holoprotein [122]. Indeed, similar for psen1, repression of psen2 function in zebrafish embryos provides notch loss of function phenotypes [141]. These studies indicate that zebrafish embryos are a valid and valuable system for the study of presenilin function and regulation.

Two homologues of APP, *appa* and *appb* have been identified in zebrafish. Both genes have approximately 70% amino acid identity to human APP-695, with 80% identity in the Aβ-42 region and 95% identity within the transmembrane domain [142]. Widespread expression of both genes is first detected at 8 hpf but at 10 hpf the distribution of expression of two genes diverges. By 24 hpf both genes have overlapping but distinct patterns of expression. Overall the expression pattern of these two genes is similar to that observed for the mouse APP-695 isoform [143]. This indicates that APP gene function is conserved during vertebrate evolution.

Zebrafish are useful for studies of the effects of environmental hazards on vertebrate cells. Similar to mammals, the zebrafish have defence mechanisms against toxic chemicals that includes the generation of oxidative stress [144]. Carvan et al. [144] treated zebrafish and human cell lines with a variety of chemicals known to induce transcription of certain protective genes in cultured mammalian cells. They observed activation of transcription of these genes in a similar dose dependent manner in the zebrafish and human cells, indicating this process to be well conserved between mammals and zebrafish [144].

Alzheimer's disease is clearly a complex, heterogenous disorder evident through extensive research spanning from oxidative stress mechanisms to vascular dysfunction. Intense research has identified genes and environmental factors that heighten the risk of developing AD. The pathogenesis of AD may occur through several pathways, with the common characteristics of Aβ deposition and to a lesser extent aberrant presenilins, which have also been demonstrated in other neurodegenerative disorders. Easily manipulable vertebrate

models, now including the zebrafish, are proving to be increasingly important in elucidating these pathways.

References

[1] K. Blennow, M.J. de Leon, H. Zetterberg, Alzheimer's disease, Lancet 368 (2006) 387–403.

[2] D. Pratico, N. Delanty, Oxidative injury in diseases of the central nervous system: focus on Alzheimer's disease, Am. J. Med. 109 (2000) 577–585.

[3] D.J. Selkoe, M.B. Podlisny, Deciphering the genetic basis of Alzheimer's disease, Annu. Rev. Genomics Hum. Genet. 3 (2002) 67–99.

[4] S. Artero, M.C. Tierney, J. Touchon, K. Ritchie, Prediction of transition from cognitive impairment to senile dementia: a prospective, longitudinal study, Acta Psychiatr. Scand. 107 (2003) 390–393.

[5] M.A. Lambon Ralph, K. Patterson, N. Graham, K. Dawson, J.R. Hodges, Homogeneity and heterogeneity in mild cognitive impairment and Alzheimer's disease: a cross-sectional and longitudinal study of 55 cases, Brain 126 (2003) 2350–2362.

[6] D.J. Selkoe, The molecular pathology of Alzheimer's disease, Neuron 6 (1991) 487–498.

[7] K. Taguchi, H.D. Yamagata, W. Zhong, K. Kamino, H. Akatsu, R. Hata, T. Yamamoto, K. Kosaka, M. Takeda, I. Kondo, T. Miki, Identification of hippocampus-related candidate genes for Alzheimer's disease, Ann. Neurol. 57 (2005) 585–588.

[8] C.W. Cotman, J.H. Su, Mechanisms of neuronal death in Alzheimer's disease, Brain Pathol. 6 (1996) 493–506.

[9] M. Aslan, T. Ozben, Reactive oxygen and nitrogen species in Alzheimer's disease, Curr. Alzheimers Res. 1 (2004) 111–119.

[10] D.A. Butterfield, S. Griffin, G. Munch, G.M. Pasinetti, Amyloid beta-peptide and amyloid pathology are central to the oxidative stress and inflammatory cascades under which Alzheimer's disease brain exists, J. Alzheimers Dis. 4 (2002) 193–201.

[11] C. Opazo, X. Huang, R.A. Cherny, R.D. Moir, A.E. Roher, A.R. White, R. Cappai, C.L. Masters, R.E. Tanzi, N.C. Inestrosa, A.I. Bush, Metalloenzyme-like activity of Alzheimer's disease beta-amyloid. Cu-dependent catalytic conversion of dopamine, cholesterol, and biological reducing agents to neurotoxic H(2)O(2), J. Biol. Chem. 277 (2002) 40302–40308.

[12] X. Huang, M.P. Cuajungco, C.S. Atwood, M.A. Hartshorn, J.D. Tyndall, G. R. Hanson, K.C. Stokes, M. Leopold, G. Multhaup, L.E. Goldstein, R.C. Scarpa, A.J. Saunders, J. Lim, R.D. Moir, C. Glabe, E.F. Bowden, C.L. Masters, D.P. Fairlie, R.E. Tanzi, A.I. Bush, Cu(II) potentiation of alzheimer abeta neurotoxicity. Correlation with cell-free hydrogen peroxide production and metal reduction, J. Biol. Chem. 274 (1999) 37111–37116.

[13] X. Huang, C.S. Atwood, M.A. Hartshorn, G. Multhaup, L.E. Goldstein, R.C. Scarpa, M.P. Cuajungco, D.N. Gray, J. Lim, R.D. Moir, R.E. Tanzi, A.I. Bush, The A beta peptide of Alzheimer's disease directly produces hydrogen peroxide through metal ion reduction, Biochemistry 38 (1999) 7609–7616.

[14] J.W. Lustbader, M. Cirilli, C. Lin, H.W. Xu, K. Takuma, N. Wang, C. Caspersen, X. Chen, S. Pollak, M. Chaney, F. Trinchese, S. Liu, F. Gunn-Moore, L.F. Lue, D.G. Walker, P. Kuppusamy, Z.L. Zewier, O. Arancio, D. Stern, S.S. Yan, H. Wu, ABAD directly links Abeta to mitochondrial toxicity in Alzheimer's disease, Science 304 (2004) 448–452.

[15] M. Sastre, T. Klockgether, M.T. Heneka, Contribution of inflammatory processes to Alzheimer's disease: molecular mechanisms, Int. J. Dev. Neurosci. 24 (2006) 167–176.

[16] T. Wyss-Coray, J.D. Loike, T.C. Brionne, E. Lu, R. Anankov, F. Yan, S.C. Silverstein, J. Husemann, Adult mouse astrocytes degrade amyloid-beta in vitro and in situ, Nat. Med. 9 (2003) 453–457.

[17] E.E. Tuppo, H.R. Arias, The role of inflammation in Alzheimer's disease, Int. J. Biochem. Cell Biol. 37 (2005) 289–305.

[18] D.T. Weldon, S.D. Rogers, J.R. Ghilardi, M.P. Finke, J.P. Cleary, E. O'Hare, W.P. Esler, J.E. Maggio, P.W. Mantyh, Fibrillar beta-amyloid induces microglial phagocytosis, expression of inducible nitric oxide synthase, and loss of a select population of neurons in the rat CNS in vivo, J. Neurosci. 18 (1998) 2161–2173.

[19] G.J. Guillemin, K.R. Williams, D.G. Smith, G.A. Smythe, J. Croitoru-Lamoury, B.J. Brew, Quinolinic acid in the pathogenesis of Alzheimer's disease, Adv. Exp. Med. Biol. 527 (2003) 167–176.

[20] N. Kitaguchi, Y. Takahashi, Y. Tokushima, S. Shiojiri, H. Ito, Novel precursor of Alzheimer's disease amyloid protein shows protease inhibitory activity, Nature 331 (1988) 530–532.

[21] M. Mullan, F. Crawford, K. Axelman, H. Houlden, L. Lilius, B. Winblad, L. Lannfelt, A pathogenic mutation for probable Alzheimer's disease in the APP gene at the N-terminus of beta-amyloid, Nat. Genet. 1 (1992) 345–347.

[22] B. De Strooper, L. Umans, F. Van Leuven, H. Van Den Berghe, Study of the synthesis and secretion of normal and artificial mutants of murine amyloid precursor protein (APP): cleavage of APP occurs in a late compartment of the default secretion pathway, J. Cell Biol. 121 (1993) 295–304.

[23] M.D. Kirkitadze, A. Kowalska, Molecular mechanisms initiating amyloid beta-fibril formation in Alzheimer's disease, Acta Biochim. Pol. 52 (2005) 417–423.

[24] M.P. Cuajungco, K.Y. Faget, Zinc takes the center stage: its paradoxical role in Alzheimer's disease, Brain Res. Brain Res. Rev. 41 (2003) 44–56.

[25] K.N. Dahlgren, A.M. Manelli, W.B. Stine Jr., L.K. Baker, G.A. Krafft, M. J. LaDu, Oligomeric and fibrillar species of amyloid-beta peptides differentially affect neuronal viability, J. Biol. Chem. 277 (2002) 32046–32053.

[26] T.D. Bird, Genetic factors in Alzheimer's disease, N. Engl. J. Med. 352 (2005) 862–864.

[27] A. Capell, H. Steiner, H. Romig, S. Keck, M. Baader, M.G. Grim, R. Baumeister, C. Haass, Presenilin-1 differentially facilitates endoproteolysis of the beta-amyloid precursor protein and Notch, Nat. Cell Biol. 2 (2000) 205–211.

[28] E.H. Corder, A.M. Saunders, W.J. Strittmatter, D.E. Schmechel, P.C. Gaskell, G.W. Small, A.D. Roses, J.L. Haines, M.A. Pericak-Vance, Gene dose of apolipoprotein E type 4 allele and the risk of Alzheimer's disease in late onset families, Science 261 (1993) 921–923.

[29] A. Kowalska, Genetic basis of neurodegeneration in familial Alzheimer's disease, Pol. J. Pharmacol. 56 (2004) 171–178.

[30] Cruts, M.a.R., R., Vol. 2006 August 2006.

[31] D.J. Selkoe, Deciphering the genesis and fate of amyloid beta-protein yields novel therapies for Alzheimer disease, J. Clin. Invest. 110 (2002) 1375–1381.

[32] T.E. Golde, The Abeta hypothesis: leading us to rationally-designed therapeutic strategies for the treatment or prevention of Alzheimer disease, Brain Pathol. 15 (2005) 84–87.

[33] J. Theuns, E. Marjaux, M. Vandenbulcke, K. Van Laere, S. Kumar-Singh, G. Bormans, N. Brouwers, M. Van den Broeck, K. Vennekens, E. Corsmit, M. Cruts, B. De Strooper, C. Van Broeckhoven, R. Vandenberghe, Alzheimer dementia caused by a novel mutation located in the APP C-terminal intracytosolic fragment, Hum. Mutat. 27 (2006) 888–896.

[34] E.S. Walker, M. Martinez, A.L. Brunkan, A. Goate, Presenilin 2 familial Alzheimer's disease mutations result in partial loss of function and dramatic changes in Abeta 42/40 ratios, J. Neurochem. 92 (2005) 294–301.

[35] Q. Chen, D. Schubert, Presenilin-interacting proteins, Expert Rev. Mol. Med. 2002 (2002) 1–18.

[36] C. Haass, C.A. Lemere, A. Capell, M. Citron, P. Seubert, D. Schenk, L. Lannfelt, D.J. Selkoe, The Swedish mutation causes early-onset Alzheimer's disease by beta-secretase cleavage within the secretory pathway, Nat. Med. 1 (1995) 1291–1296.

[37] D.M. Walsh, D.M. Hartley, M.M. Condron, D.J. Selkoe, D.B. Teplow, In vitro studies of amyloid beta-protein fibril assembly and toxicity provide clues to the aetiology of Flemish variant (Ala692–(Gly) Alzheimer's disease, Biochem. J. 355 (2001) 869–877.

[38] M.D. Kirkitadze, M.M. Condron, D.B. Teplow, Identification and characterization of key kinetic intermediates in amyloid beta-protein fibrillogenesis, J. Mol. Biol. 312 (2001) 1103–1119.

[39] Z.Z. Chong, F. Li, K. Maiese, Stress in the brain: novel cellular

mechanisms of injury linked to Alzheimer's disease, Brain Res. Brain Res. Rev. 49 (2005) 1–21.
[40] M.A. Smith, K. Hirai, K. Hsiao, M.A. Pappolla, P.L. Harris, S.L. Siedlak, M. Tabaton, G. Perry, Amyloid-beta deposition in Alzheimer transgenic mice is associated with oxidative stress, J. Neurochem. 70 (1998) 2212–2215.
[41] M. Stefani, C.M. Dobson, Protein aggregation and aggregate toxicity: new insights into protein folding, misfolding diseases and biological evolution, J. Mol. Med. 81 (2003) 678–699.
[42] M. Sjogren, K. Blennow, The link between cholesterol and Alzheimer's disease, World J. Biol. Psychiatry 6 (2005) 85–97.
[43] R. Cacabelos, L. Fernandez-Novoa, V. Lombardi, L. Corzo, V. Pichel, Y. Kubota, Cerebrovascular risk factors in Alzheimer's disease: brain hemodynamics and pharmacogenomic implications, Neurol. Res. 25 (2003) 567–580.
[44] A. Hofman, A. Ott, M.M. Breteler, M.L. Bots, A.J. Slooter, F. van Harskamp, M.A. van Duijn, C. Van Broeckhoven, D.E. Grobbee, Atherosclerosis, apolipoprotein E, and prevalence of dementia and Alzheimer's disease in the Rotterdam Study, Lancet. 349 (1997) 151–154.
[45] A. Ott, R.P. Stolk, A. Hofman, F. van Harskamp, D.E. Grobbee, M.M. Breteler, Association of diabetes mellitus and dementia: the Rotterdam Study, Diabetologia 39 (1996) 1392–1397.
[46] K. Balakrishnan, G. Verdile, P.D. Mehta, J. Beilby, D. Nolan, D.A. Galvao, R. Newton, S.E. Gandy, R.N. Martins, Plasma Abeta42 correlates positively with increased body fat in healthy individuals, J. Alzheimers Dis. 8 (2005) 269–282.
[47] B.V. Zlokovic, Neurovascular mechanisms of Alzheimer's neurodegeneration, Trends Neurosci. 28 (2005) 202–208.
[48] A.J. Dwork, E.A. Schon, J. Herbert, Nonidentical distribution of transferrin and ferric iron in human brain, Neuroscience 27 (1988) 333–345.
[49] C.J. Frederickson, Neurobiology of zinc and zinc-containing neurons, Int. Rev. Neurobiol. 31 (1989) 145–238.
[50] T.E. Droste, R.M. Smith, Neurobiology of Trace Elements, vol. 1, Humana Press, Clifton, NJ, 1983.
[51] S.L. Sensi, H.Z. Yin, S.G. Carriedo, S.S. Rao, J.H. Weiss, Preferential Zn2+influx through Ca2+-permeable AMPA/kainate channels triggers prolonged mitochondrial superoxide production, Proc. Natl. Acad. Sci. U. S. A. 96 (1999) 2414–2419.
[52] C.R. Cornett, W.R. Markesbery, W.D. Ehmann, Imbalances of trace elements related to oxidative damage in Alzheimer's disease brain, Neurotoxicology 19 (1998) 339–345.
[53] R. Sherrington, E.I. Rogaev, Y. Liang, E.A. Rogaeva, G. Levesque, M. Ikeda, H. Chi, C. Lin, G. Li, K. Holman, et al., Cloning of a gene bearing missense mutations in early-onset familial Alzheimer's disease, Nature 375 (1995) 754–760.
[54] E. Levy-Lahad, W. Wasco, P. Poorkaj, D.M. Romano, J. Oshima, W.H. Pettingell, C.E. Yu, P.D. Jondro, S.D. Schmidt, K. Wang, et al., Candidate gene for the chromosome 1 familial Alzheimer's disease locus, Science 269 (1995) 973–977.
[55] E.I. Rogaev, R. Sherrington, E.A. Rogaeva, G. Levesque, M. Ikeda, Y. Liang, H. Chi, C. Lin, K. Holman, T. Tsuda, et al., Familial Alzheimer's disease in kindreds with missense mutations in a gene on chromosome 1 related to the Alzheimer's disease type 3 gene, Nature 376 (1995) 775–778.
[56] J.H. Chyung, D.M. Raper, D.J. Selkoe, gamma-secretase exists on the plasma membrane as an intact complex that accepts substrates and effects intramembrane cleavage, J. Biol. Chem. 280 (2005) 4383–4392.
[57] B. De Strooper, M. Beullens, B. Contreras, L. Levesque, K. Craessaerts, B. Cordell, D. Moechars, M. Bollen, P. Fraser, P.S. George-Hyslop, F. Van Leuven, Phosphorylation, subcellular localization, and membrane orientation of the Alzheimer's disease-associated presenilins, J. Biol. Chem. 272 (1997) 3590–3598.
[58] L. Holcomb, M.N. Gordon, E. McGowan, X. Yu, S. Benkovic, P. Jantzen, K. Wright, I. Saad, R. Mueller, D. Morgan, S. Sanders, C. Zehr, K. O'Campo, J. Hardy, C.M. Prada, C. Eckman, S. Younkin, K. Hsiao, K. Duff, Accelerated Alzheimer-type phenotype in transgenic mice carrying both mutant amyloid precursor protein and presenilin 1 transgenes, Nat. Med. 4 (1998) 97–100.
[59] M. Citron, D. Westaway, W. Xia, G. Carlson, T. Diehl, G. Levesque, K. Johnson-Wood, M. Lee, P. Seubert, A. Davis, D. Kholodenko, R. Motter, R. Sherrington, B. Perry, H. Yao, R. Strome, I. Lieberburg, J. Rommens, S. Kim, D. Schenk, P. Fraser, P. St George Hyslop, D.J. Selkoe, Mutant presenilins of Alzheimer's disease increase production of 42-residue amyloid beta-protein in both transfected cells and transgenic mice, Nat. Med. 3 (1997) 67–72.
[60] D. Scheuner, C. Eckman, M. Jensen, X. Song, M. Citron, N. Suzuki, T.D. Bird, J. Hardy, M. Hutton, W. Kukull, E. Larson, E. Levy-Lahad, M. Viitanen, E. Peskind, P. Poorkaj, G. Schellenberg, R. Tanzi, W. Wasco, L. Lannfelt, D. Selkoe, S. Younkin, Secreted amyloid beta-protein similar to that in the senile plaques of Alzheimer's disease is increased in vivo by the presenilin 1 and 2 and APP mutations linked to familial Alzheimer's disease, Nat. Med. 2 (1996) 864–870.
[61] B. De Strooper, P. Saftig, K. Craessaerts, H. Vanderstichele, G. Guhde, W. Annaert, K. Von Figura, F. Van Leuven, Deficiency of presenilin-1 inhibits the normal cleavage of amyloid precursor protein, Nature 391 (1998) 387–390.
[62] A. Herreman, D. Hartmann, W. Annaert, P. Saftig, K. Craessaerts, L. Serneels, L. Umans, V. Schrijvers, F. Checler, H. Vanderstichele, V. Baekelandt, R. Dressel, P. Cupers, D. Huylebroeck, A. Zwijsen, F. Van Leuven, B. De Strooper, Presenilin 2 deficiency causes a mild pulmonary phenotype and no changes in amyloid precursor protein processing but enhances the embryonic lethal phenotype of presenilin 1 deficiency, Proc. Natl. Acad. Sci. U. S. A. 96 (1999) 11872–11877.
[63] R. Feng, H. Wang, J. Wang, D. Shrom, X. Zeng, J.Z. Tsien, Forebrain degeneration and ventricle enlargement caused by double knockout of Alzheimer's presenilin-1 and presenilin-2, Proc. Natl. Acad. Sci. U. S. A. 101 (2004) 8162–8167.
[64] M.J. Smith, R.A. Sharples, G. Evin, C.A. McLean, B. Dean, G. Pavey, E. Fantino, R.G. Cotton, K. Imaizumi, C.L. Masters, R. Cappai, J.G. Culvenor, Expression of truncated presenilin 2 splice variant in Alzheimer's disease, bipolar disorder, and schizophrenia brain cortex, Brain Res. Mol. Brain Res. 127 (2004) 128–135.
[65] A.L. Brunkan, A.M. Goate, Presenilin function and gamma-secretase activity, J. Neurochem. 93 (2005) 769–792.
[66] K.S. Vetrivel, Y.W. Zhang, H. Xu, G. Thinakaran, Pathological and physiological functions of presenilins, Mol. Neurodegener. 1 (2006) 4.
[67] H. Tu, O. Nelson, A. Bezprozvanny, Z. Wang, S.F. Lee, Y.H. Hao, L. Serneels, B. De Strooper, G. Yu, I. Bezprozvanny, Presenilins form ER Ca2+leak channels, a function disrupted by familial Alzheimer's disease-linked mutations, Cell 126 (2006) 981–993.
[68] P. Vito, E. Lacana, L. D'Adamio, Interfering with apoptosis: Ca(2+)-binding protein ALG-2 and Alzheimer's disease gene ALG-3, Science 271 (1996) 521–525.
[69] A. Alberici, D. Moratto, L. Benussi, L. Gasparini, R. Ghidoni, L.B. Gatta, D. Finazzi, G.B. Frisoni, M. Trabucchi, J.H. Growdon, R.M. Nitsch, G. Binetti, Presenilin 1 protein directly interacts with Bcl-2, J. Biol. Chem. 274 (1999) 30764–30769.
[70] B.J. Passer, L. Pellegrini, P. Vito, J.K. Ganjei, L. D'Adamio, Interaction of Alzheimer's presenilin-1 and presenilin-2 with Bcl-X(L). A potential role in modulating the threshold of cell death, J. Biol. Chem. 274 (1999) 24007–24013.
[71] X. Li, I. Greenwald, Additional evidence for an eight-transmembrane-domain topology for *Caenorhabditis elegans* and human presenilins, Proc. Natl. Acad. Sci. U. S. A. 95 (1998) 7109–7114.
[72] N.N. Dewji, S.J. Singer, The seven-transmembrane spanning topography of the Alzheimer disease-related presenilin proteins in the plasma membranes of cultured cells, Proc. Natl. Acad. Sci. U. S. A. 94 (1997) 14025–14030.
[73] S. Lehmann, R. Chiesa, D.A. Harris, Evidence for a six-transmembrane domain structure of presenilin 1, J. Biol. Chem. 272 (1997) 12047–12051.
[74] D. Spasic, A. Tolia, K. Dillen, V. Baert, B. De Strooper, S. Vrijens, W.

Annaert, Presenilin-1 maintains a nine transmembrane topology throughout the secretory pathway, J. Biol. Chem. (2006).
[75] H. Laudon, E.M. Hansson, K. Melen, A. Bergman, M.R. Farmery, B. Winblad, U. Lendahl, G. von Heijne, J. Naslund, A nine-transmembrane domain topology for presenilin 1, J. Biol. Chem. 280 (2005) 35352–35360.
[76] M.S. Wolfe, W. Xia, B.L. Ostaszewski, T.S. Diehl, W.T. Kimberly, D.J. Selkoe, Two transmembrane aspartates in presenilin-1 required for presenilin endoproteolysis and gamma-secretase activity, Nature 398 (1999) 513–517.
[77] W.T. Kimberly, W. Xia, T. Rahmati, M.S. Wolfe, D.J. Selkoe, The transmembrane aspartates in presenilin 1 and 2 are obligatory for gamma-secretase activity and amyloid beta-protein generation, J. Biol. Chem. 275 (2000) 3173–3178.
[78] M.B. Podlisny, M. Citron, P. Amarante, R. Sherrington, W. Xia, J. Zhang, T. Diehl, G. Levesque, P. Fraser, C. Haass, E.H. Koo, P. Seubert, P. St George-Hyslop, D.B. Teplow, D.J. Selkoe, Presenilin proteins undergo heterogeneous endoproteolysis between Thr291 and Ala299 and occur as stable N- and C-terminal fragments in normal and Alzheimer brain tissue, Neurobiol. Dis. 3 (1997) 325–337.
[79] G. Thinakaran, D.R. Borchelt, M.K. Lee, H.H. Slunt, L. Spitzer, G. Kim, T. Ratovitsky, F. Davenport, C. Nordstedt, M. Seeger, J. Hardy, A.I. Levey, S.E. Gandy, N.A. Jenkins, N.G. Copeland, D.L. Price, S.S. Sisodia, Endoproteolysis of presenilin 1 and accumulation of processed derivatives in vivo, Neuron 17 (1996) 181–190.
[80] T. Ratovitski, H.H. Slunt, G. Thinakaran, D.L. Price, S.S. Sisodia, D.R. Borchelt, Endoproteolytic processing and stabilization of wild-type and mutant presenilin, J. Biol. Chem. 272 (1997) 24536–24541.
[81] H. Steiner, A. Capell, B. Pesold, M. Citron, P.M. Kloetzel, D.J. Selkoe, H. Romig, K. Mendla, C. Haass, Expression of Alzheimer's disease-associated presenilin-1 is controlled by proteolytic degradation and complex formation, J. Biol. Chem. 273 (1998) 32322–32331.
[82] A. Capell, J. Grunberg, B. Pesold, A. Diehlmann, M. Citron, R. Nixon, K. Beyreuther, D.J. Selkoe, C. Haass, The proteolytic fragments of the Alzheimer's disease-associated presenilin-1 form heterodimers and occur as a 100–150-kDa molecular mass complex, J. Biol. Chem. 273 (1998) 3205–3211.
[83] S.S. Hebert, C. Godin, G. Levesque, Oligomerization of human presenilin-1 fragments, FEBS Lett. 550 (2003) 30–34.
[84] C. Haass, H. Steiner, Alzheimer disease gamma-secretase: a complex story of GxGD-type presenilin proteases, Trends Cell Biol. 12 (2002) 556–562.
[85] S. Cervantes, R. Gonzalez-Duarte, G. Marfany, Homodimerization of presenilin N-terminal fragments is affected by mutations linked to Alzheimer's disease, FEBS Lett. 505 (2001) 81–86.
[86] M.S. Brown, J. Ye, R.B. Rawson, J.L. Goldstein, Regulated intramembrane proteolysis: a control mechanism conserved from bacteria to humans, Cell 100 (2000) 391–398.
[87] W.T. Kimberly, M.J. LaVoie, B.L. Ostaszewski, W. Ye, M.S. Wolfe, D.J. Selkoe, Gamma-secretase is a membrane protein complex comprised of presenilin, nicastrin, Aph-1, and Pen-2, Proc. Natl. Acad. Sci. U. S. A. 100 (2003) 6382–6387.
[88] W.T. Kimberly, W.P. Esler, W. Ye, B.L. Ostaszewski, J. Gao, T. Diehl, D.J. Selkoe, M.S. Wolfe, Notch and the amyloid precursor protein are cleaved by similar gamma-secretase(s), Biochemistry 42 (2003) 137–144.
[89] N. Takasugi, T. Tomita, I. Hayashi, M. Tsuruoka, M. Niimura, Y. Takahashi, G. Thinakaran, T. Iwatsubo, The role of presenilin cofactors in the gamma-secretase complex, Nature 422 (2003) 438–441.
[90] Y. Hu, Y. Ye, M.E. Fortini, Nicastrin is required for gamma-secretase cleavage of the *Drosophila* Notch receptor, Dev. Cell 2 (2002) 69–78.
[91] G. Yu, M. Nishimura, S. Arawaka, D. Levitan, L. Zhang, A. Tandon, Y.Q. Song, E. Rogaeva, F. Chen, T. Kawarai, A. Supala, L. Levesque, H. Yu, D.S. Yang, E. Holmes, P. Milman, Y. Liang, D.M. Zhang, D.H. Xu, C. Sato, E. Rogaev, M. Smith, C. Janus, Y. Zhang, R. Aebersold, L.S. Farrer, S. Sorbi, A. Bruni, P. Fraser, P. St George-Hyslop, Nicastrin modulates presenilin-mediated notch/glp-1 signal transduction and betaAPP processing, Nature 407 (2000) 48–54.
[92] T. Li, G. Ma, H. Cai, D.L. Price, P.C. Wong, Nicastrin is required for assembly of presenilin/gamma-secretase complexes to mediate Notch signaling and for processing and trafficking of beta-amyloid precursor protein in mammals, J. Neurosci. 23 (2003) 3272–3277.
[93] Y.W. Zhang, W.J. Luo, H. Wang, P. Lin, K.S. Vetrivel, F. Liao, F. Li, P.C. Wong, M.G. Farquhar, G. Thinakaran, H. Xu, Nicastrin is critical for stability and trafficking but not association of other presenilin/gamma-secretase components, J. Biol. Chem. 280 (2005) 17020–17026.
[94] F. Chen, H. Hasegawa, G. Schmitt-Ulms, T. Kawarai, C. Bohm, T. Katayama, Y. Gu, N. Sanjo, M. Glista, E. Rogaeva, Y. Wakutani, R. Pardossi-Piquard, X. Ruan, A. Tandon, F. Checler, P. Marambaud, K. Hansen, D. Westaway, P. St George-Hyslop, P. Fraser, TMP21 is a presenilin complex component that modulates gamma-secretase but not epsilon-secretase activity, Nature 440 (2006) 1208–1212.
[95] H. Steiner, M. Kostka, H. Romig, G. Basset, B. Pesold, J. Hardy, A. Capell, L. Meyn, M.L. Grim, R. Baumeister, K. Fechteler, C. Haass, Glycine 384 is required for presenilin-1 function and is conserved in bacterial polytopic aspartyl proteases, Nat. Cell Biol. 2 (2000) 848–851.
[96] E.H. Schroeter, J.A. Kisslinger, R. Kopan, Notch-1 signalling requires ligand-induced proteolytic release of intracellular domain, Nature 393 (1998) 382–386.
[97] G. Struhl, I. Greenwald, Presenilin is required for activity and nuclear access of Notch in *Drosophila*, Nature 398 (1999) 522–525.
[98] D. Levitan, T.G. Doyle, D. Brousseau, M.K. Lee, G. Thinakaran, H.H. Slunt, S.S. Sisodia, I. Greenwald, Assessment of normal and mutant human presenilin function in *Caenorhabditis elegans*, Proc. Natl. Acad. Sci. U. S. A. 93 (1996) 14940–14944.
[99] E.H. Koo, R. Kopan, Potential role of presenilin-regulated signaling pathways in sporadic neurodegeneration, Nat. Med. 10 Suppl (2004) S26–S33.
[100] P.E. Fraser, D.S. Yang, G. Yu, L. Levesque, M. Nishimura, S. Arawaka, L.C. Serpell, E. Rogaeva, P. St George-Hyslop, Presenilin structure, function and role in Alzheimer disease, Biochim. Biophys. Acta 1502 (2000) 1–15.
[101] N. Sato, O. Hori, A. Yamaguchi, J.C. Lambert, M.C. Chartier-Harlin, P.A. Robinson, A. Delacourte, A.M. Schmidt, T. Furuyama, K. Imaizumi, M. Tohyama, T. Takagi, A novel presenilin-2 splice variant in human Alzheimer's disease brain tissue, J. Neurochem. 72 (1999) 2498–2505.
[102] S. Higashide, K. Morikawa, M. Okumura, S. Kondo, M. Ogata, T. Murakami, A. Yamashita, S. Kanemoto, T. Manabe, K. Imaizumi, Identification of regulatory cis-acting elements for alternative splicing of presenilin 2 exon 5 under hypoxic stress conditions, J. Neurochem. 91 (2004) 1191–1198.
[103] S. Matsuzaki, T. Manabe, T. Katayama, A. Nishikawa, T. Yanagita, H. Okuda, Y. Yasuda, S. Miyata, S. Meshitsuka, M. Tohyama, Metals accelerate production of the aberrant splicing isoform of the presenilin-2, J. Neurochem. 88 (2004) 1345–1351.
[104] J.B. Kwok, G.M. Halliday, W.S. Brooks, G. Dolios, H. Laudon, O. Murayama, M. Hallupp, R.F. Badenhop, J. Vickers, R. Wang, J. Naslund, A. Takashima, S.E. Gandy, P.R. Schofield, Presenilin-1 mutation L271V results in altered exon 8 splicing and Alzheimer's disease with non-cored plaques and no neuritic dystrophy, J. Biol. Chem. 278 (2003) 6748–6754.
[105] R. Crook, A. Verkkoniemi, J. Perez-Tur, N. Mehta, M. Baker, H. Houlden, M. Farrer, M. Hutton, S. Lincoln, J. Hardy, K. Gwinn, M. Somer, A. Paetau, H. Kalimo, R. Ylikoski, M. Poyhonen, S. Kucera, M. Haltia, A variant of Alzheimer's disease with spastic paraparesis and unusual plaques due to deletion of exon 9 of presenilin 1, Nat. Med. 4 (1998) 452–455.
[106] G. Evin, M.J. Smith, A. Tziotis, C. McLean, L. Canterford, R.A. Sharples, R. Cappai, A. Weidemann, K. Beyreuther, R.G. Cotton, C.L. Masters, J.G. Culvenor, Alternative transcripts of presenilin-1 associated with frontotemporal dementia, NeuroReport 13 (2002) 917–921.
[107] B. Dermaut, S. Kumar-Singh, S. Engelborghs, J. Theuns, R. Rademakers, J. Saerens, B.A. Pickut, K. Peeters, M. van den Broeck, K. Vennekens, S. Claes, M. Cruts, P. Cras, J.J. Martin, C. Van Broeckhoven, P.P. De Deyn, A novel presenilin 1 mutation associated with Pick's disease but not beta-amyloid plaques, Ann. Neurol. 55 (2004) 617–626.
[108] F. Assal, R. Sztajzel, A. Carota, J.M. Annoni, J. Bogousslavsky.

Neurodegeneration and cerebrovascular disease: causal or incidental link? Rev. Med. Suisse 2 (2006) 1180–82, 1184.
[109] A. Rovelet-Lecrux, D. Hannequin, G. Raux, N. Le Meur, A. Laquerriere, A. Vital, C. Dumanchin, S. Feuillette, A. Brice, M. Vercelletto, F. Dubas, T. Frebourg, D. Campion, APP locus duplication causes autosomal dominant early-onset Alzheimer disease with cerebral amyloid angiopathy, Nat. Genet. 38 (2006) 24–26.
[110] A. Joutel, K. Vahedi, C. Corpechot, A. Troesch, H. Chabriat, C. Vayssiere, C. Cruaud, J. Maciazek, J. Weissenbach, M.G. Bousser, J.F. Bach, E. Tournier-Lasserve, Strong clustering and stereotyped nature of Notch3 mutations in CADASIL patients, Lancet. 350 (1997) 1511–1515.
[111] M. Vikelis, M. Xifaras, D.D. Mitsikostas, CADASIL: a short review of the literature and a description of the first family from Greece, Funct. Neurol. 21 (2006) 77–82.
[112] J.E. Meredith Jr., Q. Wang, T.J. Mitchell, R.E. Olson, R. Zaczek, A.M. Stern, D. Seiffert, Gamma-secretase activity is not involved in presenilin-mediated regulation of beta-catenin, Biochem. Biophys. Res. Commun. 299 (2002) 744–750.
[113] B. De Strooper, W. Annaert, Where Notch and Wnt signaling meet. The presenilin hub, J. Cell Biol. 152 (2001) F17–F20.
[114] E. Noll, M. Medina, D. Hartley, J. Zhou, N. Perrimon, K.S. Kosik, Presenilin affects arm/beta-catenin localization and function in *Drosophila*, Dev. Biol. 227 (2000) 450–464.
[115] S. Soriano, D.E. Kang, M. Fu, R. Pestell, N. Chevallier, H. Zheng, E. H. Koo, Presenilin 1 negatively regulates beta-catenin/T cell factor/lymphoid enhancer factor-1 signaling independently of beta-amyloid precursor protein and notch processing, J. Cell Biol. 152 (2001) 785–794.
[116] M. Murayama, S. Tanaka, J. Palacino, O. Murayama, T. Honda, X. Sun, K. Yasutake, N. Nihonmatsu, B. Wolozin, A. Takashima, Direct association of presenilin-1 with beta-catenin, FEBS Lett. 433 (1998) 73–77.
[117] Z. Zhang, H. Hartmann, V.M. Do, D. Abramowski, C. Sturchler-Pierrat, M. Staufenbiel, B. Sommer, M. van de Wetering, H. Clevers, P. Saftig, B. De Strooper, X. He, B.A. Yankner, Destabilization of beta-catenin by mutations in presenilin-1 potentiates neuronal apoptosis, Nature 395 (1998) 698–702.
[118] D.E. Kang, S. Soriano, M.P. Frosch, T. Collins, S. Naruse, S.S. Sisodia, G. Leibowitz, F. Levine, E.H. Koo, Presenilin 1 facilitates the constitutive turnover of beta-catenin: differential activity of Alzheimer's disease-linked PS1 mutants in the beta-catenin-signaling pathway, J. Neurosci. 19 (1999) 4229–4237.
[119] U. Wagner, J. Brownlees, N.G. Irving, F.R. Lucas, P.C. Salinas, C.C. Miller, Overexpression of the mouse dishevelled-1 protein inhibits GSK-3beta-mediated phosphorylation of tau in transfected mammalian cells, FEBS Lett. 411 (1997) 369–372.
[120] U. Leimer, K. Lun, H. Romig, J. Walter, J. Grunberg, M. Brand, C. Haass, Zebrafish (*Danio rerio*) presenilin promotes aberrant amyloid beta-peptide production and requires a critical aspartate residue for its function in amyloidogenesis, Biochemistry 38 (1999) 13602–13609.
[121] C. Groth, S. Nornes, R. McCarty, R. Tamme, M. Lardelli, Identification of a second presenilin gene in zebrafish with similarity to the human Alzheimer's disease gene presenilin2, Dev. Genes Evol. 212 (2002) 486–490.
[122] S. Nornes, C. Groth, E. Camp, P. Ey, M. Lardelli, Developmental control of Presenilin1 expression, endoproteolysis, and interaction in zebrafish embryos, Exp. Cell Res. 289 (2003) 124–132.
[123] D.C. Crowther, K.J. Kinghorn, E. Miranda, R. Page, J.A. Curry, F.A. Duthie, D.C. Gubb, D.A. Lomas, Intraneuronal Abeta, non-amyloid aggregates and neurodegeneration in a *Drosophila* model of Alzheimer's disease, Neuroscience 132 (2005) 123–135.
[124] A. Finelli, A. Kelkar, H.J. Song, H. Yang, M. Konsolaki, A model for studying Alzheimer's Abeta42-induced toxicity in *Drosophila melanogaster*, Mol. Cell Neurosci. 26 (2004) 365–375.
[125] X. Li, I. Greenwald, HOP-1, a *Caenorhabditis elegans* presenilin, appears to be functionally redundant with SEL-12 presenilin and to facilitate LIN-12 and GLP-1 signaling, Proc. Natl. Acad. Sci. U. S. A. 94 (1997) 12204–12209.
[126] P.M. Arduengo, O.K. Appleberry, P. Chuang, S.W. L'Hernault, The presenilin protein family member SPE-4 localizes to an ER/Golgi derived organelle and is required for proper cytoplasmic partitioning during *Caenorhabditis elegans* spermatogenesis, J. Cell Sci. 111 (Pt 24) (1998) 3645–3654.
[127] S.W. L'Hernault, P.M. Arduengo, Mutation of a putative sperm membrane protein in *Caenorhabditis elegans* prevents sperm differentiation but not its associated meiotic divisions, J. Cell Biol. 119 (1992) 55–68.
[128] C.D. Link, Expression of human beta-amyloid peptide in transgenic *Caenorhabditis elegans*, Proc. Natl. Acad. Sci. U. S. A. 92 (1995) 9368–9372.
[129] S. Oddo, A. Caccamo, M. Kitazawa, B.P. Tseng, F.M. LaFerla, Amyloid deposition precedes tangle formation in a triple transgenic model of Alzheimer's disease, Neurobiol. Aging 24 (2003) 1063–1070.
[130] L.M. Billings, S. Oddo, K.N. Green, J.L. McGaugh, F.M. Laferla, Intraneuronal Abeta causes the onset of early Alzheimer's disease-related cognitive deficits in transgenic mice, Neuron 45 (2005) 675–688.
[131] K.H. Ashe, Mechanisms of memory loss in Abeta and tau mouse models, Biochem. Soc. Trans. 33 (2005) 591–594.
[132] Y. Tatebayashi, T. Miyasaka, D.H. Chui, T. Akagi, K. Mishima, K. Iwasaki, M. Fujiwara, K. Tanemura, M. Murayama, K. Ishiguro, E. Planel, S. Sato, T. Hashikawa, A. Takashima, Tau filament formation and associative memory deficit in aged mice expressing mutant (R406W) human tau, Proc. Natl. Acad. Sci. U. S. A. 99 (2002) 13896–13901.
[133] H.G. Tomasiewicz, D.B. Flaherty, J.P. Soria, J.G. Wood, Transgenic zebrafish model of neurodegeneration, J. Neurosci. Res. 70 (2002) 734–745.
[134] N. Scheer, J.A. Campos-Ortega, Use of the Gal4-UAS technique for targeted gene expression in the zebrafish, Mech. Dev. 80 (1999) 153–158.
[135] H. Steiner, E. Winkler, D. Edbauer, S. Prokop, G. Basset, A. Yamasaki, M. Kostka, C. Haass, PEN-2 is an integral component of the gamma-secretase complex required for coordinated expression of presenilin and nicastrin, J. Biol. Chem. 277 (2002) 39062–39065.
[136] W.A. Campbell, H. Yang, H. Zetterberg, S. Baulac, J.A. Sears, T. Liu, S. T. Wong, T.P. Zhong, W. Xia, Zebrafish lacking Alzheimer presenilin enhancer 2 (Pen-2) demonstrate excessive p53-dependent apoptosis and neuronal loss, J. Neurochem. 96 (2006) 1423–1440.
[137] H.F. Dovey, V. John, J.P. Anderson, L.Z. Chen, P. de Saint, L.Y. de Saint Andrieu, S.B. Fang, B. Freedman, E. Folmer, E.J. Goldbach, K.L. Holsztynska, K.L. Hu, S.L. Johnson-Wood, D. Kennedy, J.E. Kholodenko, L.H. Knops, M. Latimer, Z. Lee, I.M. Liao, R.N. Lieberburg, L.C. Motter, J. Mutter, K.P. Nietz, K.L. Quinn, P.A. Sacchi, G.M. Seubert, E.D. Shopp, J.S. Thorsett, J. Tung, S. Wu, C.T. Yang, D.B. Yin, P.C. Schenk, L.D. May, M.H. Altstiel, L.N. Bender, T.C. Boggs, J.C. Britton, D.L. Clemens, D.K. Czilli, J.J. Dieckman-McGinty, K.S. Droste, B.D. Fuson, P.A. Gitter, E.M. Hyslop, W.Y. Johnstone, S.P. Li, T.E. Little, F.D. Mabry, J.E. Miller, Functional gamma-secretase inhibitors reduce beta-amyloid peptide levels in brain, J. Neurochem. 76 (2001) 173–181.
[138] A. Geling, H. Steiner, M. Willem, L. Bally-Cuif, C. Haass, A gamma-secretase inhibitor blocks Notch signaling in vivo and causes a severe neurogenic phenotype in zebrafish, EMBO Rep. 3 (2002) 688–694.
[139] D.B. Donoviel, A.K. Hadjantonakis, M. Ikeda, H. Zheng, P.S. Hyslop, A. Bernstein, Mice lacking both presenilin genes exhibit early embryonic patterning defects, Genes Dev. 13 (1999) 2801–2810.
[140] G. Thinakaran, C.L. Harris, T. Ratovitski, F. Davenport, H.H. Slunt, D.L. Price, D.R. Borchelt, S.S. Sisodia, Evidence that levels of presenilins (PS1 and PS2) are coordinately regulated by competition for limiting cellular factors, J. Biol. Chem. 272 (1997) 28415–28422.
[141] Nornes, S.a.L., M. Manuscript in progress.
[142] A. Musa, H. Lehrach, V.A. Russo, Distinct expression patterns of two zebrafish homologues of the human APP gene during embryonic development, Dev. Genes Evol. 211 (2001) 563–567.
[143] M. Sarasa, V. Sorribas, J. Terradoa, S. Climent, J.M. Palacios, G. Mengod, Alzheimer beta-amyloid precursor proteins display specific patterns of expression during embryogenesis, Mech. Dev. 94 (2000) 233–236.
[144] M.J. Carvan III, D.M. Sonntag, C.B. Cmar, R.S. Cook, M.A. Curran, G.L. Miller, Oxidative stress in zebrafish cells: potential utility of transgenic zebrafish as a deployable sentinel for site hazard ranking, Sci. Total Environ. 274 (2001) 183–196.

I.2 Recent developments towards PSEN's function in AD

The research field of AD is quite dynamic with ever increasing evidence for the involvement of many genes and molecular pathways. Therefore, since the previous review was published, Newman *et al.* 2007, there has been further insight on the normal function of PSEN and how FAD mutations in *PSEN* are involved in AD pathogenesis.

Initially it was proposed that FAD-linked PSEN mutations result in a gain-of-toxic-function, however there is an emerging idea that loss-of-function PSEN can explain the neurodegeneration not only evident in AD but also in another neurodegenerative dementia, frontotemporal dementia (FTD). In comparison to overexpression studies of PSEN, conditional knockout of PSEN1 in the adult cerebral cortex of mice causes age-related progressive neurodegeneration (Saura et al., 2004). These mice present with many hallmarks of AD neuropathology including synaptic loss, neuronal cell death and tau hyperphosphorylation. *PSEN* FAD mutations were presumed to alter the Aβ42/Aβ40 ratio mainly through an increase in Aβ42 secretion, which is then thought to trigger neurodegeneration in the brain. Secondary analysis of the effects of these mutations on APP processing confirmed the increase in the Aβ42/Aβ40 ratio, however, in most mutants it was through a reduction in Aβ40 rather than an increase in Aβ42 peptide levels. (Bentahir et al., 2006; Kumar-Singh et al., 2006; Walker et al., 2005). Pathogenic FAD *PSEN* mutations impair γ-secretase cleavage of not only APP but also Notch and N-cadherin (reviewed in (Shen and Kelleher, 2007)). With reductions in the proteolytic release of NICD during Notch cleavage (Song et al., 1999). A general loss-of-function mechanism for AD mutations in *PSEN1* and *2* has implications for therapeutic strategies for AD, which in the past have focused on diminishing the function of PSEN to reduce Aβ42 production.

Non-proteolytic functions of presenilin have also been examined further with additional investigation of PSEN's role in calcium homeostasis. Tu *et al.* 2006 proposed that PSEN as a holoprotein is able to form calcium ion leak channels from the endoplasmic reticulum (ER) independently of its γ-secretase activity. Mouse Psen1/2 double knockouts in have increased calcium ion concentrations in the ER. While WT Psen could rescue this phenotype, two FAD mutations (M146V and N141I) could not. This supports the above "loss of PSEN function" hypothesis of FAD and also the emerging idea that there is defective calcium ion signalling in AD that is induced by PSEN FAD mutations (Tu et al., 2006).

I.3 The cell cycle hypothesis for AD Pathogenesis

The cell cycle consists of four phases that take place in a eukaryotic cell leading to its replication. Regulation of the cell cycle is crucial to ensure a homeostatic balance between cell proliferation and cell death. The four distinct phases are gap 1 (G_1) phase, synthesis (S) phase, gap 2 (G_2) phase and mitosis (M) phase, with gap 0 (G_0) a resting phase from these four distinct phases. Cyclins and cyclin-dependent kinases (CDK) are the key regulators of cell cycle progression. Disruptions to these regulators will lead to cell cycle arrest and/or cell death. Cyclin protein levels rise and fall with different stages of the cell cycle. In mammalian cells there have been 12 cyclin subtypes identified. These are cyclins A though to K and cyclin T (Kimura et al., 2001), with these proteins sharing a highly conserved motif named the 'cyclin box' (Pines and Hunter, 1989). They are classified into different groups through structural similarity, function during the cell cycle and expression regulation (Horne et al., 1996).

Previously, it has been accepted that neurons in the adult brain are in a terminally differentiated state, that is, they can no longer return to the cell cycle. The cell cycle hypothesis of AD is based on the notion that susceptible neuronal populations in the AD brain re-enter the cell cycle from G_0 into G_1 phase (Zhu et al., 2007). Normally cell cycle re-entry is followed shortly by cell-cycle arrest (G1/S phase), which allows redifferentiation to still occur. However in AD, the regulation mechanisms of G_1/S fail, allowing the neurons to go forward into DNA replication. Since neurons are unable to divide they remain in the late G_2 phase of the cell cycle (Nagy et al., 1998). These neurons are incapable of apoptosis and cell cycle mechanisms activated in G2 drive the formation of neurofibrillary tangles and amyloid plaques (Baumann et al., 1993; Tamura et al., 1993). This cell cycle hypothesis is further supported by susceptible neurons in AD cases having ectopic expression of various cyclins, CDKs and CDK inhibitors. For example, the cdc2/cyclinB1 complex shows aberrant expression in degenerating neurons (Vincent et al., 1997). There is expression of cell cycle and cell division markers in the hippocampus, the main brain region affected in AD (Nagy et al., 1997a; Nagy et al., 1997b), specifically, there is ectopic expression of cyclin D, cdk4, proliferating cell nuclear antigen (PCNA) and cyclin B1 (Busser et al., 1998). Furthermore, expression of the APP Swedish mutation in rat cortical neurons also increases the mRNA and protein levels of cyclin B1 and cyclin D1 (Ahn et al., 2008). The D-cyclins are essential to cell division and overexpression of these cyclins is involved in cancer development. Cyclin B is a mitotic cyclin and, as a complex, promotes mitosis.

Oxidative stress and damage has been observed in neurofibrillary tangles and in neurons at risk of death. Recently the “two-hit hypothesis” has been proposed by Zhu *et*

al, 2004 and 2007. They proposed that aberrant mitotic signalling and oxidative stress are both necessary and sufficient to cause AD. Recently, it was found that expression of β-secretase or BACE1 is stimulated by oxidative stress. This mechanism requires γ-secretase activity and occurs in normal cells, but not in cells lacking PSEN or APP (Tamagno et al., 2008). This provides a specific link between oxidative stress and increased Aβ accumulation.

I.4 The Function of Cyclin G1

CCNG1 was isolated as a novel member of the cyclin family though its homology with the *c*-src family (Tamura et al., 1993) and also through differential screening for transcriptional targets of p53 (Zauberman et al., 1995). CCNG1 protein has a cyclin domain but lacks the protein destabilising (PEST) domain that is present in other cyclin members. The function of CCNG1 has not been completely elucidated. It is currently proposed to play a role in p53 dependent apoptosis as it has p53 binding sites and is induced under p53 inducing conditions (Okamoto and Beach, 1994). Furthermore, CCNG1 has been shown to be induced in a p53 dependent manner in response to DNA damage (Bates et al., 1996). Ccng1 null mice are phenotypically normal. However, further analysis of Ccng1 function reveals a role in G2/M arrest, damage recovery and growth promotion after cellular stress (Kimura et al., 2001). As CCNG1 appears to be non-essential for cell survival (as null mice are viable) it may function through p53 dependent apoptosis in regulating the above pathways. The *CCNG1* paralogue, *CCNG2* has 60% nucleotide sequence identity and 53% amino acid identity to *CCNG1* (Horne et al., 1996). There is contrasting mRNA expression of the two paralogs, with *CCNG1* being constitutively expressed and *CCNG2* oscillating through the cell cycle. These paralogs also have contrasting tissue-specific

expression (Horne et al., 1996). Similar to CCNG1, the function of CCNG2 has not been investigated in detail however it does appear that CCNG2 expression inhibits G1 to S phase transition. Both CCNG1 and CCNG2 directly interact with the catalytic subunit of protein phosphatase 2A (PP2A) (Bennin et al., 2002), this complex may function to inhibit cell cycle progression. The mechanism by which CCNG2 expression is regulated during the cell cycle is unknown.

Accumulating evidence suggests that CCNG1 may play a role in AD pathogenesis. There is an observed increase in immunoreactivity of CCNG1 in the cytoplasm of neurons in human AD brains (Jordan-Sciutto et al., 1999) and CCNG1 protein is also upregulated in the hippocampus of brains of patients with mild cognitive impairment (MCI) (Sultana and Butterfield, 2007). The hippocampus is severely affected during AD pathology and MCI is regarded as an intermediate stage leading to the more severe cognitive decline evident in AD.

The zebrafish orthologue of *CCNG1*, *ccng1*, is upregulated in zebrafish embryos as a result of interference with normal splicing of the AD related genes, *psen1* and *psen2* (paper 3). *CCNG1* also has identified orthologues in *Mus musculus, Rattus norvegicus, Bos Taurus, Drosophila melanogaster,* and *Xenopus tropicalis*. *Danio rerio* also contains an orthologue of *CCNG2* (*ccng2*).

I.5 Aims of the PhD Research Project

AD is a heterogenous disorder with the genetic mechanisms underpinning FAD having been characterised to a certain extent. Intense research has identified genes and environmental factors that heighten the risk of developing the more common sporadic

form of AD. However the pathogenesis of AD is complex and may occur through several pathways, with the deposition of Aβ peptides and oxidative stress playing important roles. Easily manipulable vertebrate models, now including the zebrafish, are proving to be increasingly important in elucidating these pathways. This thesis uses the zebrafish model in attempt to investigate genes with potential links with AD pathogenesis.

I.6 Summary of papers II-IV and links between them

In paper 2, altering *psen1* splicing in zebrafish embryos revealed that aberrant splicing of exon 8 splicing leads to low-levels of truncated peptide species that have dominant negative affects on normal Psen1 function. In human AD cases, no mutations in *PSEN1* have been found that lead to aberrant splicing or protein truncation after exon 6. This paper demonstrated that interference with splicing in between exons 6-8 causes dominant negative activity that appears to suppress notch signalling, indicating a loss of Psen1 activity. Also, blocking Psen1 activity triggers a compensation mechanism that leads to an increase in transcription of normal *psen1*. Such mutations causing peptide truncation, when occurring *de novo,* would be expected to be dominant lethal to human embryogenesis, as changes to Psen1 function affecting Notch signalling are lethal in mice. This explains why such mutations have not been observed in human pedigrees. Over 90% of AD cases are sporadic, while the majority of FAD cases are attributed to mutations in *PSEN1*. Since both familial and sporadic forms of AD present with similar pathologies, genetic analysis of familial AD may elucidate molecular mechanisms in the more common, sporadic, form of AD. The results from paper 2, raise the question that aberrant splicing of *PSEN1* may play a role in sporadic forms of AD, as increased aberrant splicing has been observed in

aged cells. It is suggested that reductions in PSEN1 activity are a cause of FAD and that, therefore, reductions in PSEN1 activity through somatic cellular changes (such as aberrant splicing) may promote irregular APP cleavage and lead to sporadic forms of AD.

Blockage of splicing to exon 8 of *psen1* or *psen2* transcripts in zebrafish embryos, results in very similar effects on embryo development are observed. By 48 hpf there is evident hydrocephalus in the hindbrain with a reduction in pigmentation and yolk extension. In an attempt to identify the common changes in gene expression that might account for these phenotypes, a microarray experiment was undertaken in paper 3. Of the 12 genes that showed the highest degree of divergent regulation in both treatments, one in particular, *ccng1*, held the most interest. There have been numerous hypotheses for the initiation and development of AD. One hypothesis for which evidence is accumulating, is the cell cycle hypothesis, in which susceptible neuronal populations in the AD brain are proposed to re-enter the cell cycle. This, together with increased oxidative stress may result in the increased neuronal death observed in AD. Of the 12 genes identified above, the others with known function are: *prosaposin* (*psap*), *cathepsin Lb* (*ctslb*), *heat shock protein 70kDa* (*hsp70*) and *hatching enzyme 1* (*he1*). Paper 3 provides a discussion on how regulation of these genes may potentially have links to AD pathogenesis. In particular PSAP is involved in lipid metabolism in cell membrane rafts. Recently, PSEN was found to be present in these rafts.

Since the function of Ccng1 in zebrafish is unknown, paper 4 employed morpholino anitsense technology to investigate this. Similar to the mouse knockout of *Ccng1,* knockdown of zebrafish Ccng1 leads to no gross abnormalities in the developing

embryo. However, apparent truncation of Ccng1 after the first exon (88 amino acids) leads to developmental defects in the notochord, brain and developing somites by 22 hpf. Interestingly, this appears to phenocopy the effect of reduced Ccng2 translation. Potentially, truncated Ccng1 species have a dominant negative activity effect on Ccng2 function, a phenomenon that should be investigated further.

CHAPTER II

Research Paper II

Interference with splicing of Presenilin transcripts has potent dominant negative effects on Presenilin activity.

Svanhild Nornes[1], Morgan Newman[1], Giuseppe Verdile[2,3,4], Simon Wells[1], CristiL. Stoick-Cooper[5,6], Ben Tucker[1], Inna Frederich-Sleptsova[2,3], Ralph Martins [2,3,4] and Michael Lardelli[1]

[1]Discipline of Genetics, School of Molecular and Biomedical Science, The University of Adelaide, SA 5005, Australia, [2]Centre of Excellence for Alzheimer's Disease Research and Care, School of Exercise, Biomedical and Health, [3]SirJames McCusker Alzheimer's Disease Sciences, Edith Cowan University, Joondalup, WA 6027, Australia, [4]Research Unit, Hollywood Private Hospital, Nedlands, WA 6009, Australia, School of Psychiatry and Clinical, [5]Neurosciences, University of Western Australia, Crawley, WA 6009, Australia, Department of Pharmacology, Howard, [6]Graduate Program in Neurobiology Hughes Medical Institute, Institute for Stem Cell and Regenerative Medicine and Behavior, University of Washington School o f Medicine, Seattle, WA 98195, USA

Human Molecular Genetics, 2008, Vol17, No3 402-4122.2

STATEMENT OF AUTHORSHIP

Interference with splicing of Presenilin transcripts has potent dominant negative effects on Presenilin activity.

Human Molecular Genetics, 2008, Vol17, No3 402-4122.2

Morgan Newman (Candidate)

- editing of paper
- presenilin morpholino injections
- Development of PCR primers and RT- and Q- PCR analysis on:
    - presenilin morpholino injected embryos (depicted in figure 1)
    - DAPT treated embryos and HEK-293 cells

Certification that the statement of contribution is accurate and permission is given for the inclusion of the paper in the thesis

Signed…….Date

Svanhild Nornes (co-author)

- editing of paper
- presenilin morpholino and mRNA injections
- presenilin protein analysis
- whole mount *in situ* hybridisation on morphants for *neurogenin 1*and *tbx16* expression followed by statistical analysis

Certification that the statement of contribution is accurate and permission is given for the inclusion of the paper in the thesis

Signed

…….Date……

Simon Wells (co-author)

Discovered that DoLa neuron number respond to change in presenilin 2, not presenilin 1. Counting of DoLa neurons in whole mount *in situ* hybridised embryos for *tbx16* expression.

Certification that the statement of contribution is accurate and permission is given for the inclusion of the paper in the thesis

Signed

…….Date……

Ben Tucker (co-author)

Assisted with imaging of morpholino injected embryos.

Certification that the statement of contribution is accurate and permission is given for the inclusion of the paper in the thesis

Signed

…….Date……

Michael Lardelli (co-author)

Planned the research, wrote the manuscript, acted as corresponding author and supervised development of work for Newman, Nornes, Wells and Tucker.

Certification that the statement of contribution is accurate and permission is given for the inclusion of the paper in the thesis

Signed

…….Date……

Giuseppe Verdile (co-author)

Treated Hek-293 cells with a γ-secretase inhibitor, DAPT, for QPCR analysis.

Certification that the statement of contribution is accurate and permission is given for the inclusion of the paper in the thesis

Signed

……. ….. …. ……Date…..

Inna Frederich-Sleptsova (co-author)

Validated morpholino injections.

Certification that the statement of contribution is accurate and permission is given for the inclusion of the paper in the thesis

Signed

…… ……Date

Ralph Martins (co-author)

Supervised development of work for Verdile and Frederich-Sleptsova.

Certification that the statement of contribution is accurate and permission is given for the inclusion of the paper in the thesis

Signed

…… ……Date.

Cristi L. Stoick-Cooper (co-author)

Injected presenilin morpholinos into zebrafish bearing the TOPdGFP transgene and analysed morphants by QPCR.

Certification that the statement of contribution is accurate and permission is given for the inclusion of the paper in the thesis

Signed

Date ...

Nornes, S., Newman, M., Verdile, G. Wells, S., Stoick-Cooper, C., Tucker, B., Frederich-Sleptsover, I., Martins, R. and Lardelli, M. (2008) Interference with slicing of Presenilin transcripts has potent dominant negative effects on Presenilin activity. *Human Molecular Genetics, v. 17 (3), pp. 402-412, February 2008*

NOTE: This publication is included in the print copy of the thesis held in the University of Adelaide Library.

It is also available online to authorised users at:

http://dx.doi.org/doi:10.1093/hmg/ddm317

CHAPTER III

Research Paper III

Altering *presenilin* gene activity in zebrafish embryos causes changes in expression of genes with potential involvement in Alzheimer's Disease pathogenesis.

Morgan Newman[1], Ben Tucker[1], Svanhild Nornes[1], Alister Ward[2] and Michael Lardelli[1]

[1]Discipline of Genetics, School of Molecular and Biomedical Science, The University of Adelaide, SA 5005, Australia

[2]School of Medicine, Deakin University, Waurn Ponds, 3217 VIC, Australia

Journal of Alzheimer's Disease, 2008, Accepted manuscript

STATEMENT OF AUTHORSHIP

Altering *presenilin* gene activity in zebrafish embryos causes changes in expression of genes with potential involvement in Alzheimer's Disease pathogenesis.

Journal of Alzheimer's Disease, June 2008, Accepted manuscript

Morgan Newman (Candidate)

Performed all experiments apart from where Ben Tucker and Svanhild Nornes contributed (see below). Wrote manuscript and acting as corresponding author.

Certification that the statement of contribution is accurate

Signed

…….Date……

Ben Tucker (co-author)

Injected presenilin morpholinos into embryos and prepared RNA from these presenilin morphants for the Adelaide Microarray Facility.

Certification that the statement of contribution is accurate

Signed

…….Date……

Svanhild Nornes (co-author)

Characterisation of morpholino phenotypes before publication.

Certification that the statement of contribution is accurate

Signed

…….Date……

Alister Ward (co-author)

Developed the microarray slides printed with the Compugen Zebrafish OligoLibrary™.

Certification that the statement of contribution is accurate

Signed

.....Date...

Michael Lardelli (co-author)

Planned the research and supervised development of work.

Certification that the statement of contribution is accurate

Signed

.....Date.....

Title:

Altering *presenilin* gene activity in zebrafish embryos causes changes in expression of genes with potential involvement in Alzheimer's Disease pathogenesis.

Authors:

Morgan Newman*^, Ben Tucker^, Svanhild Nornes^, Alistar Ward[#] and Michael Lardelli^

Affiliations:

^Discipline of Genetics, School of Molecular and Biomedical Science, The University of Adelaide, SA, 5005, Australia

[#]School of Medicine, Deakin University, Warun Ponds, VIC, 3217, Australia

*** Corresponding author:**

Morgan Newman

Discipline of Genetics, School of Molecular and Biomedical Science, The University of Adelaide, SA, 5005, Australia

Tel: +61 8 303 4863

Fax: +61 8 303 4362

Email: morgan.newman@adelaide.edu.au

Abstract

Aberrant splicing and point mutations in the human presenilin genes, *PSEN1* and *PSEN2*, have been linked to familial forms of Alzheimer's disease. We have previously described that low-level aberrant splicing of exon 8 in zebrafish *psen1* transcripts in zebrafish embryos produces potent dominant negative effects that increase *psen1* transcription, cause a dramatic hydrocephalus phenotype, decreased pigmentation and other developmental defects. Similar effects are also observed after low-level interference with splicing of exon 8 of *psen2*. To determine the molecular aetiology of these effects we performed microarray analyses of global gene expression changes. Of the 100 genes that showed greatest dysregulation after either *psen1* or *psen2* manipulation, 12 genes were common to both treatments. Five of these have known function and showed increased expression: *cyclin* G1 (*ccng1*), *prosaposin* (*psap*), *cathepsin Lb* (*ctslb*), *heat shock protein 70kDa* (*hsp70*) and *hatching enzyme 1* (*he1*). We used phylogenetic and conserved synteny analysis to confirm the orthology of zebrafish *ccng1* with human *CCNG1*. We analysed the expression of zebrafish *ccng1* in developing embryos to 24 hours post fertilization (hpf). Decreased *ccng1* expression does not rescue the hydrocephalus or pigmentation phenotypes of embryos with aberrant splicing of *psen1* exon 8.

Key Words

presenilin, zebrafish, Alzheimer's disease, cyclin G1, prosaposin

Introduction

The presenilins (PSEN) are ubiquitously expressed transmembrane proteins that function within the γ-secretase complex. Presenilin is found to be the catalytic core of this complex which regulates the proteolysis of a number of type I membrane proteins, including Notch and the amyloid-β protein precursor (AβPP) [1]. The aberrant cleavage of AβPP is proposed to play a major role in the pathogenesis of Alzheimer's disease (AD) and point mutations in the *PSEN1* gene have been linked to familial forms of AD and frontotemporal dementia (FTD) including Pick disease (reviewed by [2]). Mutations affecting the splicing of *PSEN1* have been also demonstrated in the familial forms of these diseases. The G183V mutation affects the donor site of *PSEN1* exon 6 and results in FTD [3]. In some of the resulting transcripts exon 6 is lost and the mRNA codes for a truncated protein. The *PSEN1* L271V mutation identified in AD cases leads to transcripts lacking exon 8 (a naturally occurring isoform). In this case the reading frame is maintained and the translated protein lacks γ-secretase activity [4]. Furthermore, loss of *PSEN2* exon 5 generates a truncated form of the *PSEN2* protein which has been detected in sporadic AD cases [5, 6]. It is important to note that AD has a complex aetiology with a range of proposed mechanisms for disease pathogenesis such as cell cycle dysregulation, increased oxidative stress, disturbed lysosomal function and lipid raft mediated amyloidogenic AβPP processing. Therefore, aberrant presenilin activity is potentially involved at multiple points in a network of mechanisms proposed to lead to this disease. In particular, cyclin G1 and cyclin dependent kinase 2 and 5 proteins are upregulated in the hippocampus of brains of patients with mild cognitive impairment (MCI) [7]. Presenilin and BACE (another enzyme essential for AβPP processing) are

enriched in lipid rafts [8, 9]. Sphingolipids are essential components of these rafts and have been shown to strongly influence Aβ production [10, 11].

Zebrafish possess orthologues of the human *PSEN1* and *PSEN2* genes denoted *psen1* and *psen2.* As previously described in Nornes *et al.* 2007, manipulation of zebrafish embryos can be used to analyse the effects of interfering with *psen1* splicing. Morpholino antisense oligonucleotides ("morpholinos") are short polymers of morpholino-nucleotides that can inhibit mRNA translation or interfere with transcript splicing in a gene-directed fashion. In the Nornes *et al.* study, morpholinos interfering with splicing were designed with the intention of promoting exclusion of exon 8 from *psen1* or *psen2* transcripts. Upon injection into zebrafish embryos, a low-level of aberrant splicing of *psen1* transcripts in exon 8 was detected and this produced potent dominant negative affects that increased *psen1* transcription appeared to suppress Notch signalling and caused pigment loss and severe hydrocephalus by 48 hours post fertilisation (hpf). Reduced pigmentation and hydrocephalus was also evident after injection of a morpholino interfering with splicing to exon 8 of *psen2* transcripts.

In the work described in this paper we used microarray analysis of zebrafish embryos to detect similar patterns of gene dysregulation underlying the common phenotype that results from interference with splicing to exon 8 in either psen1 or psen2. Of the 100 genes that showed greatest dysregulation from interference with psen1 or psen2 splicing, 12 genes were common to both sets. One of these genes, a putative orthologue of human CYCLIN G1 showed visibly increased transcript concentration by whole mount *in situ* hybridisation. We confirm the orthology of this gene to human

CYCLIN G1 and show that suppression of cyclin G1 activity does not alleviate the hydrocephalus or pigmentation phenotypes.

Materials and Methods

Microinjection of morpholino antisense oligonucleotides and control DNA.

Morpholinos were obtained from Gene Tools (LLC, Corvallis, OR, USA). The *psen1* and *psen2* splice blocking morpholinos were designed over the splice acceptor site of exon 8:

Mopsen1Ac8 GCCAGAAGATCTACACAAGAGCAGG

Mopsen2Ac8 ATCTGAAAAACACACGACACTCACA

The Ccng1 translation blocking morpholino binds to the 5'UTR of ccng1 mRNA:

MoCcng1Tln CGTTTCGGTCACCTGGTTCAATCATC

All Mopsen1Ac8 and Mopsen2Ac8 injections were compared to the standard negative control morpholino:

MoCont CCTCCTACCTCAGTTACAATTTATA

Fertilised embryos were injected before cleavage. Embryos were always injected with morpholino solutions at 1mM total concentration to ensure consistency. Dilution of Mopsen1Ac8 and MoCcng1Tln was carried out by mixing with MoCont, to a final injection solution concentration of 1mM. The maximum injection concentration of splice blocking morpholino was 0.5mM (ie. A mixture of 0.5mM MoCont and 0.5mM Mopsen1Ac8). For the morpholino co-injection experiments all morpholinos were mixed with MoCont to their desired final concentration prior to co-injection (ie. A mixture of 0.1mM MoTlnCcng1, 0.3mM Mopsen1Ac8 and 0.6mM MoCont, with total morpholino concentration being 1mM). Injected embryos were then maintained at 28.5°C under standard conditions [12] until the desired developmental stage. As a

control to show the binding specificity of MoCcng1Tsl to *ccng1*, the first 295 bases of the *ccng1* coding sequence was fused in frame to GFP in the N1-EGFP plasmid. This plasmid was linearised prior to co-injection with either MoCcng1Tsl or MoCont alone and then MoCont mixture. Embryos were then observed for GFP fluorescence at ~10hpf using fluorescent microscopy.

Hybridisation and data analysis.

Total RNA was extracted from embryos at 48hpf after injection at the 1 cell stage with either, Mopsen1Ac8, Mopsen2Ac8, or MoCont using the 'QIAGEN RNAeasy Mini Kit' (QIAGEN Hilden, Germany). RNA was precipitated with lithium chloride (Ambion Austen, Texas, USA) and treated with 1 unit of RQ1 DNase (Promega Corp. Madison, WI, USA) at 37ºC for 30 min. RNA quality was checked on a 1% agarose/Tris-borate-EDTA gel and quantity was determined by UV light absorbance with A_{260} correpsonding to 40μg/mL of RNA. cDNA synthesis from total RNA (up to 60μg) and hybridisation to microarray slides printed with the Compugen Zebrafish OligoLibrary^{TM} was performed by the Adelaide Microarray Facility (Australia). The OligoLibrary consists of 16399 oligos representing 16228 LEADS^{TM} clusters plus 171 controls. One oligo was designed for each zebrafish gene identified in GenBank 127 and genes represented by only one EST were not included. Data analysis was performed in R (www.r-project.org) using the Limma package of Bioconductor [13, 14] and in-house scripts. Arrays were normalized using intensity-dependent spatial normalization and scale normalization [15]. Spatial loess was also applied to a subset of arrays [16]. Linear modeling and F-test-based classifications were performed with the Limma package of bioconductor [13]. These procedures and the subsequent data analysis were as described in Brown *et al*, 2006 [17].

Reverse Transcription for RT-PCR.

A mixture of 1-5µg of total RNA, 1µl of random primers and 1µl of 10nM dNTPs was incubated at 65 °C for 5 min followed by -20 °C for 1 min. 4µl of a 5X reaction buffer containing (250 mM Tris–HCl pH 8.3, 375 mM KCl and 15 mM $MgCl_2$), 1µl of 100 mM DTT, 1µl of SuperScript III (200 units/µl) (Invitrogen Corp. Carlsbard, CA, USA), 1µl of Rnase Inhibitor (20U/ µl) (Ambion) was added and incubated at 25 °C for 5 min, followed by 50°C for 60 min. The mixture was then heat inactivated at 70°C for 15 min. Gene specific primers for the amplification of WT and morpholino injected cDNA were designed and synthesised by Gene Works Pty Ltd (Adelaide, Australia) or Proligo (Boulder, Colorado, USA).

Quantitative PCR.

The relative standard curve method for quantification was used to determine the expression of experimental samples compared to a basis sample. For experimental samples, target quantity was determined from the standard curve and then compared to the basis sample to determine fold changes in expression. Gene specific primers were designed using Primer Express software (Applied Biosystems Foster City, CA, USA) for *ccng1*, *psap*, *ctslb* and the ubiquitously expressed control gene *ef-1a*. The starting cDNA quantity was from a pool of 30-60 embryos. The reaction mixture consisted of 100ng/µl (RNA equivalent) of cDNA. 18µM of forward and reverse primers and SYBR green master mix PCR solution (Applied Biosystems). For generation of the standard curve cDNA was serially diluted (100ng, 50ng, 25ng, 12.5ng). Each sample and standard curve reaction was performed in triplicate for the control gene and experimental genes. Amplification conditions were 2 min at 50°C

followed by 10 min at 95°C and then 40-45 cycles of 15 s at 95°C and 1 min at 60°C. Amplification was performed on an ABI 7000 Sequence Detection System (Applied Biosystems) using 96 well plates. Cycle thresholds obtained from each triplicate were averaged and normalised against the expression of *ef-1a*, which has been previously demonstrated as a suitable normalisation gene for zebrafish QPCR [18]. Each experimental sample was then compared to the control sample to determine fold changes of expression.

Cyclin sequence analysis.

Danio rerio (Dr), *Homo sapiens* (Hs) and *Mus musculus* (Mm) cyclin protein sequences were taken from NCBI entrez protein (http://www.ncbi.nlm.nih.gov/sites/entrez?db=protein&cm) (Table 2).

Dr cyclin G1 and G2 protein sequences were used as a query in TBLASTN (BLAST, basic local alignment search tool) [19] searches of the human genome. TBLASTN parameters used were default values specified by the NCBI site (http://www.ncbi.nlm.nih.gov/blast/Blast.cgi).

Phylogenetic analysis of cyclin sequences.

Phylogenetic analysis was performed using the Biomanager facility provided by the Australian National Genomic Information Service (ANGIS, http://angis.org.au/). The protein multiple sequence alignment was performed using ClustalW (accurate) [20]. Parameters were as follows: Protein weight matrix Blosum30, gap opening penalty=10, gap extension penalty=0.05, an end gap separation penalty, gap separation distance=8 and with residue specific and hydrophilic gap penalties. The alignment was then refined to a subregion where the first and last residue contained

identical amino acid residues for all protein sequences (see Table 2). The alignment subregion was prepared for publication using Prettyplot. The alignment subregion was analysed by protein distance methods (Protdist) to create a distance matrix followed by neighbour-joining (Neighbour) to give a phylogeny with branch lengths [21]. Parsimony analysis was also conducted using Protpars [21] with no jumbles and no parsimony threshold. Bootstrap analysis was performed using Seqboot [21] to produce 1,000 resampled datasets that were then analysed by Neighbour and Protpars followed by Consense [21].

Conserved synteny analysis.

The Ensembl genome browser (version 45, release date June 2007, http://www.ensembl.org/index.html) was used to define regions of conserved synteny on the chromosome surrounding the *CCNG1* gene location in various species. Human genes surrounding *CCNG1* where then compared to the zebrafish genome using TBLASTN with the parameters set to default values specified by the NCBI site (http://www.ncbi.nlm.nih.gov/blast/Blast.cgi).

Whole-Mount *In Situ* Hybridisation (WISH).

For each EST, cDNA was PCR amplified from wild type untreated zebrafish cDNA. Primers (sequences in supplementary information) were synthesised by Proligo (Boulder, Colorado, USA) to amplify the full target regions of >500bp. A 25-μL PCR reaction included 1 μL of each cDNA gene-specific primer (10 mM), 10 mM dNTPs, Dynazyme DNA polymerase (Finnzymes Oy, Espoo, Finland). PCR was performed for 30-35 cycles with temperature at 94 °C for 30 s, at 50 °C for 1 min, and at 72 °C for 2 min on a PTC-200, Peltier Thermal cycler (MJ Research Inc. Waltham, MA,

USA). The PCR product was purified from a1-2% agarose/Tris–Acetate–EDTA gels prior to cloning into the pGEMT vector system (Promega Corp. Madison, WI, USA). A Digoxigenin 11-uridine 5' triphosphate (DIG) antisense labelled RNA probe was then generated using SP6 or T7 RNA polymerase from cDNA amplified from a clone using M13 primers. Embryos were fixed in 4% formalaldehyde in embryo medium before manual dechorionation. Whole-mount ISH was then performed as previously described [22].

Results and Discussion

What transcripts are dysregulated in embryos with aberrant *psen1* or *psen2* splicing?

The similar pigmentation and hydrocephalus phenotypes that result from interference with the splicing of exon 8 of either *psen1* or *psen2* imply some overlap in the sets of genes whose regulation is affected. We sought to identify these common gene regulatory changes using a microarray strategy. Embryos were injected with morpholinos Mopsen18Ac, Mopsen28Ac or MoCont (described in methods) at the 1-cell stage. After injection, morpholinos occasionally do not spread throughout the embryo as expected or the physical disruption caused by the injection process may lead to developmental deformities. Therefore, to increase the signal-to-noise ratio for detection of changes in gene regulation, embryos showing the expected consensus phenotypes for Mopsen18Ac and Mopsen28Ac after 48 hours of development were selected for preparation of mRNA for microarray analysis. Although morpholinos have an ultimately transient effect on gene expression, their effects are known to persist beyond the 48 hpf at which we made our observations.

Analysis of microarray expression data analysis was as described in Brown *et al.* 2006. Of the 100 genes each that showed greatest change in expression after manipulation of *psen1* or *psen2* splicing, 12 genes were identified as commonly regulated in both treatments (Table 1a). There were ten upregulated transcripts, which had fold changes ranging from 1.5 to 4.4, while there were 2 downregulated transcripts with fold changes ranging from 1.8 to 3.3. Of these 12 transcripts five were from genes of known function: *cyclin G1* (*ccng1*), *prosaposin* (*psap*), *cathepsin Lb* (*ctslb*), *heat shock protein 70kDa* (*hsp70*) and *hatching enzyme* (*he1*). Two transcripts had putative functions based on similarity to another gene: *similar to plakophilin 3 isoform 3* and *similar to rat glycine n-methyltransferase*. The remaining transcripts had unknown functions. We used these remaining sequences to search the human genome using BLAST but did not identify any potential functions or regions of sequence similarity to characterised human genes.

Confirmation of changes in expression of *ccng1*, *ctslb* and *psap* by QPCR.

To confirm that the microarray analysis had revealed real changes in gene transcription, semi-quantitative real time RT-PCR analyses (QPCR) were performed for three of the genes identified as dysregulated in common in Mopsen1Ac8- and Mopsen2Ac8-injected embryos. Embryo injection, cDNA synthesis and QPCR were performed twice for each gene. The QPCR data is summarised in Table 1b. In every case, Mopsen1Ac8- and Mopsen2Ac8- injected embryos show upregulated expression of *ccng1*, *ctslb* and *psap* comparable to the fold changes observed in the microarray analysis.

Dysregulation of the cell cycle has been discussed as a hypothesis for the progression of AD pathology [23-25]. In mammalian cells there have been 12 cyclin subtypes identified, cyclins A though to K and cyclin T [26]. These proteins share a highly conserved motif named the 'cyclin box' [27] and are classified into different groups through their structural similarity, function during the cell cycle and expression regulation [28]. Mammalian *CCNG1* was isolated as a novel member of the cyclin family though its homology with the *c*-src family [29] and also through differential screening for transcriptional targets of p53 [30]. The function of CCNG1 protein has not been defined in detail. It is currently proposed to play a role in p53-dependent apoptosis. Ccng1 has a proposed role in p53-dependent apoptosis due to the presence of p53 binding sites and its induction under conditions that activate p53 [31]. Furthermore, CCNG1 is induced in a p53-dependent manner in response to DNA damage [32]. *Ccng1* null mice appear grossly phenotypically normal. However, further analysis has revealed roles in G2/M arrest, damage recovery and growth promotion after cellular stress [26]. In mammals, *CCNG1* and *CCNG2* show contrasting levels of mRNA expression in different tissues. Whereas *CCNG1* mRNA levels do not appear to oscillate with the cell cycle, *CCNG2* does show this characteristic [28]. There is also increasing evidence that CCNG1 may play a role in AD pathology. Increased CCNG1 protein can be detected by immunohistochemistry in the cytoplasm of neurons in the hippocampus and neocortex in human AD brains [33] and CCNG1 protein is also upregulated in the hippocampus of brains of patients with mild cognitive impairment (MCI) [7]. The hippocampus is severely affected during AD pathology and MCI is regarded as an intermediate stage leading to more severe cognitive decline evident in AD.

The *prosaposin* gene encodes a multifunctional protein which is the precursor of four saposins, A, B, C and D. These glycoprotein activator proteins are required for the activation of specific lysosomal hydrolases leading to the degradation of glycosphingolipids (GSLs) [34]. The saposin C active site has an *in vitro* nerve regenerating function [35] and human neurotrophic activity [36]. Specifically, the rat hydrophilic sequence of saposin C protected hippocampal CA1 neurons against lethal forebrain ischemia [37] and neurons against chronic hypoxic stress [38], with prosaposin mRNA levels increasing by more than 400% in ischemic brains compared to control brains [39]. Therefore, prosaposin may also act as an antioxidant agent. Deficiency of the saposins leads to lysosomal storage diseases, which usually have a neurological phenotype resulting from the storage of GSLs in central nervous system cells. Mutations in *prosaposin* cause different types of lysosomal storage diseases [40-43] all of these diseases show a commonality of being neurodegenerative disorders with associated pathological lipid metabolism. Sphingolipids are an essential component of rafts and rafts constitute lipid microdomains in the matrix of cellular membranes and allow the compartmentalisation of membrane processes. A current hypothesis is that lipid rafts may mediate amyloidogenic AβPP processing, as presenilin and BACE (another enzyme essential for AβPP processing) are enriched in lipid rafts [8, 9]. Interestingly, presenilin deficient cells display altered lipid raft composition [44]. As sphingolipids have been shown to strongly influence Aβ production [10, 11], mutations in prosaposin (which is required for sphingolipid degradation) potentially affect lipid raft composition and consequently, may affect presenilin regulation in the raft and contribute to AD pathology.

The cathepsin Lb gene encodes a lysosomal cysteine protease. In zebrafish, this protein has a specific role in hatching [45]. Plakophilin 3 is a desmosomal plaque protein and a member of the armadillo repeat multi-gene family. PSEN1 has been shown to interact with armadillo members, β-catenin [46] and plakoglobin [47] (which is also a desmosomal plaque protein). Potentially, PSEN1 may also interact with the plakohilins. Thus, the dominant negative activity of zebrafish Psen brought about by aberrant exon 8 splicing may upregulate plakophilin 3 as a compensatory mechanism. Heat shock protein 70kDa (HSP70) is the most abundant and conserved HSP. Induction of HSPs usually results as a protective mechanism against various stressors of the cell. Increased oxidative stress in cells can induce expression of several heat shock proteins [48]. Together with dysregulation of the cell cycle, oxidative stress is proposed to be a triggering mechanism for AD pathogenesis [23, 24]. The embryo injection process itself invokes stress on the cell and induces the expression of hsp70 (Ben Tucker, unpublished results). However, in our analysis the MoPS1Ac8- and MoPS2Ac8-injected embryos are compared to MoCont-injected controls and so all embryo cohorts have been subjected to the same level of injection stress. Therefore, it is likely that the injection of MoPS1Ac8 or MoPS2Ac8 causes additional stress, such as oxidative stress, that further induces the expression of hsp70. To confirm that oxidative stress is occurring we could potentially observe protein carbonyl levels, which displays if there is oxidative damage [49].

Does Mopsen1Ac8 or Mopsen2Ac8 injection alter the expression pattern of the dysregulated transcripts?

The increases in gene expression observed from our microarray analysis may result from increased expression in cells already expressing a gene or from ectopic gene

expression, or both. The region of gene expression may also give clues to the function of that gene in generation of a phenotype. Whole mount *in situ* transcript hybridisation (WISH) is useful for examining differences in the spatial expression of genes between embryos (in comparison to QPCR which examines changes in global gene expression). Therefore we used WISH to observe the distribution pattern of the 12 identified genes/transcripts dysregulated in common between Mopsen1Ac8- and Mopsen2Ac8-injected embryos, in an attempt to assess how their expression may be perturbed. A DIG-labelled cRNA probe was generated for each transcript. (Note that we were unable amplify cDNA to allow generation of a probe for the transcript identified by AI964267). Uninjected, MoCont-, Mopsen1Ac8- or Mopsen2Ac8-injected embryos were fixed at 24 hpf and 48 hpf of development and subjected to WISH using these probes. The observed expression patterns for each transcript are summarised in supplementary table 2. Some wild-type expression data is also available for the five genes of known function from the Zebrafish Information Network (ZFIN, www.zfin.org) with which we could compare our results. In uninjected and MoCont-injected embryos, the genes *ccng1*, *ctsl1b*, *hsp70* and *he1* had expression patterns consistent with the ZFIN data. However, we could not detect *psap* expression in all expected regions with our probe in uninjected, MoCont-, Mopsen1Ac8- or Mopsen2Ac8-injected embryos. Upon injection of Mopsen1Ac8 or Mopsen2Ac8, *ccng1* expression increased markedly and occurred in areas outside those observed in uninjected or MoCont-injected embryos (figure 1a). *ctsl1b* showed strong expression in the hatching gland, but we could not observe any marked increase in expression in Mopsen1Ac8- or Mopsen2Ac8-injected embryos (figure 1b). *he1* also showed strong expression in the hatching gland. *hsp70* showed strong expression in the lens as expected but, upon injection of Mopsen1Ac8 or

Mopsen2Ac8 additional, lower intensity expression was also observed in the spinal cord, possibly indicating a region of stress induction (data not shown). *Psap* showed some weak expression in the yolk syncytial layer at both 24 hpf and 48 hpf and there was a marginal increase in the expression of this gene in Mopsen1Ac8- or Mopsen2Ac8-injected embryos. Note that aberrant presenilin splicing caused by Mopsen1Ac8- or Mopsen2Ac8-injection leads to a reduction in the size of the yolk extension and so the specific expression of psap in the yolk syncytial layer may reflect an association worthy of further investigation. The remaining transcripts (plakophilin 3 and those represented by ESTs AI793467 and BM101640) have widespread but weak expression in the brain and spinal cord. For the majority of the previously uncharacterised genes identified as dysregulated in common, transcript expression was similar in embryos injected with either Mopsen1Ac8 or Mopsen2Ac8 with some differences at 24 hpf for BM101640.

Phylogenetic analysis indicates the orthology of human *CCNG1* and zebrafish *ccng1*

ccng1 was chosen for further analysis due to the induction of ectopic *ccng1* expression in Mopsen1Ac8 or Mopsen2Ac8 injected embryos and the accumulating evidence for a role of CCNG1 in AD pathogenesis. The *CCNG1* homologue, *CYCLIN G2* (*CCNG2*) has 60% nucleotide sequence identity and 53% amino acid residue identity with *CCNG1* [28]. CCNG1 has been conserved during evolution. Orthologue's of human *CCNG1* have reportedly been identified in the vertebrates *Mus musculus, Rattus norvegicus, Bos Taurus, Xenopus laevis* (African clawed toad), *Danio rerio* (zebrafish) and in the fruitfly, *Drosophila melanogaster.* To confirm the orthology between the nominal *ccng1* orthologue in zebrafish and human *CCNG1*, we

conducted TBLASTN searches of the zebrafish genome using CCNG1 and CCNG2 protein sequences. This produced alignments with highest significance with zebrafish genes denoted in the Ensemble database (version 45, release date June 2007, http://www.ensembl.org/index.html) as *ccng1* (in linkage group/chromosome 14) and *ccng2* (in linkage group/chromosome 21, see Table 4). TBLASTN searches back onto the human genome using putative protein sequences derived from the zebrafish *ccng1* and *ccng2* genes gave alignments of highest significance to human *CCNG1* (in linkage group/chromosome 5) and *CCNG2* (in linkage group/chromosome 4) respectively indicating the probable orthology of these zebrafish and human gene pairs (Table 2b). (Note that the TBLASTN search with putative zebrafish Ccng1 protein sequence also detected the existence of a processed pseudogene in an intron of the human *VANIN1* gene on chromosome 6 that gives an alignment of higher apparent significance than to CCNG1 due to the pseudogene's lack of introns).

Phylogenetic analysis was then performed using ANGIS web based software (http://angis.org.au/). A ClustalW protein alignment of putative zebrafish Ccng1 and human CCNG1 proteins sequences demonstrates 62.8% amino acid residue identity between these proteins. A clustalW multiple protein alignment was then performed using Cyclin G1 and Cyclin G2 proteins from human, mouse and zebrafish and also included a third zebrafish cyclin protein, Ccnf (figure 2a). There is a 4 amino acid gap in the alignment for all sequences except zebrafish Ccng1 due to the latter having an insertion of the residues PVPS between conserved glutamic acid and leucine residues (Figure 3a). The phylogenies generated by neighbour-joining and parsimony analysis both show human *CCNG1* and mouse *ccng1* in a clade with zebrafish *ccng1* and not grouping with *ccng2* sequences. The Neighbour tree with branch lengths is displayed

in Figure 3b. Bootstrap analysis gave strong statistical support to these groupings. (The values obtained for the neighbour-joining analysis are placed on the initial Neighbour tree in Figure 2b.) This supports that zebrafish *ccng1* is orthologous to human *CCNG1*.

Conserved synteny analysis of the genomic location spanning CCNG1 supports zebrafish ccng1 as an orthologue.

Analysis of synteny in the chromosomal region around human *CCNG1* demonstrated conservation between human and zebrafish. In humans, the *NudC domain containing 2* gene (*NUDCD2*) is syntenic with *CCNG1*. This is also observed for the putative zebrafish orthologue (*nudcd2* Table 2c) and TBLASTN searches of the zebrafish genome with the human *NUDCD2* protein sequence gave hits of highest alignment significance to the putative orthologue above (Table 2d). Since *CCNG1* and *NUDCD2* have no known close functional interaction, this supports that the zebrafish genes are, in fact, orthologs of these human genes. This chromosomal region was also found to be conserved in a number of vertebrate species including mouse, rat and *Bos taurus* (data not shown).

WISH transcript hybridisation analysis of *ccng1* expression in the developing embryo predicts a role in somite formation.

In situ hybridisation was performed on embryos from approximately the 256 cell stage (data not shown) through to the 26 somites stage to determine the areas of *ccng1* expression during this time and so further elucidate the function of *ccng1* during early zebrafish development. At the 256 cell stage *ccng1* is expressed ubiquitously indicating a maternal contribution of *ccng1* mRNA to the embryo. The expression is

also uneven with some cells sporadically showing a greater concentration of transcript than others. This confirms previous observations [50]. This uneven ubiquitous expression continues until myotome formation begins at which time *ccng1* transcript appears to be relatively concentrated towards the centre of myotomes and excluded from the horizontal myoseptum (Figure 43a and a'). At 24 hpf *ccng1* expression is observed to be ubiquitous with higher relative levels in the tectum, lens and retina (Figure 3a, b, c, d). The neural expression of *ccng1* is consistent with a role in neural function comparable to the rat brain, where Ccng1 protein levels increase in the cerebral cortex during development, reaching a maximal level in the adult brain [51]. In normal human adult brains CCNG1 protein is expressed at low levels in the frontal cortex and hippocampus [33]. However, in MCI patients, CCNG1 is upregulated in the hippocampus [7], and there is also increased immunoreactivity in the frontal cortex and hippocampus in AD brains [33]. Therefore, the increased neural expression of cyclin G1 protein in the human AD brain and cyclin G1 transcript in zebrafish embryos with altered presenilin splicing, may indicate a role for cyclin G1 in response to neural injury.

Can reduction of ccng1 activity alleviate hydrocephalus in embryos with aberrant splicing of psen1 exon 8?

Of the 11 genes whose expression we attempted to observe with WISH, ccng1 showed the most dramatic upregulation and ectopic expression spreading to all brain regions. Therefore, this induction of expression is potentially involved in the hydrocephalus phenotype that is common between Mopsen1Ac8- and Mopsen2Ac8-injected embryos. If increased *ccng1* expression contributes to these phenotypes then reducing its activity in these embryos might partially alleviate (rescue) them. To test

this we developed a morpholino, MoCcng1Tln, which can inhibit translation of *ccng1* mRNA. Reduction of *ccng1* mRNA translation in otherwise normal embryos does not visibly interrupt zebrafish embryo development (Newman and Lardelli, manuscript in preparation). This is consistent with the phenotype of *Ccng1* knockout mice [26].

We tested the ability of reduced *ccng1* activity to rescue the hydrocephalus and pigmentation phenotype of Mopsen1Ac8-injected embryos by co injecting 0.4mM Mopsen1Ac8 mixed with either 0.1mM or 0.5mM MoCcng1Tln. (The 0.4mM concentration of Mopsen1Ac8 was chosen as a low concentration that still gives a consistent phenotype.) Each mixture was tested twice but no rescue of either hydrocephalus or pigmentation phenotypes at 48hpf was observed relative to embryos injected with only MoPS1Ac8 (data not shown). In a separate experiment the morpholinos were injected separately without prior mixing. Once again there was no rescue of either hydrocephalus or pigmentation defects in the embryos at 48 hpf. This indicates that the hydrocephalus and pigmentation phenotypes are not solely caused by dysregulation of *ccng1*. Indeed, one study proposed that *ccng1* may function in growth promotion after cellular stress [26] in which case the upregulation of *ccng1* may be a response to the aberrant gene regulation and embryo development caused by injection of Mopsen1Ac8.

Conclusion

We conducted a microarray study to compare gene regulation in embryos with disturbed splicing of transcripts from *psen1* or *psen2*. Of the 100 genes each that showed the greatest dysregulation after either *psen1* or *psen2* manipulation, 12 were common to both treatments. Of these 12, only five had characterised gene function.

Upregulated *ccng1* held particular interest because of its normal widespread expression pattern and dramatic dysregulation in embryos with disturbed *psen1/2* splicing. Phylogenetic and conserved synteny analyses indicate that zebrafish *ccng1* is the zebrafish orthologue of human *CCNG1* and that the genomic region including this gene is evolutionarily conserved in a number of vertebrates. *In situ* expression analysis indicates potential roles for *ccng1* in somite differentiation and neural development in zebrafish. Reduction of Ccng1 translation in zebrafish embryos failed to rescue the hydrocephalus or pigmentation phenotypes in Mopsen1Ac8 injected embryos, indicating that these phenotypes are not solely cause by *ccng1* dysregulation. Future work will involve more detailed functional analysis of *ccng1* in zebrafish development.

Acknowledgments

This research was funded by the Australian National Health and Medical Research Council under Project Grant 453622. Additional support was from the Australian Research Council (ARC) Special Research Centre for the Molecular Genetics of Development. Student funding was from the School of Molecular and Biomedical Science, The University of Adelaide. The microarrays were produced under an ARC Linkage Infrastructure, Equipment and Facilities grant, “FishWorks - collaborative infrastructure for zebrafish research”.

Table 1. Summary of genes regulated in common from microarray data analysis and qPCR data confirming microarray fold changes. (**A**) Of the 100 genes that showed the greatest dysregulation after manipulation of splicing of either *psen1* or *psen2* by morpholino injection, 12 genes were common to both treatments. Comparisons were made to MoCont injected embryos. Where known the encoding *Danio rerio* gene is listed. The genes are ordered by relative fold change. Arrows up/down represent increased/decreased expression relative to control respectively. (**B**) For each injection type (MoCont, Mopsen1Ac8 or Mopsen2Ac8) two separate batches of embryos were injected and then separate cDNA syntheses were performed for each batch. For each of the three genes, *ccng1*, *ctslb* and *psap* triplicates within each experiment were performed for each batch to confirm the fold change observed from the microarray data. Each experiment was normalised against *ef-1a*.

A

Presenilin 1

EST ID	Gene bank ID	Danio rerio Gene	Fold Change
AI877922	BC098595	*hatching enzyme 1*	3.2↑
AF006007	NM_131397	*hsp70*	2.8↑
AW077091			2.6↑
BI881145	XM_679912	*plakophilin 3*[#]	2.5↑
AI959372	NM_199481	*cyclin G1*	2.5↑
BE017682	BC062527	*GNMT**	2.3↑
Y08321	NM_131198	*cathepsin L1b*	2.2↑
AI793467			1.9↑
AF108655	NM_131883	*prosaposin*	1.7↑
BM101640	BC049306		1.6↑
AI931056			1.8↓
AI964267			2.1↓

Presenilin 2

EST ID	Gene bank ID	Danio rerio Gene	Fold Change
BI881145	XM_679912	*plakophilin 3* [#]	4.4↑
AW077091			3.9↑
BE017682	BC062527	*GNMT**	2.8↑
Y08321	NM_131198	*cathepsin L1b*	2.6↑
AF006007	NM_131397	*hsp70*	2.5↑
AI877922	BC098595	*hatching enzyme 1*	2.3↑
AI793467			1.9↑
AI959372	NM_199481	*cyclin G1*	1.8↑
AF108655	NM_131883	*prosaposin*	1.5↑
BM101640	BC049306		1.5↑
AI964267			3.2↓
AI931056			3.3↓

*similar to rat glycine n-methyltransferase
[#] similar to plakophilin 3 isoform 3

B

Presenilin 1

Gene	Expt 1.	Expt 2.	Microarray
ccng1	2.6	1.9	2.5
ctslb	1.6	2.2	2.2
psap	2.2	3	1.7

Presenilin 2

Gene	Expt 1.	Expt 2.	Microarray
ccng1	1.4	1.9	1.8
ctslb	1.8	1.8	2.6
psap	1.8	3.6	1.5

Table 2. NCBI accession numbers for cyclin sequences used in TBLASTN searches of human and zebrafish genomes and conserved synteny analysis of the genomic region around *ccng1*.

Cyclin protein accession numbers and the amino acid residues used for the multiple protein alignment in Fig 1A are indicated. (**B**) Sequences of human and putative zebrafish Cyclin G1 and G2 proteins were used in TBLASTN searches of zebrafish and human genome sequences to find the alignments of highest statistical significance. Note: The TBLASTN analysis of the human genome with zebrafish putative Cyclin G1detected a psuedogene within an intron of the human *VANIN1* gene that has a higher E-value than alignments with human *CYCLIN G1* or *G2* due to its lack of introns. (**C**) *ccng1* lies within a region of conserved synteny. *nudcd2* is situated close to *ccng1* in both zebrafish and human genomes on chromosomes 14 and 5 respectively. (**D**) TBLASTN analysis of human NUDCD2 against the zebrafish genome and the reciprocal analysis of zebrafish Nudcd2 against the human genome shows that zebrafish *nudcd2* is most similar to human *NUDCD2* and thus supports the orthology of human *CCNG1* with zebrafish *ccng1*.

A

Protein	NCBI Accession Number		
	Nucleotide	Protein	Amino acid residues
Danio rerio			
Cyclin G1	NM_199481	NP_955775	28 - 292
Cyclin G2	NM_213172	NP_998337	17 - 280
Cyclin F	NM_207048	NP_996931	281 - 552
Homo sapiens			
Cyclin G1	NM_004060	NP_004051	24 - 288
Cyclin G2	NM_004354	NP_004345	28 - 291
Mus musculus			
Cyclin G1	NM_009831	NP_033961	23 - 287
Cyclin G2	NM_007635	NP_031661	28 - 291

B

Protein	Target genome	Highest quality alignments (NCBI descriptions)	Quality (E value)
Danio rerio Cyclin G1	*Homo sapiens*	NT_023133.12 Hs5_23289 *Homo sapiens* chromosome 5 genomic contig *CYCLIN G1*	9.00E-26
		NT_016354.18 Hs4_16510 *Homo sapiens* chromosome 4 genomic contig *CYCLIN G2*	3.00E-15
Danio rerio Cyclin G2	*Homo sapiens*	NT_016354.18 Hs4_16510 *Homo sapiens* chromosome 4 genomic contig *CYCLIN G2*	4.00E-42
		NT_023133.12 Hs5_23289 *Homo sapiens* chromosome 5 genomic contig *CYCLIN G1*	7.00E-35
Homo sapiens CYCLIN G1	*Danio rerio*	NW_001511049.1 Dr14_WGA2017_2 *Danio rerio* chromosome 14 genomic contig cyclin G1	2.00E-56
		NW_001512342.1 Dr21_WGA3149_2 *Danio rerio* chromosome 21 genomic contig cyclin G2	3.00E-15

C

Species	Chromosome No.	Gene and map position	
Danio rerio	14	*ccng1* 18.912- 18.920 Mb	*nudcd2* 18.920 - 18.932 Mb
Homo sapiens	5	*CCNG1* 162.794 - 162.804 Mb	*NUDCD2* 162.813 - 162.819 Mb

D

Protein and Accession No.	Target Genome	Highest quality alignments (NCBI descriptions)	Quality (E-value)
NUDCD2 NP_660309	*danio rerio*	NW_001511049.1 Dr14_WGA2017_2 Danio rerio chromosome 14 genomic contig LOC791909 XM_001330894 NP_001003539 NudC domain containing 2 no significant additional homologue detected	3.00E-20
nudcd2 NP_001003539	*homo sapien*	NT_023133.12 Hs5_23289 Homo sapiens chromosome 5 genomic contig NM_145266 NP_660309 NudC domain containing 2 (only one hit)	3.00E-17

Supplementary Table 1. Primer sequenced used to amplify microarray genes from cDNA.

	Primer seqeunce	
Genbank ID	**Sense 5'-3'**	**Antisense 5'-3'**
AF006007 (*hsp70*)	GGATGCAGGAGTCATCGC	CAGTTCTCTGCCGTTGAAGA
AW077091	CACACTACATACAGCACTGGAAATAT	TCATGCTCCGCTGTGTATAAG
AI959372 (*ccng1*)	TTGATTGACCAGGTGACCG	GCAATGGCATGCCTTTAACTG
Y08321 (*ctslb*)	ACTTGAGAAAAATTGAGCAACACAA	GCCCTAACAGCAGAACAACTTGATA
AI793467	TGGAGAGAAAAAAAACCAAACA	CACTCTGCACCCCTTTTAAAA
BE017682	TCAATAAAGAACAAGCATCAAGAAT	CCTATGACTACATCATTGAGCCTG
AI877922 (*he1*)	GCATCCTGAAGACAACATGG	CGTACTGGTTCACGATCGCT
BI881145	GGAATCTGTCCTATCAGGTG	TGTCTCGTGCGGCCAACAT
AF108655 (*psap*)	TGTGATCTGTGCAAAGAGGTGT	ATCGGCCTCCTGCACAA
BM101640	TCCCCTTCATTTTATTAAACATCA	AGGATTCAGTGCGAGCAAGT

Supplementary Table 2. Summary of expression analysis for whole mount *in situ* hybridisation. A DIG labelled probe was generated for each of the 12 commonly regulated genes except AI931056 and AI964267 for which no cDNA could be amplified. Uninjected, MoCont, Mopsen1Ac8 or Mopsen2Ac8 injected embryos at 24 and 48 hpf were subjected to WISH analysis for each gene to determine expression patterns in normal and injected embroys and whether these suggested any involvement in the hydrocephalus and pigmentation-loss phenotypes.

GenBank ID		Zebrafish gene	Expression in control embryos	Expression in psen1 ex8 morphants	Expression in psen2 ex8 morphants
AF006007	**NM_131397**	***hsp70***	strong expression specifically in the lens of the eye	less expression in the lens of the eye with increased expression in the spinal cord relative to control embryos	same as for psen1 ex8 morphants
AW077091			weak, ubiquitous expression which appears stronger in 24hpf embryos	increased expression specifically in the spinal cord/notochord in 48hpf embryos	same as for psen1 ex8 morphants
AI959372	**NM_199481**	***ccng1***	ubiquitous expression particularly in the somites, eye and brain regions	overall increased expression relative to control embryos	same as for psen1 ex8 morphants
AI964267	No ISH probe				
Y08321	**NM_131198**	***Ctsl1b***	specific strong expression in the hatching gland, anterior end of the yolk	in 48hpf embryos hatching gland expression appears more laterally spread across the yolk	similar to control embryos
AI793467			weak expression in brain in 48hpf embryos only	weak brain expression evident from 24hpf which is slightly increased at 48hpf relative to control embryos	expression appears to be decreased in the regions observed in control embryos
BE017682	**BC062527**	***GNMT****	weak expression in spinal cord	similar to control embryos	similar to control embryos
AI877922	**BC098595**	***he1***	specific strong expression in the hatching gland, anterior end of the yolk	similar to control embryos in a reduced yolk extension	same as for psen1 ex8 morphants
BI881145	**XM_679912**	***plakophilin 3#***	at 24hpf weak ubiquitous expression and at 48hpf expression in spinal cord	slightly increased expression relative to control embryos	same as for psen1 ex8 morphants
AI931056	No ISH probe				
AF108655	**NM_131883**	***psap***	weak expression along yolk extension in the yolk syncitial layer in 48hpf embryos only	slightly increased expression relative to control embryos in a reduced yolk extension	similar to psen1 with expression evident from 24hpf
BM101640	**BC049306**		weak brain expression in 48hpf embryos only	weak expression is evident from 24hpf embryos onwards	no expression observed in 24hpf embryos and increased expression in 48hpf embryos relative to control embryos

Figure 1. Phylogenetic analysis of cyclin sequences. (**A**) The clustalW alignment of cyclin protein sequences used for phylogenetic analysis. A multiple alignment was performed using *Danio rerio* (*Dr*), *Homo sapiens* (*Hs*) and *Mus Musculus* (*Mm*) cyclin G1 and G2 and *Dr* Cyclin F (Ccnf) protein sequences. The alignment was then refined to a subregion where the first and last residue contained identical amino acid residues for all protein sequences. Black boxes indicate identical residues. (**B**) Phylogenetic tree derived by protein distance and neighbour-joining methods of the alignment in A. Branch lengths are indicated and confidence values (as % within the fork of the node in bold numbering) from analysis of 1,000 resampled datasets indicate the frequency at which all sequences after a node were found to be grouped. The tree is unrooted as there is no basis for assigning any particular sequence as ancestral to the others. The double bars over the *Dr* Ccnf branch indicate that this branch is longer than actually shown.

Figure 1.

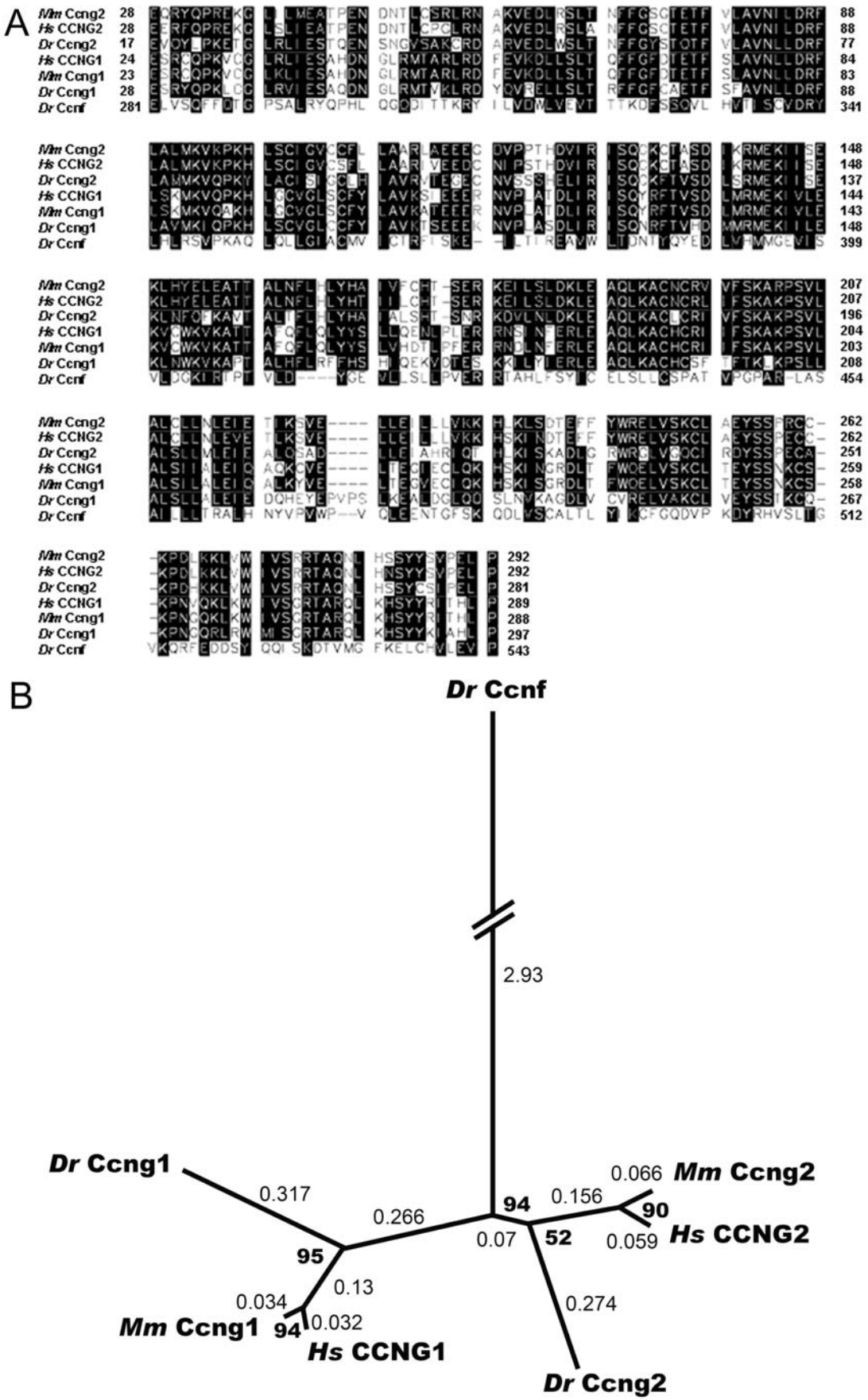

A
Mm Ccng2
Hs CCNG2
Dr Ccng2
Hs CCNG1
Mm Ccng1
Dr Ccng1
Dr Ccnf
B
Dr Ccnf
2.93
Dr Ccng1
0.317
0.266
95
0.13
0.034
Mm Ccng1
94
0.032
Hs CCNG1
94
0.07
0.156
0.066
Mm Ccng2
90
0.059
Hs CCNG2
52
0.274
Dr Ccng2

Figure 2. WISH analysis of *ccng1* and *ctslb* expression in MoCont-, Mopsen1Ac8- and Mopsen2Ac8-48hpf injected embryos. The morpholino injected is indicated for each row and WISH probe for each column. There is an obvious increased expression in the somites (S) and an induction of neural (N) ectopic expression of *ccng1* in the MopsenAc8 embryos. *Ctslb* displays strong expression in the hatching gland (H) which is consistent in the Cont and MoPSAc8 embryos.

Figure 2.

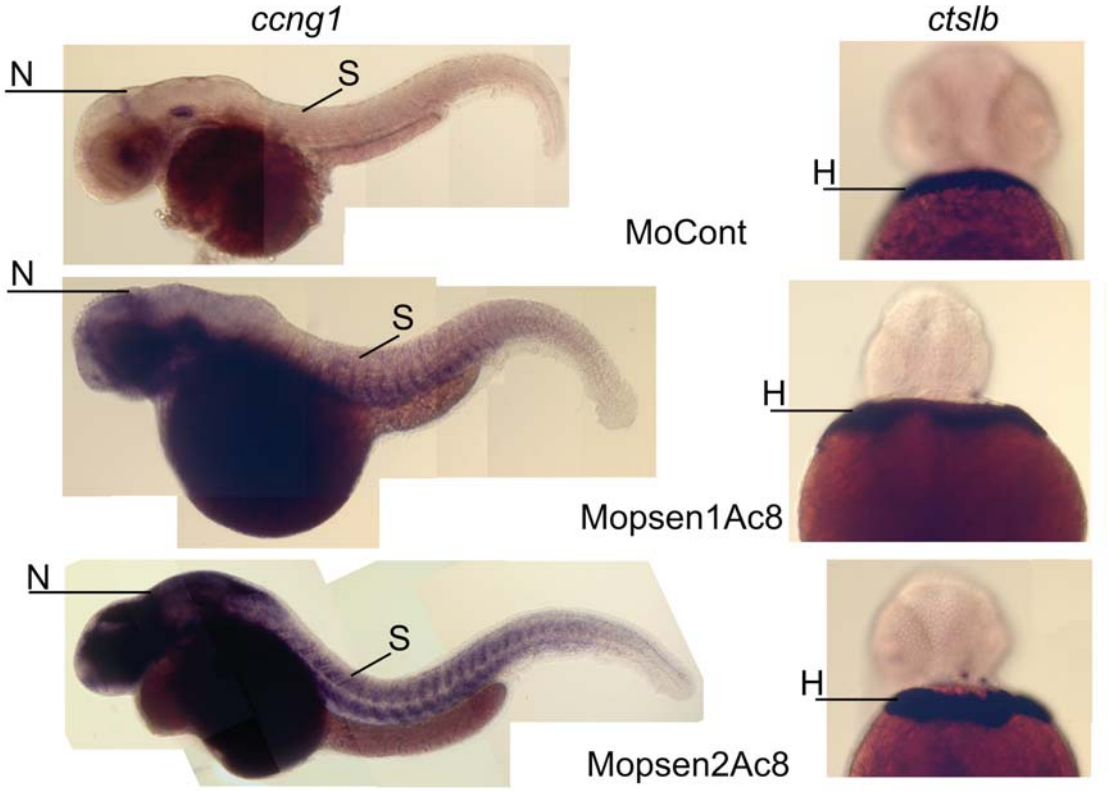
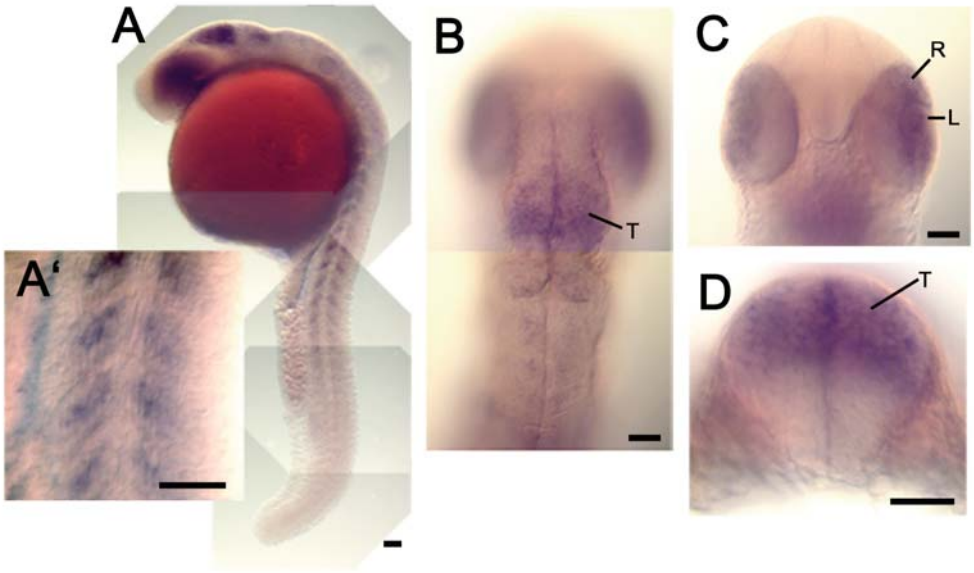


Figure 3. *ccng1* expression in the zebrafish embryo at 24 hpf.

(**A**), Embryo at 24hpf, lateral view with anterior to top and dorsal to right. *ccng1* appears ubiquitous but has relatively high levels of expression in myotomes (but not in the myoseptum). (**A'**), Higher magnification view of this embryo in the region dorsal to the yolk extension showing myotome expression. (**B**) and (**C**), dorsal views of mesencephalon and eyes respectively showing expression in tectum (**T**), retina (**R**) and lens (**L**). (**D**), Transverse optical section through the mesencephalon showing higher relative expression in the tectum. Size bars indicate 50μm.

Figure 3.



References

[1] A. Capell, H. Steiner, H. Romig, S. Keck, M. Baader, M.G. Grim, R. Baumeister and C. Haass, Nat Cell Biol 2 (2000) 205-11.

[2] B. Dermaut, S. Kumar-Singh, R. Rademakers, J. Theuns, M. Cruts and C. Van Broeckhoven, Trends Genet 21 (2005) 664-72.

[3] B. Dermaut, S. Kumar-Singh, S. Engelborghs, J. Theuns, R. Rademakers, J. Saerens, B.A. Pickut, K. Peeters, M. van den Broeck, K. Vennekens, S. Claes, M. Cruts, P. Cras, J.J. Martin, C. Van Broeckhoven and P.P. De Deyn, Ann Neurol 55 (2004) 617-26.

[4] J.B. Kwok, G.M. Halliday, W.S. Brooks, G. Dolios, H. Laudon, O. Murayama, M. Hallupp, R.F. Badenhop, J. Vickers, R. Wang, J. Naslund, A. Takashima, S.E. Gandy and P.R. Schofield, J Biol Chem 278 (2003) 6748-54.

[5] N. Sato, O. Hori, A. Yamaguchi, J.C. Lambert, M.C. Chartier-Harlin, P.A. Robinson, A. Delacourte, A.M. Schmidt, T. Furuyama, K. Imaizumi, M. Tohyama and T. Takagi, J Neurochem 72 (1999) 2498-505.

[6] M.J. Smith, R.A. Sharples, G. Evin, C.A. McLean, B. Dean, G. Pavey, E. Fantino, R.G. Cotton, K. Imaizumi, C.L. Masters, R. Cappai and J.G. Culvenor, Brain Res Mol Brain Res 127 (2004) 128-35.

[7] R. Sultana and D.A. Butterfield, Neurochem Res 32 (2007) 655-62.

[8] K.S. Vetrivel, H. Cheng, W. Lin, T. Sakurai, T. Li, N. Nukina, P.C. Wong, H. Xu and G. Thinakaran, J Biol Chem 279 (2004) 44945-54.

[9] J.M. Cordy, N.M. Hooper and A.J. Turner, Mol Membr Biol 23 (2006) 111-22.

[10] Q. Zha, Y. Ruan, T. Hartmann, K. Beyreuther and D. Zhang, Mol Psychiatry 9 (2004) 946-52.

[11] M.O. Grimm, H.S. Grimm, A.J. Patzold, E.G. Zinser, R. Halonen, M. Duering, J.A. Tschape, B. De Strooper, U. Muller, J. Shen and T. Hartmann, Nat Cell Biol 7 (2005) 1118-23.

[12] M. Westerfield, The Zebrafish Book: A guide to the laboratory use of Zebrafish (Danio rerio), University of Oregon Press, Eugene 1995.

[13] G.K. Smyth, Stat Appl Genet Mol Biol 3 (2004) Article3.

[14] R.C. Gentleman, V.J. Carey, D.M. Bates, B. Bolstad, M. Dettling, S. Dudoit, B. Ellis, L. Gautier, Y. Ge, J. Gentry, K. Hornik, T. Hothorn, W. Huber, S. Iacus, R. Irizarry, F. Leisch, C. Li, M. Maechler, A.J. Rossini, G. Sawitzki, C. Smith, G. Smyth, L. Tierney, J.Y. Yang and J. Zhang, Genome Biol 5 (2004) R80.

[15] Y.H. Yang, S. Dudoit, P. Luu, D.M. Lin, V. Peng, J. Ngai and T.P. Speed, Nucleic Acids Res 30 (2002) e15.

[16] X. Cui, M.K. Kerr and G.A. Churchill, Stat Appl Genet Mol Biol 2 (2003) Article4.

[17] A.L. Brown, C.R. Wilkinson, S.R. Waterman, C.H. Kok, D.G. Salerno, S.M. Diakiw, B. Reynolds, H.S. Scott, A. Tsykin, G.F. Glonek, G.J. Goodall, P.J. Solomon, T.J. Gonda and R.J. D'Andrea, J Leukoc Biol 80 (2006) 433-47.

[18] B. Tucker, R. Richards and M. Lardelli, Dev Genes Evol 214 (2004) 567-74.

[19] S.F. Altschul, T.L. Madden, A.A. Schaffer, J. Zhang, Z. Zhang, W. Miller and D.J. Lipman, Nucleic Acids Res 25 (1997) 3389-402.

[20] J.D. Thompson, D.G. Higgins and T.J. Gibson, Nucleic Acids Res 22 (1994) 4673-80.

[21] J. Felsenstein, Cladistics 5 (1989) 164-166.

[22] T. Jowett, Tissue in situ hybridization, John Wiley and Sons, New York, 1997.

[23] X. Zhu, H.G. Lee, G. Perry and M.A. Smith, Biochim Biophys Acta 1772 (2007) 494-502.

[24] X. Zhu, A.K. Raina, G. Perry and M.A. Smith, Lancet Neurol 3 (2004) 219-26.

[25] Z. Nagy, Biochim Biophys Acta 1772 (2007) 402-8.

[26] S.H. Kimura, M. Ikawa, A. Ito, M. Okabe and H. Nojima, Oncogene 20 (2001) 3290-300.

[27] J. Pines and T. Hunter, Cell 58 (1989) 833-46.

[28] M.C. Horne, G.L. Goolsby, K.L. Donaldson, D. Tran, M. Neubauer and A.F. Wahl, J Biol Chem 271 (1996) 6050-61.

[29] K. Tamura, Y. Kanaoka, S. Jinno, A. Nagata, Y. Ogiso, K. Shimizu, T. Hayakawa, H. Nojima and H. Okayama, Oncogene 8 (1993) 2113-8.

[30] A. Zauberman, A. Lupo and M. Oren, Oncogene 10 (1995) 2361-6.

[31] K. Okamoto and D. Beach, Embo J 13 (1994) 4816-22.

[32] S. Bates, S. Rowan and K.H. Vousden, Oncogene 13 (1996) 1103-9.

[33] K.L. Jordan-Sciutto, K. Morgan and R. Bowser, J Alzheimers Dis 1 (1999) 409-417.

[34] E.G. Rorman and G.A. Grabowski, Genomics 5 (1989) 486-92.

[35] X. Qi, K. Kondoh, D. Krusling, G.J. Kelso, T. Leonova and G.A. Grabowski, Biochemistry 38 (1999) 6284-91.

[36] J.S. O'Brien, G.S. Carson, H.C. Seo, M. Hiraiwa and Y. Kishimoto, Proc Natl Acad Sci U S A 91 (1994) 9593-6.

[37] Y. Kotani, S. Matsuda, T.C. Wen, M. Sakanaka, J. Tanaka, N. Maeda, K. Kondoh, S. Ueno and A. Sano, J Neurochem 66 (1996) 2197-200.

[38] K. Igase, J. Tanaka, Y. Kumon, B. Zhang, Y. Sadamoto, N. Maeda, S. Sakaki and M. Sakanaka, J Cereb Blood Flow Metab 19 (1999) 298-306.

[39] M. Hiraiwa, J. Liu, A.G. Lu, C.Y. Wang, R. Misasi, T. Yamauchi, I. Hozumi, T. Inuzuka and J.S. O'Brien, J Neurotrauma 20 (2003) 755-65.

[40] W. Schlote, K. Harzer, H. Christomanou, B.C. Paton, B. Kustermann-Kuhn, B. Schmid, J. Seeger, U. Beudt, I. Schuster and U. Langenbeck, Eur J Pediatr 150 (1991) 584-91.

[41] J. Matsuda, A. Yoneshige and K. Suzuki, J Neurochem 103 Suppl 1 (2007) 32-8.

[42] J. Matsuda, M.T. Vanier, Y. Saito, J. Tohyama and K. Suzuki, Hum Mol Genet 10 (2001) 1191-9.

[43] R. Spiegel, G. Bach, V. Sury, G. Mengistu, B. Meidan, S. Shalev, Y. Shneor, H. Mandel and M. Zeigler, Mol Genet Metab 84 (2005) 160-6.

[44] E. Kojro, G. Gimpl, S. Lammich, W. Marz and F. Fahrenholz, Proc Natl Acad Sci U S A 98 (2001) 5815-20.

[45] A. Tingaud-Sequeira and J. Cerda, Gene 386 (2007) 98-106.

[46] M. Murayama, S. Tanaka, J. Palacino, O. Murayama, T. Honda, X. Sun, K. Yasutake, N. Nihonmatsu, B. Wolozin and A. Takashima, FEBS Lett 433 (1998) 73-7.

[47] I. Raurell, J. Castano, C. Franci, A. Garcia de Herreros and M. Dunach, J Biol Chem 281 (2006) 1401-11.

[48] M.A. Pappolla, R.A. Omar, K.S. Kim and N.K. Robakis, Am J Pathol 140 (1992) 621-8.

[49] M.A. Smith, G. Perry, P.L. Richey, L.M. Sayre, V.E. Anderson, M.F. Beal and N. Kowall, Nature 382 (1996) 120-1.

[50] B. Thisse, Pfumio, S., Fürthauer, M., Loppin B., Heyer, V., Degrave, A., Woehl, R., Lux, A., Steffan, T., Charbonnier, X.Q. and Thisse, C., Vol. 2008, ZFIN on-line publication 2001.

[51] M. van Lookeren Campagne, K. Okamoto, C. Prives and R. Gill, Brain Res Mol Brain Res 64 (1999) 1-10.

CHAPTER IV

Research Paper IV

Changes in cyclin G1 and cyclin G2 activity that affect zebrafish embryo development.

Morgan Newman and Michael Lardelli

Discipline of Genetics, School of Molecular and Biomedical Science, The University of Adelaide, SA 5005, Australia

Manuscript

STATEMENT OF AUTHORSHIP

Changes in cyclin G1 and cyclin G2 activity that affect zebrafish embryo development.

Manuscript

Morgan Newman (Candidate)

Performed all experiments and wrote manuscript.

Certification that the statement of contribution is accurate

Signed

…….Date……

Michael Lardelli (co-author)

Planned the research and supervised development of work.

Certification that the statement of contribution is accurate

Signed

…….Date……

Title:

Changes in cyclin G1 and cyclin G2 activity that affect zebrafish embryo development.

Authors:

Morgan Newman and Michael Lardelli

Affiliations:

Discipline of Genetics, School of Molecular and Biomedical Science, The University of Adelaide, SA, 5005, Australia

Abstract

cyclin G1 (*ccng1*) was identified in a microarray analysis as upregulated after interference with splicing to exon 8 of the presenilin1 (*psen1*) or presenilin 2 (*psen2*) genes in zebrafish embryos. The function of human CCNG1 has not been investigated in great depth. However a role as been proposed in p53-dependent apoptosis and there is increasing evidence that CCNG1may be involved in Alzheimer's disease (AD) pathology as increased CCNG1 protein can be detected by immunohistochemistry in the cytoplasm of neurons in human AD brains. The function of *ccng1* and its paralogue *cyclin G2* (*ccng2*) in zebrafish is unknown. Here we use morpholino antisense oligonucotides to interfere with splicing of *ccng1* transcripts or to reduce translation of Ccng1 or Ccng2 proteins in zebrafish embryos. Interference with splicing causes truncation of the *ccng1* open reading frame at codon 88 and increases the concentration of normal *ccng1* transcript. Defects in brain, notochord and somite development are observed by 22 hours post fertilisation (hpf). Decreasing Ccng2

translation shows very similar phenotypic effects on zebrafish development while decreased Ccng1 translation has no obvious effect on zebrafish embryo development. This suggests that truncated forms of Ccng1 may interfere with Ccng2 function. Overexpression of Ccng1 by mRNA injection also produced similar phenotypes, suggesting that normal Ccng2 function may involve interaction with Ccng1.

Introduction

Cyclins are proteins that generally play important roles in the control of cell cycle progression, with most cyclin protein levels rising and falling corresponding to different stages of the cell cycle. In mammalian cells 12 cyclin subtypes have been identified, cyclins A though to K and cyclin T (Kimura et al., 2001). These proteins share a highly conserved motif named the 'cyclin box' (Pines and Hunter, 1989). The cyclins are classified into different groups through structural similarity, function during the cell cycle and expression regulation (Horne et al., 1996). Mammalian *cyclin G1* (*CCNG1)* was isolated as a novel member of the cyclin family though its homology with the *c*-src family (Tamura et al., 1993) and also through differential screening for transcriptional targets of p53 (Zauberman et al., 1995). CCNG1 protein has a cyclin domain but lacks the protein destabilising (PEST) domain that is present in other cyclin members. The function of CCNG1 protein has not been defined in detail, however it is currently proposed to play a role in p53-dependent apoptosis as it has p53 binding sites and is induced under conditions that activate p53 (Okamoto and Beach, 1994). Furthermore, CCNG1 is induced in a p53-dependent manner in response to DNA damage (Bates et al., 1996). *Ccng1* null mice are phenotypically normal. However, further analysis has revealed roles in G2/M arrest, damage recovery and growth promotion after cellular stress (Kimura et al., 2001). The *CCNG1*

paralogue, *CCNG2* has 60% nucleotide sequence identity and 53% amino acid residue identity with *CCNG1* (Horne et al., 1996). In mammals, *CCNG1* and *CCNG2* show contrasting levels of mRNA expression in different tissues. Whereas *CCNG1* mRNA levels do not appear to oscillate with the cell cycle, *CCNG2* does show this characteristic and is shown to be an ubiquitous cell cycle regulator (Horne et al., 1996). Similar to CCNG1, the function of CCNG2 has not been completely investigated. However, its expression does appear to inhibit G_1 to S phase transition. Both CCNG1 and CCNG2 directly interact with the catalytic subunit of protein phosphatase 2A (PP2A) (Bennin et al., 2002) and this complex may function to inhibit cell cycle progression. The mechanism by which CCNG2 expression is regulated during the cell cycle is unknown.

Ccng1 was identified from a microarray analysis to be upregulated as a result of interference with splicing to exon 8 of transcripts of either *psen1* or *2* in zebrafish embryos (Newman et al., 2008). The predicted orthology of this gene to human *CCNG1* was confirmed and whole mount in situ hybridisation showed visibly increased transcript concentration in embryos with altered exon 8 splicing for either *psen1* or *2*. The PSEN proteins are ubiquitously expressed transmembrane proteins that function within the γ-secretase complex. γ-secretase activity regulates the proteolysis of a number of type I membrane proteins, including Notch and the amyloid-β precursor protein (APP) (Capell et al., 2000). The aberrant cleavage of APP is proposed to play a major role in the pathogenesis of Alzheimer's disease (AD) and point mutations in the *PSEN1* gene have been linked to familial forms of AD and frontotemporal dementia (FTD) including Pick disease (reviewed by (Dermaut et al., 2005). Mutations affecting the splicing of *PSEN1* have also been demonstrated in the

familial forms of these diseases. There is also increasing evidence that CCNG1 may play a role in AD pathology. Increased levels of CCNG1 protein can be detected by immunohistochemistry in the cytoplasm of neurons in human AD brains (Jordan-Sciutto et al., 1999) and CCNG1 protein is also upregulated in the hippocampus of brains of patients with mild cognitive impairment (MCI) (Sultana and Butterfield, 2007). The hippocampus is severely affected during AD pathogenesis and MCI is regarded as an intermediate stage leading to the more severe cognitive decline evident in AD. Dysregulation of the cell cycle has been suggested as a mechanism by which neuronal death in AD may be initiated (Nagy, 2007).

The function of *ccng1* and *ccng2* in zebrafish is unknown. At 24 hpf *ccng1* expression is ubiquitous with specific expression in the lens, midbrain-hindbrain boundary and somites (Newman et al., 2008; Thisse, 2001), while, *ccng2* shows expression in the CNS, somites and in the pronephric duct (Thisse, 2001). In the work described in this paper we investigate the function of Ccng1 and Ccng2 in zebrafish embryo development. We use morpholino antisense oligonucotides (Mo) to decrease Ccng1 and Ccng2 translation. Two splice blocking morpholinos are used to cause deletion of the 3rd exon from *ccng1* transcripts to give divergence from the normal ORF . Decreased Ccng1 translation does not result in any gross morphological defects in the embryo which is consistent with the phenotype of mice lacking Ccng1 activity (Kimura et al., 2001). However, a minor level of loss of the normal *ccng1* ORF after codon 88 (through exon 3 deletion) does not decrease levels of normal *ccng1* transcript, but results in defects in the brain, notochord and somites of developing embryos by 22hpf. Interestingly, decreased Ccng2 translation causes similar developmental defects. This suggests that truncated forms of Ccng1 protein may disturb development by decreasing

ccng2 function in a dominant negative manner and increasing *ccng1* transcription (or stabilising these transcripts). Overexpression of Ccng1 by mRNA injection gives similar effects, suggesting that normal Ccng1 can influence Ccng2 function.

Materials and Methods

Microinjection of morpholino antisense oligonucleotides, GFP-DNA, RNA.

Morpholinos were obtained from Gene Tools (LLC, Corvallis, OR, USA).
The Ccng1 translation blocking morpholino, MoCcng1Tln, binds over the -1 nucleotide and the first codons of the *ccng1* ORF. The Ccng2 translation blocking morpholinos, MoCcng2Tln and MoCcng2Tln.2 bind to non-overlapping sites in the 5' untranslated region (5'UTR) of ccng2 mRNA. The first *ccng1* splice blocking morpholino, MoCcng1Do, was designed to bind over the splice site donor site of exon2 (the first translated exon) and a second splice blocking morpholino, MoCcng1Ac, was designed to bind over the splice acceptor site of exon 3 (the second translated exon). The effects of all morpholino injections were compared to those resulting from injection of the standard negative control morpholino MoCont. A second morpholino control was used which blocks the translation of p53. This serves to attenuate off-target affects of gene-specific morpholinos (Robu et al., 2007). Morpholino sequences are displayed in Table 2.

Full-length ORF (288 amino acids), truncated (first 88 amino acids) and control (stop codon engineered at codon 3 of full-length) (Figure 1) *ccng1* cDNA was cloned into the BamHI/EcoRI sites of the pcGlobin2 expression vector (Ro et al., 2004) (primers listed in Table 2). pcGlobin2 DNA was linearised prior to *in vitro* mRNA transcription using the mMessage mMachine T7 kit (Ambion Austin, Texas, USA).

mRNA was diluted to the desired concentration in 1XTE buffer prior to injection. Active morpholinos were mixed with MoCont so that embryos were always injected with morpholino solutions at a final concentration of 1mM. The maximum injection concentration of any active morpholino was 0.5mM (ie. A mixture of 0.5mM MoCont and 0.5mM active morpholino). Fertilised embryos were injected before first cleavage. Injected embryos were then maintained at 28.5°C under standard conditions (Westerfield, 1995) until the desired developmental stage.

As a control to show the ability of MoCcng1Tln to suppress *ccng1* mRNA translation, the first 295 bases of the *ccng1* coding sequence was fused in frame to EGFP at the EcoRI/AgeI sites of the N1-EGFP plasmid vector (BD Biosciences, NJ, USA) (Primers listed in Table 2),. This plasmid was linearised prior to co-injection with either 0.5 mM MoCcng1Tln mixed with MoCont or MoCont alone. Embryos were then observed for GFP fluorescence at ~10hpf using fluorescence microscopy.

RNA Extraction and Reverse Transcription for RT-PCR.

Total RNA was extracted from embryos at 24 hpf after injection at the 1 cell stage with either MoCcng1Ac or MoCont using the 'QIAGEN RNAeasy Mini Kit' (QIAGEN Hilden, Germany). RNA was precipitated with lithium chloride (Ambion) and treated with 1 unit of RQ1 DNase (Promega Corp. Madison, WI, USA) at 37ºC for 30 min. Concentration was determined and RNA quality was checked on a 1% agarose/Tris-borate-EDTA gel. For reverse transcription, a mixture of 1-5µg of total RNA, 1µl of random hexamer primers and 1µl of 10nM dNTPs was incubated at 65 °C for 5 min followed by -20 °C for 1 min. 4µl of a 5X reaction buffer containing 250 mM Tris–HCl pH 8.3, 375 mM KCl, 15 mM $MgCl_2$ was mixed with 1µl of 100 mM DTT, 1µl of

SuperScript III (200 units/µl) (Invitrogen Corp. Carlsbard, CA, USA) and 1µl of Rnase Inhibitor (20U/ µl) (Ambion) was added and incubated at 25 °C for 5 min, followed by 50°C for 60 min. The mixture was then heat inactivated at 70°C for 15 min. Gene specific primers for the amplification of cDNA synthesised from embryos injected with MoCont and *ccng1* splice blocking morpholinos were designed using Primer Express software (Applied Biosystems Foster City, CA, USA) and synthesised by or Proligo (Boulder, Colorado, USA). Sequences are listed in Table 2. *Ccng1F* and *ccng1(3rdexon)R* amplifies from the start site to codon 97 in exon 3. *ccng1F* and *ccng1(lastexon)R* amplifies from the start site to codon 272 in the last exon (listed in Table 2).

Sequencing of Splicing Isoforms.

Purified amplified cDNA products were cloned in the pGEMT easy vector system (Promega Corp., Madison, Wisconsin, USA) for cycle sequencing using M13 primers and Big Dye Terminator Mix (Applied Biosystems) according to the manufacturer's instructions. The products were analysed on an ABI DNA sequencer (Applied Biosystems).

Quantitative PCR.

The relative standard curve method for quantification was used to determine the expression of experimental samples compared to a basis sample. For experimental samples, target quantity was determined from the standard curve and then compared to the basis sample to determine fold changes in expression. Primers spaning the first exon-exon junction of the ORF of *ccng1* were designed using Primer Express software (*Qccng1F* and *Qccng1R*) (Applied Biosystems) and primers for the

ubiquitously expressed control gene *ef-1a (Qef-1aF* and *Qef-1aR*) have previously been described in (Tucker et al., 2004) (listed in Table 2). The starting cDNA quantity was from a pool of 30-60 embryos. The reaction mixture consisted of 50ng/µl of RNA used to generate cDNA. 18µM of forward and reverse primers and SYBR green master mix PCR solution (Applied Biosystems). For generation of the standard curve cDNA was serially diluted (50ng, 25ng, 12.5ng and 6.25ng). Amplification conditions were 2 min at 50°C followed by 10 min at 95°C and then 40-45 cycles of 15 s at 95°C and 1 min at 60°C. Amplification was performed on an ABI 7000 Sequence Detection System (Applied Biosystems) using 96 well plates. Cycle thresholds obtained from each triplicate were averaged and normalised against the expression of *ef-1a*. Each experimental sample was then compared to the control sample to determine fold changes of expression. Each QRT-PCR experiment was replicated four times. Thus, for each experiment four independent injections and subsequent cDNA preparations were performed with MoCont and MoCcng1Ac and then each cDNA preparation was subjected to three standand curve reactions each for both *ef-1a* and the *ccng1*.

Whole-Mount In Situ Hybridisation (WISH).

WISH against *Sonic hedgehog* (*shh*), has previously been described (Amack et al., 2007). A *ccng1* digoxigenin 11-uridine 5' triphosphate (DIG) labelled probe was previously generated by Newman *et al.* 2008. A DIG antisense labelled RNA probe for *shh* was generated using T7 RNA polymerase from DNA amplified using M13 primers. Embryos were fixed in 4% formalaldehyde in embryo medium before manual dechorionation. WISH was then performed as previously described (Jowett, 1997).

Acridine orange staining of apoptotic cells.

Embryos were manually dechorionated and placed in 5µg/ml acridine orange solution diluted in 1mL of E3 medium for 30 minutes in darkness. Embryos were then rinsed three times in E3 medium, and observed for GFP fluorescence using fluorescence microscopy.

Results

Altered *ccng1* and *ccng*2 expression in zebrafish embryos.

To determine the function of *ccng1* and *ccng*2 in zebrafish development, several non-overlapping morpholinos were designed to target each gene. For *ccng1* a translation blocking morpholino (MoCcng1Tln) and two splice blocking morpholinos were designed. One was designed to bind to the donor site of the first translated exon (exon 2) of *ccng1* (MoCcng1Do) and the other to bind to the acceptor site of the second translated exon (exon 3) of *ccng1* (MoCcng1Ac) (Figure 1A), both with the intention of causing deletion of the second translated exon to give a frameshifted mRNA encoding a severely truncated (and presumably functionless) peptide (Figure 1A,C). For *ccng2* two non-overlapping translation-blocking morpholinos were designed (MoCcng2Tln and MoCcng2Tln.2) (Figure 1B), to confirm that any phenotypic affects observed are specifically the result of inhibition of *ccng2* mRNA translation.

To support the ability of MoCcng1Tln to block translation of its target mRNA, the start of the *ccng1* ORF encompassing the target region was fused in frame to EGFP to form construct ccng1EGFP, (see Materials and Methods). Injection of ccng1EGFP at a concentration of 125ng/µl at the 1-cell stage resulted in mosaic GFP expression evident by observed fluorescence at 10hpf (90%, n=30). Co-injection of MoCont (1mM) with

ccng1EGFP DNA did not affect GFP expression (90%, n=20) (Figure 2A). Co-injection of MoCcng1Tln (0.5mM) with ccng1EGFP DNA inhibited GFP expression (100%, n=25) (Figure 2B) supporting the ability of this morpholino to block translation of *ccng1* mRNA.

The effect of MoCcng1Do and MoCcng1Ac on *ccng1* splicing (ie. its ability to exclude the second translated exon, exon 3, from transcripts) was analysed by RT-PCR. Primarily, a RT-PCR was undertaken to confirm deletion of exon 3. Primers were designed to amplify from the start of the ORF to codon 272 in the last exon (Figure 1A, Table 2) so that any size difference in *ccng1* mRNAs isolated from MoCcng1Ac-(0.3mM) injected embryos and MoCont-injected embryos at 24 hpf could be determined. Figure 2C shows the products of this RT-PCR, with the product from normal *ccng1* mRNA being 816bp and, upon MoCcng1Ac injection, there is a low level of deletion, indicated by a smaller PCR product of 561bp (see 'del' in Figure 2C). This deletion product was sequenced and, as expected, revealed an absence of exon3 sequence (255bp deletion) causing a frameshift and resulting in a novel lysine codon followed by a stop codon after normal codon 88. A second aberrant splicing product is evident from the RT-PCR analysis that appears to have a smaller deletion (see '2nddel' in Figure 2C). However, we could not resolve this sufficiently from the RT-PCR product of normal mRNA to permit cloning and analysis. For analysis of *ccng1* transcription in MoCcng1Do injected embryos, primers were used to amplify from the start of the ORF to codon 97 in exon 3 (Figure 1A, Table 2). Figure 2D shows the products of this RT-PCR, with the product from normal *ccng1* mRNA being 290bp and, upon MoCcng1Do injection, there is a low level of deletion indicated by a smaller PCR product of 191bp (see 'del' in Figure 2D). Sequencing of the deletion product indicated

a 99bp deletion from codon 56 in exon 2 to codon 88 at the end of exon 2. This deletion still maintains the reading frame into exon 3. There were also transcripts showing inclusion of additional sequence as indicated by the larger PCR product (see 'inc' in Figure 2 E). This inclusion product could not be resolved sufficiently from the RT-PCR product of normal mRNA to permit cloning and analysis. However, the size difference between the inclusion product and the normal product is approximately 100bp and so potentially corresponds to inclusion of the 97bp intron between exon 2 and 3. This would cause a frameshift leading to seven novel amino acid codons followed by a premature stop codon following the end of exon 2.

The effect of MoCcng1Ac injection on *ccng1* transcription was also analysed by QRT-PCR. Primers for QRT-PCR analysis were designed to detect only the normal product and not mRNA lacking exon 3 sequence as the downstream primer binds within exon 3. Four complete replicates were performed comparing levels of normal *ccng1* transcript from MoCcng1Ac-injected and MoCont-injected embryos at 24 hpf embryos using transcripts from the *ef1a* gene as a standard against which to normalise the results. Results from these replicates were very variable. One replicate showed increased normal *ccng1* transcript (0.62-fold, $p<0.003$), two displayed minor decreases (-0.23-fold, $p<0.02$ and -0.2-fold $p<0.02$) and one showed no significant change (not sig) in normal *ccng1* mRNA levels (Figure 2E). This is consistent with the RT-PCR analysis that showed only a low-level of transcripts lacking exon 3.

Developmental consequences of altered *ccng1* and *ccng*2 expression in zebrafish.

Reduced translation of Ccng1 and Ccng2 has different gross morphological effects on development. Injection of MoCcng1Tln to reduce Ccng1 translation causes no gross

morphological effects which is consistent with the phenotype of mice lacking *ccng1* (Kimura et al., 2001) (fig. 3A). In contrast, injection of MoCcng1Ac (which causes ORF truncation after codon 88) causes irregular development of the somites and notochord with evident necrosis throughout the embryo especially in the brain (Figure 3B). MoCcng1Do injected embryos (deletion of exon 2 coding sequence and potential insertion of intron 2-3 sequence) also displays this irregular development (data not shown). Interestingly, injection of MoCcng2Tln or MoCcng2Tln.2 causes similar developmental defects to MoCcng1Ac injection (Figure 3D,H). (Note that the similar phenotypes from injection of MoCcng2Tln or MoCcng2Tln.2 provide evidence for the specific action of these morpholinos on Ccng2 translation). Therefore, termination of the ORF of *ccng1* after codon 88, (presumably generating a truncated protein), appears to phenocopy the effects seen from reduced Ccng2 translation (Figure 3C). Figure 4B shows the U-shaped somites seen in embryos injected with MoCcng1Ac compared to the normal V-shaped somites of MoCont-injected embryos at 22 hpf (Figure 4A). As described above injection of MoCcng1Ac causes only a minor proportion of exon 3 deletion (Figure 2C). However, the presumably, low level of truncated protein formed appears to affect severely embryo development. Table 1 displays the results of embryo injections with the morpholinos described above.

To address the possibility that off-target effects of MoCcng1Ac and MoCcng2Tln injection may cause the observed phenotype, each of these morpholinos was co-injected with Mop53Tln (0.5mM), that attenuates such effects, by blocking p53 activity (Robu et al., 2007). The blockage of p53 translation together with injection of MoCcng1Ac and MoCcng2Tln did not affect the specific phenotypes of these morpholinos (Table 1). Therefore, this supports that the phenotypes observed are not artifactual.

Expression of truncated Ccng1 in zebrafish embryos.

To test the idea that the effect of MoCcng1Ac injection is due to generation of a Ccng1 peptide truncated after amino acid 88, mRNA was synthesised *in vitro* corresponding to the Ccng1 ORF truncated after exon 2 sequence (mRNAccng1Tr) (Figure 1C). This mRNA was injected into embryos at the 1-cell stage (injection concentration 150ng/µl) and caused similar effects on embryo development at 24hpf to those observed in MoCcng1Ac-injected embryos (Figure 3D) (Table 1). This supports that the phenotype of the MoCcng1Ac-injected embryos is indeed due to the production of truncated Ccng1 species. Two controls were also performed. In one, mRNA encoding the complete *ccng1* ORF (mRNAccng1Full) was synthesised *in vitro* and injected into embryos at the 1-cell stage (injection concentration 150-200ng/µl). This produced variable results. Half of the embryos (51% n=86) presented with a milder form of the phenotypes observed in embryos injected with mRNAccng1Tr, MoCcng1Ac and MoCcng2Tln (Figure 3E) and half showed no effect (Table 1). This may be due to the less consistent spread of mRNA in an embryo after injection compared to morpholinos and other factors affecting mRNA. The second control for the *ccng1* mRNA injections, was injection of mRNA engineered to posses a stop codon at the fourth codon of the *ccng1* ORF (mRNAccng1Cont). Injection of this mRNA at 150ng/µl had no affect on embryo development (Figure 3F) (Table 1).

Altered Ccng1 and Ccng2 expression leads to aberrant notochord development.

Loss of *sonic hedgehog* (*shh*) gene function typically produces U-shaped somites similar to those observed in our experiments above (Nasevicius and Ekker, 2000). Therefore, to examine the phenotypic effects of disturbed *ccng1* and *ccng2* expression in more detail, we performed WISH for *sonic hedgehog* (*shh*) expression on embryos

fixed at 24 hpf of development. At 24 hpf *shh* expression can clearly be seen in the notochord and floorplate. Observations of *shh* expression in MoCcng1Ac (76%, n=21) and MoCcng2Tln injected (54%, n=39) embryos by WISH revealed an irregular notochord development (DN) at the posterior end of the developing tail in comparison to MoCont injected embryos (Figure 4E,F). There also is a thickening of the notochord particular to MoCcng1Ac-injected embryos, with an increased region of *shh* expression in the chordo-neural hinge (CH) compared to MoCont injected embryos (52%, n=21) (Figure 4E). As WISH is not a quantitative technique for gene expression levels, *shh* expression remains to be quantified by QRT-PCR.

Altering Ccng1 and Ccng2 expression increases apoptosis .

As Ccng1 and Ccng2 proteins are proposed to have roles in cell cycle progression we investigated the effect of altered *ccng1* and *ccng2* expression on apoptosis in MoCcng1Tln, MoCcng1Ac, MoCcng2Tln and MoCont injected embryos. Whole mount staining of embryos with acridine orange solution, when viewed under UV illumination, marks apoptotic cells. Injection of all morpholinos gave increased apoptosis in the dorsal somites (D) compared to MoCont (n=10 for each group), with a more pronounced increase observed in the dorsal somites in MoCcng1Ac and MoCcng2Tln injected emrbyos (Figure 5A-D). MoCcng1Tln and MoCcng2Tln both display no or minimal apoptosis in the notochord (N) which is also observed in MoCont. As the notochord is not as evident in MoCcng1Ac- compared to MoCcng1Tln-, MoCcng2Tln- and MoCont-injected embryos (where it is visible by an absence of apoptosis), it is possible that apoptosis is raised in the notochord in these embryos.

Discussion

Interference with splicing to exon 8 of either *psen1* or *psen2* in zebrafish embryos has severe dominant negative effects on Psen1 activity (Nornes et al., 2007). *Ccng1* was identified in a microarray analysis as upregulated following such interference. (Newman et al., 2008). Presenilin is the major locus for mutations causing FAD. Human CCNG1 has been found to be upregulated in AD brains (Jordan-Sciutto et al., 1999; Sultana and Butterfield, 2007) and there is accumulating evidence suggesting that dysregulation of the cell cycle may be an initiating mechanism for AD pathogenesis. (Nagy, 2007). Apart from its proposed role in p53-dependent apoptosis the function of CCNG1 has not been the subject of intense investigation. Therefore, this study employed morpholino antisense technology to investigate the normal role of *ccng1* in developing zebrafish embryos.

Reduction of Ccng1 translation in zebrafish embryos resulted in no gross morphological defects in embryo development, consistent with loss of Ccng1 activity in mice. However, when attempting to reduce Ccng1 activity using a morpholino blocking splicing to the acceptor site of exon 3, severe effects on embryogenesis were observed. Subsequent cloning and sequencing of an aberrant splice product indicated truncation of the open reading frame after exon 2. This potentially produces an mRNA encoding a form of Ccng1 protein truncated after exon 2 sequence (i.e. after codon 88). Furthermore, upon investigating the effects of reduction of translation of the ccng1 paralogue *ccng2* it appears that partial Ccng1 truncation and reduction of Ccng2 translation produce similar phenotypes. The truncated Ccng1 species possibly have a dominant negative effect on normal Ccng2 function. Overexpression of full-length Ccng1 by mRNA injection also produces similar but milder phenotypes. Thus it is

possible that Ccng1 and Ccng2 may interact either directly or indirectly and that truncation of Ccng1 or overexpression of normal Ccng1 causes interference with Ccng2 function. An interaction between these two similar proteins has not previously been shown. In humans, both CCNG1 and CCNG2 proteins form a complex with PP2A to affect cell cycle progression and this may provide a link to explain how aberrant CCNG1 activity affects CCNG2 function.

The altered *shh* expression in MoCcng1Ac- and MoCcng2Tln-injected embryos indicates that disruption of Ccng1 or Ccng2 activity alters formation of the notochord. The notochord arises from the mesodermal germ layer and induces ectoderm to become neuroectoderm, the precursor of the nervous system. The notochord provides essential signalling for midline patterning (Cleaver and Krieg, 2001). In particular, hedgehog protein signalling in zebrafish embryos induces somitic mesoderm to form slow-twitch muscle (Barresi et al., 2000). The abnormal morphology of the notochord we observed would probably affect hedgehog signalling. This would have downstream effects on somite, myotome and neural development. Such defects are observed at 24 hpf in the MoCcng1Ac- and MoCcng2Tln-injected embryos (Figure 3D), where there is evident dysmorphogenesis of the brain and somites.

Splicing changes are frequently observed in aged cells (Meshorer and Soreq, 2002) and in cancer (Pajares et al., 2007). In Nornes *et al.,* 2008, we speculated that alterations in *psen1* gene splicing might play a role in sporadic forms of AD, as aberrant splicing between exons 6 and 8 of this gene dominantly reduce Psen1 activity. In the work described in this paper it appears that aberrant splicing of *ccng1* transcripts causing deletion of exon 3 of the ORF may affect the activity of the related gene *ccng2*.

Previous research as suggested that the normal function of CCNG2 is to inhibit cell cycle progression. Therefore, the possible dominant negative action of truncated Ccng1 on Ccng2 may allow cell cycle progression whereas under normal conditions it would be inhibited. The abolition of cell cycle check-points is a common feature of cancer.

Upon injection of MoCcng1Ac, it was expected that levels of normal *ccng1* transcript would be decreased. However, four completely independent replicates of a QRT-PCR experiment to measure relative levels of normal *ccng1* in MoCcng1Ac-injected and MoCont-injected embryos did not show any reproducible decrease in transcription. . This finding has potential implications for observations in AD cases where increases in *CCNG1* mRNA and CCNG1 protein levels in neurons have been observed. Perhaps the increased levels of CCNG1 are induced by aberrant splicing of *CCNG1, which* could be stimulated by oxidative stress or simply the failure of correct splicing in aging cells.

Further experiments to complete this manuscript for submission.

To validate the phenotypic effects of reducing Ccng2 translation, full-length *ccng2* mRNA must to be engineered and injected into embryos already injected with MoCcng2Tln to attempt to rescue the observed developmental defects. Note however, that if Ccng2 expression in zebrafish is cyclic (as in mammals) then injection of Ccng2 mRNA may not be able to correctly substitute for blocked endogenous *ccng2* mRNA. The ability of the MoCcng2Tln and MoCcng2Tln.2 morpholinos to block Ccng2 translation must also formally be demonstrated by their ability to suppress translation from mRNA consisting of a fusion of *ccng2* 5'UTR sequences and a GFP ORF. To support the idea that a truncated Ccng1 peptide generated by interference with *ccng1* splicing is affecting Ccng2 activity it will be necessary to show that the apparently

truncated Ccng1 and Ccng2 proteins interact. This could be achieved by tagging these proteins and a non-interacting protein (negative control) with separate tags such as GFP, FLAG and His. Messenger RNAs coding for each construct would be mixed with mRNAs coding for the other two constructs separately (i.e. truncated Ccng1 with Ccng2, truncated Ccng1 with non-interacting protein and Ccng2 with non interacting protein) and injected into embryos followed by subsequent analysis for protein interactions, for example, by co-immunoprecipitation and western blotting.

In the context of how CCNG1 and CCNG2 may play a role in AD pathogenesis it will be important to determine to what degree the developing brains of zebrafish embryos are affected by aberrant expression of Ccng1 and Ccng2. In zebrafish embryos at 24 hpf *ccng1* is expressed in the midbrain-hindbrain boundary and *ccng2* is expressed in the telencephalon and hindbrain. Therefore, the development of these structures may be affected by aberrant *ccng1* or *ccng2* expression. To observe such defective development, WISH for *fibroblast growth factor 8* (*fgf8*) and other markers of brain subregions will be useful. *Fgf8* is expressed in the forebrain, midbrain, somites and tail bud and so will also aid in closer examination of the defective somitogenesis we have observed. Examination of *dystrophin* (*DMD*) expression that marks somite boundaries as well as the hypochord, floorplate and chordo-neural hinge will also help in this regard. As CCNG1and CCNG2 are proposed to play a role in cell cycle progression, it will be important to determine if aberrant Ccng1 or Ccng2 expression affects mitotic activity. A whole mount antibody stain using the phospho-Histone H3 antibody can identify mitotic cells in embryos (Stern et al., 2005).

Acknowledgements

Would like to thank the authors of (Ro et al., 2004), for use of the pcGlobin2 plasmid.

Table 1. Results of morpholino and mRNA injections. Results of embryo injection with the phenotypic effects on development summarised as disrupted development

Treatment (conc. injected)	Intended Action	Phenotypic Effects at 24 hpf	% with disrupted development
MoCont (1mM)	Negative control	none	13% n=89
MoCcng1Tln (0.5mM)	Translation block	none	11% n=61
MoCcng1Ac (0.3-0.5mM)	Exon 3 acceptor block	disrupted development	100% n=70 +Mop53Tln 90% n=31
MoCcng1Do (0.5mM)	Exon 2 donor block	disrupted development	95% n=112
MoCcng2Tln (0.5mM)	Translation block	disrupted development	82% n=77 +Mop53Tln 100% n=31
MoCcng2Tlnno.2 (0.3-0.5mM)	Translation block	disrupted development	100% n=64
Mop53Tln (0.5mM)	Translation block	none	8% n=38
mRNAccng1Cont (150ng/µl)	Expression of first 3 codons	none	17% n=45
mRNAccng1Full (150-200ng/µl)	Expression of full length ORF	mild disrupted development	51% n=86
mRNAccng1Tr (150ng/µl)	Expression of first 88 codons	disrupted development	81% n=88

Table 2. Primer and Morpholino Sequences. *Ccng1EcoRIF* and *ccng1BamHIF* amplify from the start site. *Ccng1stopBamHIF* is used to mutate codon 4 (**T**) to a stop codon, together with *ccng1fullEcoRIR* amplifyies the entire *ccng1* ORF. *Ccng1truncEcoRIR* with *ccng1BamHIF* amplify the first 88 codons only, corresponding to the proposed truncation by MoCcng1Ac injection. *Ccng1exon3AgeIR* with *ccng1EcoRIF* amplifies the first 295 bases of the ORF for fusion to EGFP. Restriction sites are denoted by italics in the primer sequences.

Name	**Sequence (5'-3')**
ccng1F	ATGATTGACCAGGTGACCGA
ccng1(3rdexon)R	ACACAAGACAGATGCTTGGG
ccng1(lastexon)R	CATCCACCGCAGTCTCTGG
Qccng1F	TGGCTGTGTGAAGATTCAG
Qccng1R	CACTGGCCAGAGGACATT
Qef-1aF	CCAACTTCAACGCTCAGGTCA
Qef-1aR	CAAACTTGCAGGCGATGTGA
ccng1BamHIF	CG*GGATCC*ATGATTGACCAGGTGACC
ccng1stopBamHIF	CG*GGATCC*ATGATTGAC**T**AGGTGACC
ccng1EcoRIF	CG*GAATTC*ATGATTGACCAGGTGACC
ccng1fullEcoRIR	CG*GAATTC*ATAGTCTTAACAAGCATAT
ccng1truncEcoRIR	CG*GAATTC*TTACTTCATCACAGCCAGGAA
ccng1exon3AgeIR	*ACCGGT*ACCCACACAAGACAGATG
MoCcng1Tln	CGTTTCGGTCACCTGGTTCAATCATC
MoCcng1Ac	GGGCTGAATCTGAAGAAAGAACAAA
MoCcng1Do	ATATTGGAGCACACATACCTTCATC
MoCcng2Tln	GGCCTCCATTTTTACTGTTTGTTTG
MoCcng2Tln.2	TGTTTGTTTGTGTTTCAAGTCTTCA
MoCont	CCTCCTACCTCAGTTACAATTTATA
Mop53Tln	GCGCCATTGCTTTGCAAGAATTG

Figure 1. Schematic diagram of *ccng1* and *ccng2* transcripts showing mRNA structure and positions of morpholinos and PCR primers. For A-D the 5'UTR is in grey. **A.** *Ccng1* full-length ORF with binding positions indicated for translation (orange) and splice blocking morpholinos (MoCcng1Do -light blue, MoCcng1Ac- dark blue). PCR primers for RT-PCR, Q- PCR and for cDNA construction for mRNA synthesis are also indicated. **B.** *Ccng1* construct for *in vitro* synthesis of ccng1 mRNA truncated after codon 88 with primers used for its construction indicated. Dotted red line indicates deleted exon 3. **C.** *Ccng1* control constructs. Primers indicated in black were used to mutate codon 4 to a stop codon for *in vitro* synthesis of negative control mRNA. Primers indicated in green amplify the first 295 bases of coding sequence for fusion to EGFP in the N1-EGFP plasmid. **D.** *Ccng2* ORF with the position of translation blocking morpholinos (orange) indicated. Exons are not drawn to scale. Primer names are above their corresponding arrows.

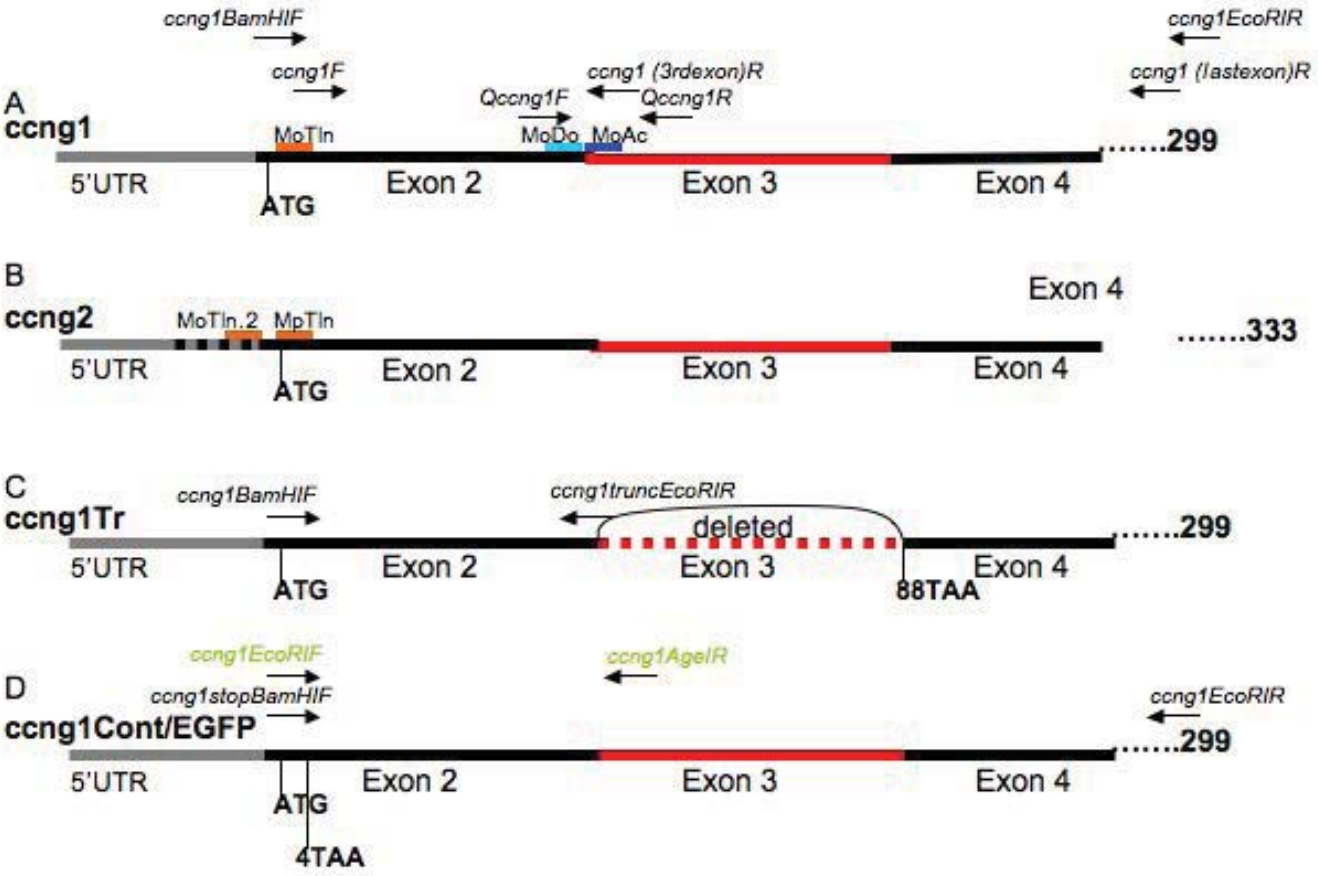

A
ccng1
ccng1BamHIF
ccng1F
Qccng1F
ccng1 (3rdexon)R
Qccng1R
ccng1EcoRIR
ccng1 (lastexon)R
MoTIn
MoDo
MoAc
.....299
5'UTR
ATG
Exon 2
Exon 3
Exon 4
B
ccng2
MoTIn.2
MpTIn
Exon 4
.....333
5'UTR
ATG
Exon 2
Exon 3
Exon 4
C
ccng1Tr
ccng1BamHIF
ccng1truncEcoRIR
deleted
.....299
5'UTR
ATG
Exon 2
Exon 3
88TAA
Exon 4
D
ccng1Cont/EGFP
ccng1EcoRIF
ccng1stopBamHIF
ccng1AgeIR
ccng1EcoRIR
.....299
5'UTR
ATG
4TAA
Exon 2
Exon 3
Exon 4

Figure 2. Confirmation of effectiveness of morpholino injection. Co-injection of DNA encoding the ccng1EGFP sequence, **A.** MoCont (**A[1].** EGFP expressing) or **B.** MoCcng1Tln (**B[1].** not EGFP expressing) into embryos at the 1-cell stage followed by observation under UV illumination at ~10 hpf. One representative embryo is shown. Size bars indicate 100µm. **C.** RT-PCR to amplify cDNA from *ccng1* mRNA from embryos injected with MoCcng1Ac or MoCont. Lane 1: 2-log DNA ladder. Lane 2: Moccng1Ac-injected embryos. Lane 3: MoCont-injected embryos. The normal PCR product is 0.816kb. Loss of exon3 sequence (del) gives a product of, 0.561kb. Another RT-PCR product of ~0.7 kb size (2^{nd} del) from MoCcng1Ac-injected embryos could not be resolved sufficiently for sequence analysis. **D.** RT-PCR to amplify cDNA from *ccng1* mRNA from embryos injected with MoCcng1Do or MoCont. Lane 1: 2-log DNA ladder. Lane 2: MoCont-injected embryos Lane 3: MoCcng1Ac-injected embryos, normal product is 0.29kb. Loss of exon3 sequence (del) gives a product of 0.191kb. Another RT-PCR product of ~0.38 kb size (inc) from MoCcng1Do-injected embryos could not be resolved sufficiently for sequence analysis **E.** Four independent replicates of a QRT-PCR analysis of cDNA from embryos injected with MoCcng1Ac with the reverse primer binding in the region of *ccng1* lost in MoCcng1Ac-injected embryos (i.e. exon 3). P-values were generated from a two-tailed t-test.

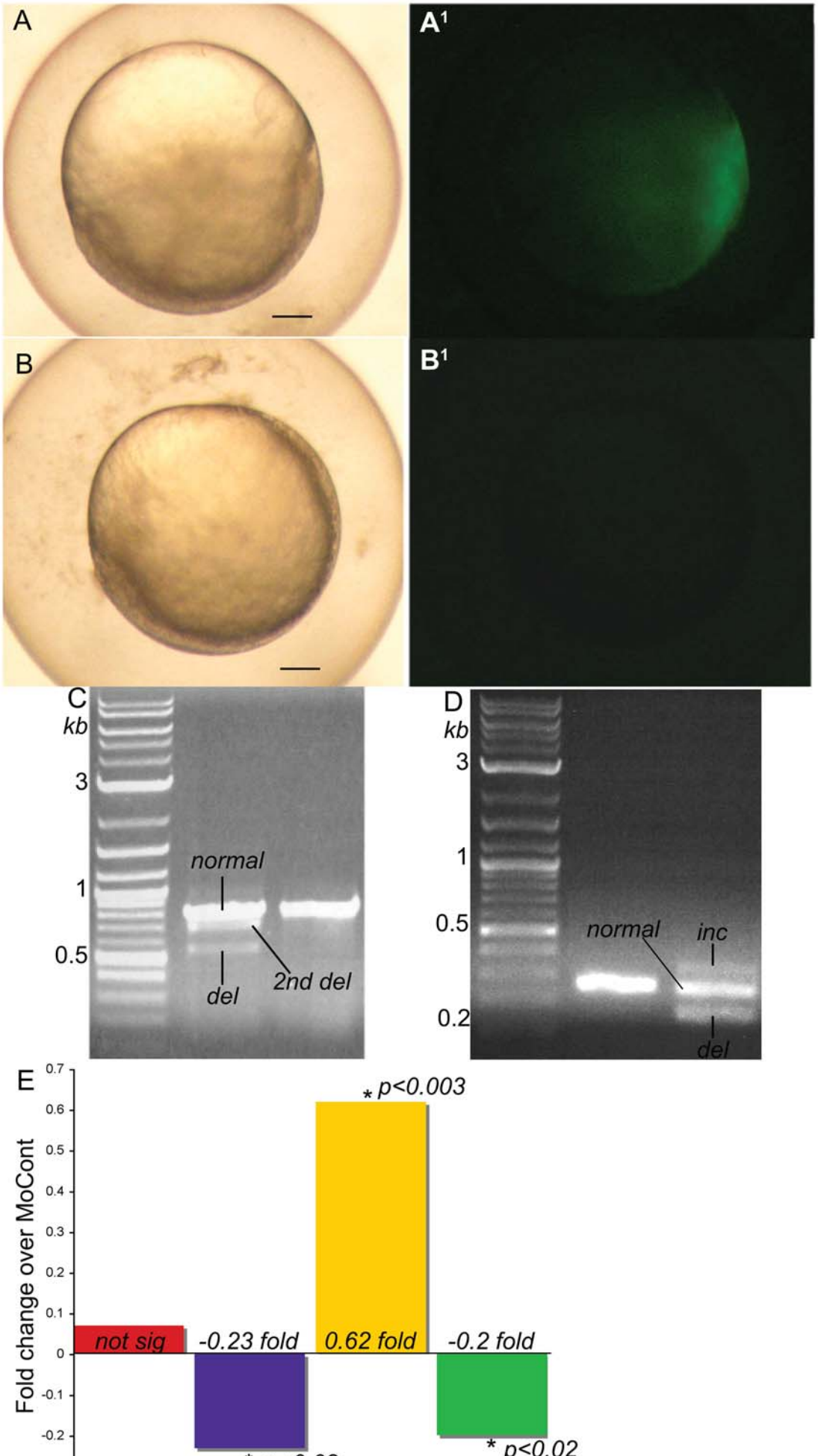

A
A1
B
B1
C
kb
3
1
0.5
normal
del
2nd del
D
kb
3
1
0.5
0.2
normal
inc
del
E
Fold change over MoCont
0.7
0.6
0.5
0.4
0.3
0.2
0.1
0
-0.1
-0.2
-0.3
not sig
-0.23 fold
0.62 fold
-0.2 fold
* p<0.003
* p<0.02
* p<0.02

Figure 3. Developmental phenotype of altered *ccng1* and *ccng*2 expression in zebrafish embryos after morpholino or mRNA injection at 24hpf. Injection of **A.** MoCont, **B.** MoCcng1Tln, **C.** MoCcng1Ac, **D.** MoCcng2Tln, **E.** mRNAccng1Cont, **F.** mRNAccng1Full, **G.** mRNAccng1Tr and **H.** MoCcng2Tln.2. Necrosis in the brain (**N)** and irregular somites (**S**) are indicated. Size bar indicates 100μm, applicable to A-H.

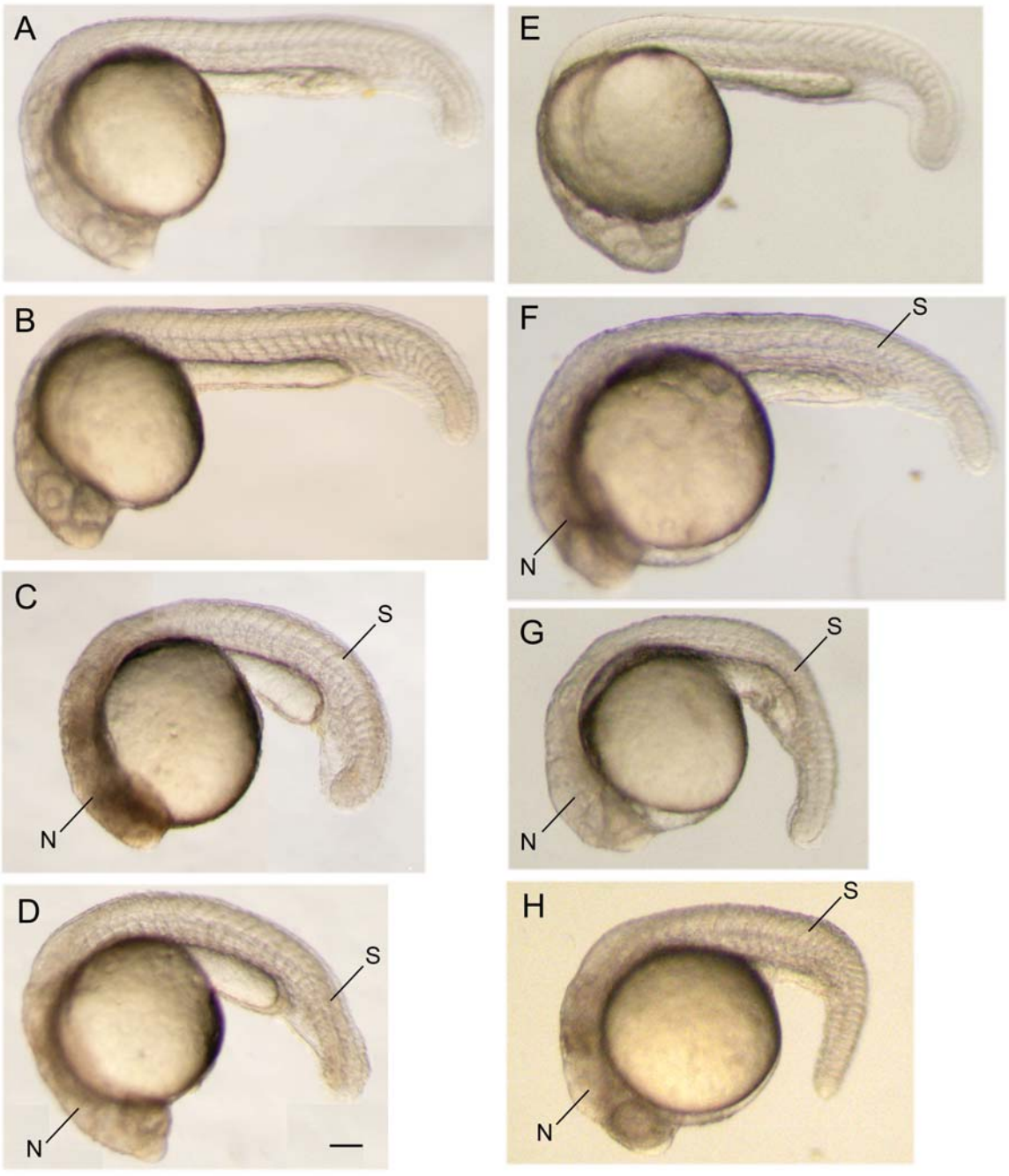

A
B
C
S
N
D
S
N
E
F
S
N
G
S
N
H
S
N

Figure 4. Developmental consequences of altered *ccng1* and *ccng*2 expression in zebrafish embryos at 24 hpf. Posterior somites of **A.** MoCont-, (v-shape somite indicated) and **B.** MoCcng1Ac-injected embryos (u-shaped somite indicated) at 22 hpf. Sizebars indicate 100µm. *Shh* expression in embryos injected with **C.** MoCont, **D.** MoCcng1Tln, **E.** MoCcng1Ac**, F.** MoCcng2Tln. Irregular notochord development (**DN**) is observed in **E** (76%, n=21) and **F** (54%, n=39). **E** has an increased area of expression of *shh* **in t**he chordo-neural hinge (**CH**) compared to **C** (52%, n=21). Size bars indicate 100µm.

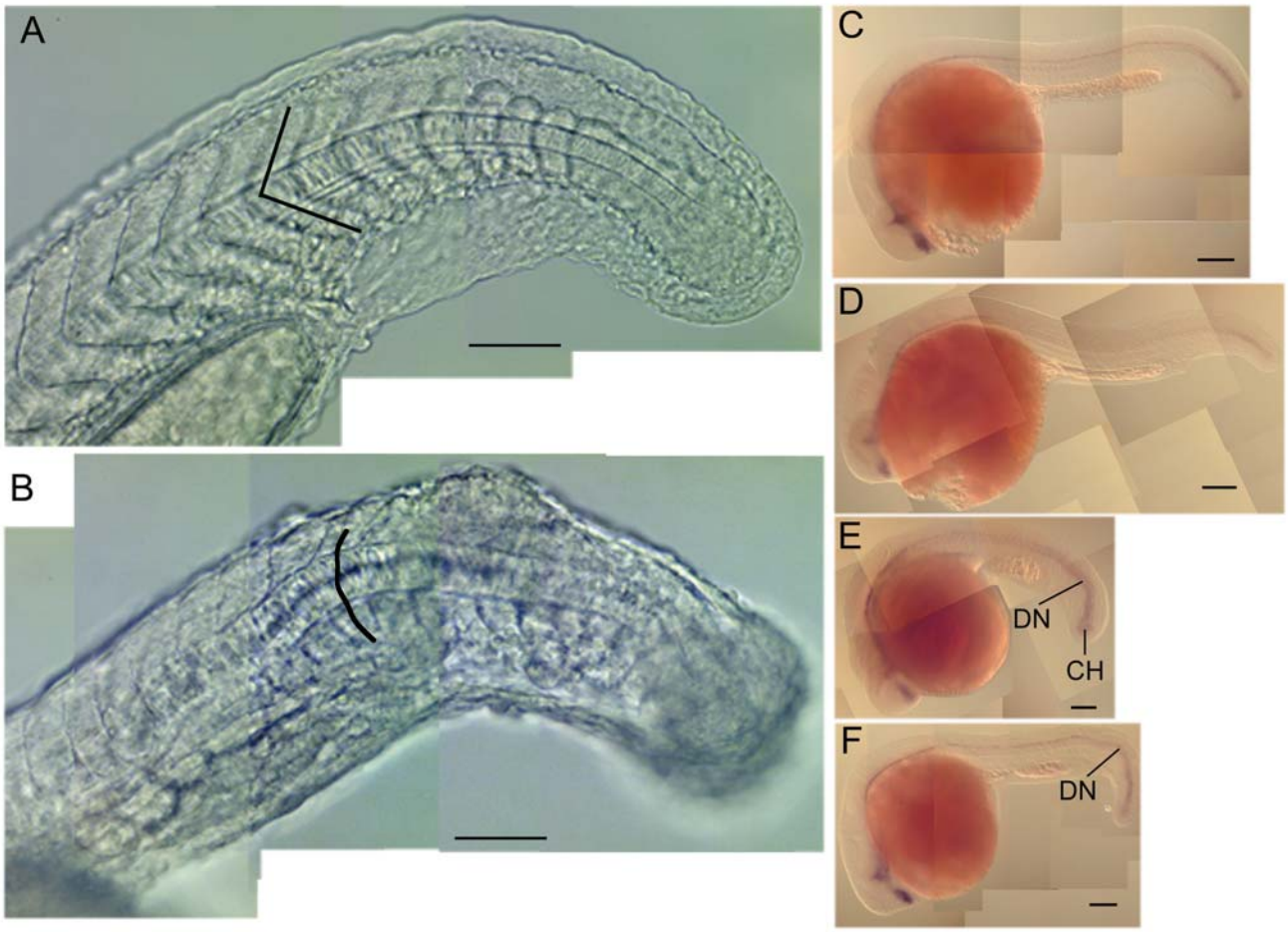
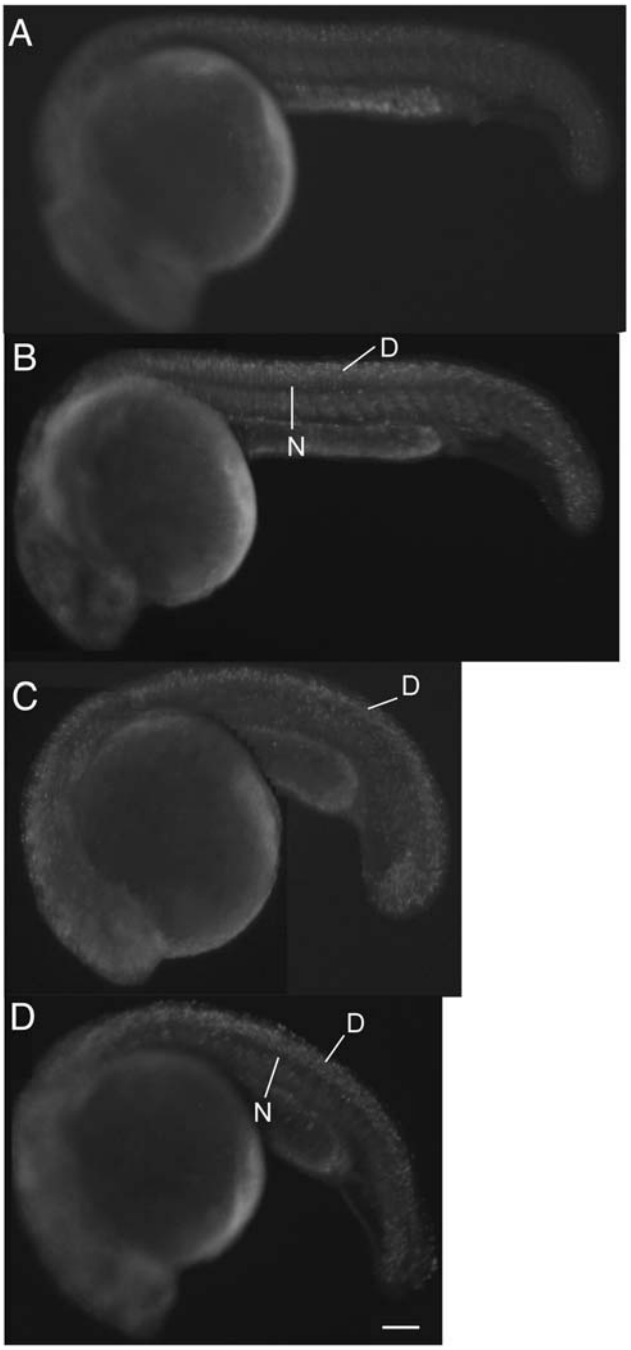

A
B
C
D
E
DN
CH
F
DN

Figure 5. Analysis of apoptosis in morpholino injected embryos. Embryos were injected with **A.** MoCont, **B.** MoCcng1Tln, **C.** MoCcng1Ac, **D.** MoCcng2Tln before staining with acridine orange at 24 hpf and observation under UV illumination to reveal apoptotic cells. Size bar indicates 100μm, applicable to A-D. The notochord (**N**) and dorsal somites (**D**) are indicated.


A
B
D
N
C
D
D
D
N

References

Amack, J.D., Wang, X., and Yost, H.J. (2007). Two T-box genes play independent and cooperative roles to regulate morphogenesis of ciliated Kupffer's vesicle in zebrafish. Dev Biol *310*, 196-210.

Barresi, M.J., Stickney, H.L., and Devoto, S.H. (2000). The zebrafish slow-muscle-omitted gene product is required for Hedgehog signal transduction and the development of slow muscle identity. Development *127*, 2189-2199.

Bates, S., Rowan, S., and Vousden, K.H. (1996). Characterisation of human cyclin G1 and G2: DNA damage inducible genes. Oncogene *13*, 1103-1109.

Bennin, D.A., Don, A.S., Brake, T., McKenzie, J.L., Rosenbaum, H., Ortiz, L., DePaoli-Roach, A.A., and Horne, M.C. (2002). Cyclin G2 associates with protein phosphatase 2A catalytic and regulatory B' subunits in active complexes and induces nuclear aberrations and a G1/S phase cell cycle arrest. J Biol Chem *277*, 27449-27467.

Capell, A., Steiner, H., Romig, H., Keck, S., Baader, M., Grim, M.G., Baumeister, R., and Haass, C. (2000). Presenilin-1 differentially facilitates endoproteolysis of the beta-amyloid precursor protein and Notch. Nat Cell Biol *2*, 205-211.

Cleaver, O., and Krieg, P.A. (2001). Notochord patterning of the endoderm. Dev Biol *234*, 1-12.

Dermaut, B., Kumar-Singh, S., Rademakers, R., Theuns, J., Cruts, M., and Van Broeckhoven, C. (2005). Tau is central in the genetic Alzheimer-frontotemporal dementia spectrum. Trends Genet *21*, 664-672.

Horne, M.C., Goolsby, G.L., Donaldson, K.L., Tran, D., Neubauer, M., and Wahl, A.F. (1996). Cyclin G1 and cyclin G2 comprise a new family of cyclins with

contrasting tissue-specific and cell cycle-regulated expression. J Biol Chem *271*, 6050-6061.

Jordan-Sciutto, K.L., Morgan, K., and Bowser, R. (1999). Increased Cyclin G1 Immunoreactivity During Alzheimer's Disease. J Alzheimers Dis *1*, 409-417.

Jowett, T. (1997). Tissue in situ hybridization (New York, John Wiley and Sons).

Kimura, S.H., Ikawa, M., Ito, A., Okabe, M., and Nojima, H. (2001). Cyclin G1 is involved in G2/M arrest in response to DNA damage and in growth control after damage recovery. Oncogene *20*, 3290-3300.

Meshorer, E., and Soreq, H. (2002). Pre-mRNA splicing modulations in senescence. Aging Cell *1*, 10-16.

Nagy, Z. (2007). The dysregulation of the cell cycle and the diagnosis of Alzheimer's disease. Biochim Biophys Acta *1772*, 402-408.

Nasevicius, A., and Ekker, S.C. (2000). Effective targeted gene 'knockdown' in zebrafish. Nat Genet *26*, 216-220.

Newman, M., Tucker, B., Nornes, S., Ward, A., and Lardelli, M. (2008). Altering presenilin gene activity in zebrafish embryos causes changes in expression of genes with potential involvement in Alzheimer’s Disease pathogenesis. The Journal of Alzheimer's Disease *Accepted Manuscript*.

Nornes, S., Newman, M., Verdile, G., Wells, S., Stoick-Cooper, C., Tucker, B., Frederich-Sleptsova, I., Martins, R., and Lardelli, M. (2007). Interference with splicing of Presenilin transcripts has potent dominant negative effects on Presenilin activity. Hum Mol Genet.

Okamoto, K., and Beach, D. (1994). Cyclin G is a transcriptional target of the p53 tumor suppressor protein. Embo J *13*, 4816-4822.

Pajares, M.J., Ezponda, T., Catena, R., Calvo, A., Pio, R., and Montuenga, L.M. (2007). Alternative splicing: an emerging topic in molecular and clinical oncology. Lancet Oncol *8*, 349-357.

Pines, J., and Hunter, T. (1989). Isolation of a human cyclin cDNA: evidence for cyclin mRNA and protein regulation in the cell cycle and for interaction with p34cdc2. Cell *58*, 833-846.

Ro, H., Soun, K., Kim, E.J., and Rhee, M. (2004). Novel vector systems optimized for injecting in vitro-synthesized mRNA into zebrafish embryos. Molecules and cells *17*, 373-376.

Robu, M.E., Larson, J.D., Nasevicius, A., Beiraghi, S., Brenner, C., Farber, S.A., and Ekker, S.C. (2007). p53 activation by knockdown technologies. PLoS Genet *3*, e78.

Stern, H.M., Murphey, R.D., Shepard, J.L., Amatruda, J.F., Straub, C.T., Pfaff, K.L., Weber, G., Tallarico, J.A., King, R.W., and Zon, L.I. (2005). Small molecules that delay S phase suppress a zebrafish bmyb mutant. Nat Chem Biol *1*, 366-370.

Sultana, R., and Butterfield, D.A. (2007). Regional expression of key cell cycle proteins in brain from subjects with amnestic mild cognitive impairment. Neurochem Res *32*, 655-662.

Tamura, K., Kanaoka, Y., Jinno, S., Nagata, A., Ogiso, Y., Shimizu, K., Hayakawa, T., Nojima, H., and Okayama, H. (1993). Cyclin G: a new mammalian cyclin with homology to fission yeast Cig1. Oncogene *8*, 2113-2118.

Thisse, B., Pfumio, S., Fürthauer, M., Loppin B., Heyer, V., Degrave, A., Woehl, R., Lux, A., Steffan, T., Charbonnier, X.Q. and Thisse, C. (2001). Expression of the zebrafish genome during embryogenesis. (ZFIN on-line publication).

Tucker, B., Richards, R., and Lardelli, M. (2004). Expression of three zebrafish orthologs of human FMR1-related genes and their phylogenetic relationships. Dev Genes Evol *214*, 567-574.

Westerfield, M. (1995). The Zebrafish Book: A guide to the laboratory use of Zebrafish (Danio rerio) (University of Oregon Press, Eugene).

Zauberman, A., Lupo, A., and Oren, M. (1995). Identification of p53 target genes through immune selection of genomic DNA: the cyclin G gene contains two distinct p53 binding sites. Oncogene *10*, 2361-2366.

Significance of The PhD Research Project and Future Directions

AD has a complex aetiology. The genetic mechanisms underpinning FAD have been characterised in greater depth than those behind the common, sporadic, form of AD. Therefore, one current goal of AD researchers is to find molecular commonalities between these two separate forms of the disease, to provide clues to early detection of the late onset sporadic form of AD. This thesis has investigated genes with potential relevance to AD by altering their expression and function in the zebrafish development model. Aberrant splicing of these genes (*psen1* and *ccng1*) has affects on gene function and regulation. As splicing changes with increased age in cells, aberrant splicing of particular genes may play a role in sporadic forms of AD and perhaps in other neurodegenerative diseases.

Future directions for further investigation of Ccng1 function were outlined in paper 4. An interesting result that requires further investigation from paper 2 was the effect of *psen1* exon 6 splice donor site blockage. This causes complex effects on transcription, and, unexpectedly, does not appear to increase *neurogenin1* expression. (increased *neurogenin1* transcription implies decreased γ-secretase activity), despite a marked reduction in Psen1 protein. The exon 6 donor block corresponds to a FTD mutation that effects the exon 6 donor site of *PSEN1* in humans (Dermaut et al., 2004). Investigating if similar changes in splicing of human *PSEN1* causes similar changes in γ-secretase activity, would provide strong evidence for aberrant splicing of *PSEN1* contributing to neurodegenerative dementias.

References

Ahn, K.W., Joo, Y., Choi, Y., Kim, M., Lee, S.H., Cha, S.H., Suh, Y.H., and Kim, H.S. (2008). Swedish amyloid precursor protein mutation increases cell cycle-related proteins in vitro and in vivo. J Neurosci Res.

Bates, S., Rowan, S., and Vousden, K.H. (1996). Characterisation of human cyclin G1 and G2: DNA damage inducible genes. Oncogene *13*, 1103-1109.

Baumann, K., Mandelkow, E.M., Biernat, J., Piwnica-Worms, H., and Mandelkow, E. (1993). Abnormal Alzheimer-like phosphorylation of tau-protein by cyclin-dependent kinases cdk2 and cdk5. FEBS Lett *336*, 417-424.

Bennin, D.A., Don, A.S., Brake, T., McKenzie, J.L., Rosenbaum, H., Ortiz, L., DePaoli-Roach, A.A., and Horne, M.C. (2002). Cyclin G2 associates with protein phosphatase 2A catalytic and regulatory B' subunits in active complexes and induces nuclear aberrations and a G1/S phase cell cycle arrest. J Biol Chem *277*, 27449-27467.

Bentahir, M., Nyabi, O., Verhamme, J., Tolia, A., Horre, K., Wiltfang, J., Esselmann, H., and De Strooper, B. (2006). Presenilin clinical mutations can affect gamma-secretase activity by different mechanisms. J Neurochem *96*, 732-742.

Busser, J., Geldmacher, D.S., and Herrup, K. (1998). Ectopic cell cycle proteins predict the sites of neuronal cell death in Alzheimer's disease brain. J Neurosci *18*, 2801-2807.

Dermaut, B., Kumar-Singh, S., Engelborghs, S., Theuns, J., Rademakers, R., Saerens, J., Pickut, B.A., Peeters, K., van den Broeck, M., Vennekens, K.*, et al.* (2004). A novel presenilin 1 mutation associated with Pick's disease but not beta-amyloid plaques. Ann Neurol *55*, 617-626.

Horne, M.C., Goolsby, G.L., Donaldson, K.L., Tran, D., Neubauer, M., and Wahl, A.F. (1996). Cyclin G1 and cyclin G2 comprise a new family of cyclins with contrasting tissue-specific and cell cycle-regulated expression. J Biol Chem *271*, 6050-6061.

Jordan-Sciutto, K.L., Morgan, K., and Bowser, R. (1999). Increased Cyclin G1 Immunoreactivity During Alzheimer's Disease. J Alzheimers Dis *1*, 409-417.

Kimura, S.H., Ikawa, M., Ito, A., Okabe, M., and Nojima, H. (2001). Cyclin G1 is involved in G2/M arrest in response to DNA damage and in growth control after damage recovery. Oncogene *20*, 3290-3300.

Kumar-Singh, S., Theuns, J., Van Broeck, B., Pirici, D., Vennekens, K., Corsmit, E., Cruts, M., Dermaut, B., Wang, R., and Van Broeckhoven, C. (2006). Mean age-of-onset of familial alzheimer disease caused by presenilin mutations correlates with both increased Abeta42 and decreased Abeta40. Hum Mutat *27*, 686-695.

Nagy, Z., Esiri, M.M., Cato, A.M., and Smith, A.D. (1997a). Cell cycle markers in the hippocampus in Alzheimer's disease. Acta Neuropathol *94*, 6-15.

Nagy, Z., Esiri, M.M., and Smith, A.D. (1997b). Expression of cell division markers in the hippocampus in Alzheimer's disease and other neurodegenerative conditions. Acta Neuropathol *93*, 294-300.

Nagy, Z., Esiri, M.M., and Smith, A.D. (1998). The cell division cycle and the pathophysiology of Alzheimer's disease. Neuroscience *87*, 731-739.

Okamoto, K., and Beach, D. (1994). Cyclin G is a transcriptional target of the p53 tumor suppressor protein. Embo J *13*, 4816-4822.

Pines, J., and Hunter, T. (1989). Isolation of a human cyclin cDNA: evidence for cyclin mRNA and protein regulation in the cell cycle and for interaction with p34cdc2. Cell *58*, 833-846.

Saura, C.A., Choi, S.Y., Beglopoulos, V., Malkani, S., Zhang, D., Shankaranarayana Rao, B.S., Chattarji, S., Kelleher, R.J., 3rd, Kandel, E.R., Duff, K.*, et al.* (2004). Loss of presenilin function causes impairments of memory and synaptic plasticity followed by age-dependent neurodegeneration. Neuron *42*, 23-36.

Shen, J., and Kelleher, R.J., 3rd (2007). The presenilin hypothesis of Alzheimer's disease: evidence for a loss-of-function pathogenic mechanism. Proc Natl Acad Sci U S A *104*, 403-409.

Song, W., Nadeau, P., Yuan, M., Yang, X., Shen, J., and Yankner, B.A. (1999). Proteolytic release and nuclear translocation of Notch-1 are induced by presenilin-1 and impaired by pathogenic presenilin-1 mutations. Proc Natl Acad Sci U S A *96*, 6959-6963.

Sultana, R., and Butterfield, D.A. (2007). Regional expression of key cell cycle proteins in brain from subjects with amnestic mild cognitive impairment. Neurochem Res *32*, 655-662.

Tamagno, E., Guglielmotto, M., Aragno, M., Borghi, R., Autelli, R., Giliberto, L., Muraca, G., Danni, O., Zhu, X., Smith, M.A.*, et al.* (2008). Oxidative stress activates a positive feedback between the gamma- and beta-secretase cleavages of the beta-amyloid precursor protein. J Neurochem *104*, 683-695.

Tamura, K., Kanaoka, Y., Jinno, S., Nagata, A., Ogiso, Y., Shimizu, K., Hayakawa, T., Nojima, H., and Okayama, H. (1993). Cyclin G: a new mammalian cyclin with homology to fission yeast Cig1. Oncogene *8*, 2113-2118.

Tu, H., Nelson, O., Bezprozvanny, A., Wang, Z., Lee, S.F., Hao, Y.H., Serneels, L., De Strooper, B., Yu, G., and Bezprozvanny, I. (2006). Presenilins form ER Ca2+ leak channels, a function disrupted by familial Alzheimer's disease-linked mutations. Cell *126*, 981-993.

Vincent, I., Jicha, G., Rosado, M., and Dickson, D.W. (1997). Aberrant expression of mitotic cdc2/cyclin B1 kinase in degenerating neurons of Alzheimer's disease brain. J Neurosci *17*, 3588-3598.

Walker, E.S., Martinez, M., Brunkan, A.L., and Goate, A. (2005). Presenilin 2 familial Alzheimer's disease mutations result in partial loss of function and dramatic changes in Abeta 42/40 ratios. J Neurochem *92*, 294-301.

Zauberman, A., Lupo, A., and Oren, M. (1995). Identification of p53 target genes through immune selection of genomic DNA: the cyclin G gene contains two distinct p53 binding sites. Oncogene *10*, 2361-2366.

Zhu, X., Lee, H.G., Perry, G., and Smith, M.A. (2007). Alzheimer disease, the two-hit hypothesis: an update. Biochim Biophys Acta *1772*, 494-502.

Amendments to thesis after examination.

- Page 10, line 5, delete the word “in” after “double knockouts”.

- Page 11, last line and page 12, first line, “*et al.”* should not be italicised to remain consistent with other “et al.” citations.

- Page 14, paragraph 1.6, line 2, delete the word “splicing” after “aberrant splicing of exon 8”.

- Page 15, first sentence of main paragraph, delete “are observed” at end of sentence.

- 2 references are missing volume and page numbers
    - in the last manuscript, vol 17 no.3 402-12 should be added to the Nornes et al., 2007 reference.
    - on page 28, vol 86, no.11 2476-87 should be added to the Ahn et al., 2008 reference.

- The supplementary information for Paper 2 “Interference with splicing of Presenilin transcripts has potent dominant negative effects on Presenilin activity” is included.

Supplementary Data 1: Details of coding sequence changes following morpholino injection (Data showing novel stop codons from areas sequenced from fragments cloned after RT-PCR on embryos injected with morpholinos). Areas sequenced correspond to those shown in Figure 1B. Intron-derived sequence is shown in bold text. In-frame stop codons are indicated in red.

Sequence from area "1a" – From cDNA amplified with Primers *2F* and *2R* following injection of Mo6Do

Exon 5
CTC ATG CTC AAC GCC ATC ATC ATG ATC AGT TGG TGA TCG TGG

TCA TGA CCC TGG GTG CTG GTG GTG CTC TAC AAG TAC AGA TGC
Intron 5
TAC AAG **GTT TGC TCC ACA TGA TGC TGA ATA CTC ATC AGC TAT**

TCT TTT ANA GGN NTT CAN GAA TTA CGA TTT GTT TTT NTT TTN GGN
Exon 6
AGG

Sequence from area "1b" – From cDNA amplified with Primers *3F* and *3R* following injection of Mo6Do

Exon 6
GTG ATT CAA GCC TGG CTG TTC TTC TCC AAC CTC CTC CTG CTC
Intron 6 (88bp)
TTC TTT TTC TCC TTA ATT TAT TTG GG**G TGA GTT TCG CTT GTT AGA**

TTA GTG TTT GTG CTG CGT TTG GAG TGT AAA CAC AAC CTC AAA
Exon 7
TCA CCT TAA GTC TGC CAC ACA CAC AGG GGA AGT GTT CAA GAC G

TA TAA CGT GGC GAT GGA TTA CTT CAC GCT GGC GTT GAT CAT CTG

GAA CTT CGG TGT GGT GGG AAT GAT CTG CAT CCA CTG GAA GGG

GCC GCT GCG GCT CCA GCA GGC CTA TCT GAT CAT GAT CAG CGC

TCT CAT GGC TCT GGT CTT CAT CAA GTA TCT CCC CGA GTG GAC

CGC ATG GCT CAT CCT CGC TGC TAT TTC AGT CTA CG

Sequence from area "2". From cDNA amplified with Primers *1F* and *1R* following injection of Mo8Ac

Exon 7
G GAA GTG TTC AAG ACG TAT AAC GTG GCG ATG GAT TAC TTC ACG

CTG GCG TTG ATC ATC TGG AAC TTC GGT GTG GTG GGA ATG ATC

TGC ATC CAC TGG AAG GGG CCG CTG CGG CTC CAG CAG GCC TAT

CTG ATC ATG ATC AGC GCT CTC ATG GCT CTG GTC TTC ATC AAA

TAT CTC CCC GAG TGG ACC GCA TGG CTC ATC CTC GCT GCT ATT TC
Intron 7
A GTC TAC G**GT CAG TCA GTC TGC AAA CAG AGC AAC AAA TTC AC**

C TCT GTT TAC TGT TTA TTG TTC TGT AAA TCT GCT TTG GAA CAA

TAA TTA GCC TGA AAA GAA TTG AAT AAT TTC AAA AAC ACA GCC
Exon 8
CCT TAA ATG TCT TTC CTG CTC CTG TGT AGA TCT TCT GGC AGT

GTT GTG TCC GAA AGG CCC TCT GCG AAT CCT TGT GGA AAC AGC

TCA AGA GAG GAA TGA GGC CAA GGC CCT CTG CGA ATC CTT GTG

GAA ACA GCT CAA GAG AGG AAT GAG GCC ATT TTC CCA GCG CTC

ATC TAC TCC T

Sequence from area “3”. From cDNA amplified with Primers *1F* and *1R* following injection of Mo9Ac

Exon8
AT CTT CTG GCA GTG TTG TGT CCG AAA GGC CCT CTG CGA ATC CAT

GTG GAA ACG GCT CAA GAG AGG AAT GAG GCC ATT TTC CCA GCG
Intron 8
CTC ATC TAC TCC T**GT AAG AAA AAC CCC TCA GCA CTT CCA TCT**

TCT CAG ACT GTG AAT GTC CAT CTG TTT AGT TGT GTT ATC GTC
Exon9
ACG TTT CTA TGA AAT TTC TCC TTC GATTTG TCA GCT ACG ATG GTG

TGG CTC TTC AAT ATG GCG GAC AGT GCT GAA ACC AGG AAT AAT

TCC AGT CAT CCA GTC CCT CAG CAG GAG AAC CAG G

Sequence amplified by RT-PCR primers *1F* and *4R* following injection of Mo7Ac

Exon 6
CC TGG CTG TTC TTC TCC AAC CTC CTC CTG CTC TTC TTT TTC TCC
Intron 6
TTA ATT TAT TTG GG**G TGA GTT TCG CTT GTT AGA TTA GTG TTT GTG**

CTG CGT TTG GAG TGT AAA CAC AAC CTC AAA TCA TTT TAA GTC TGC

CAC ACA CAG GTG AGT GGG TTT GAC AAG CCA CCT GTA GAA ACA TT

TTC ACT CTG TAA AAC GTC TTC TCT GAC CAC AAA CAG TTC CTC TGT

GTA ATT AGC AGT TGT GTG TAT TGC ATC TTC TTG TTG AAT CGC CGA

AAT CCT CTT TAA TAT TAT TGG ACA AAA GTG TCT GAT CAT GCT AAA

TGT AAA TAA TAG TGA ATA AAA TAA AAG TCA AAA GAT AGT GAC CAT

TGT TAC AGA TGT TGA CAG ATT GTC GTA CAG ATG ATC T (plus an additional 446 bp within intron 6)

Supplementary Data 2: Details of results from QRT-PCR on DAPT-treated zebrafish embryos and HEK-293 cells.

***psen1* expression for DAPT-treated zebrafish embryos**

Repeat 1

	psen1/*ef-1α*	Standard Deviation	DAPT/DMSO ratio	p-value
Untreated	1.01	0.16		
DMSO	1.30	0.14		
DAPT	0.56	0.15	0.43	<0.004

Repeat 2

	psen1/*ef-1α*	Standard Deviation	DAPT/DMSO ratio	p-value
Untreated	7.03	1.02		
DMSO	4.87	0.49		
DAPT	6.02	0.84	1.24	<0.4

Repeat 3

	psen1/*ef-1α*	Standard Deviation	DAPT/DMSO ratio	p-value
Untreated	2.57	0.35		
DMSO	1.91	0.04		
DAPT	2.36	0.08	1.24	<0.04

***PSEN1* expression for DAPT-treated HEK-293 cells**

Repeat 1

	PSEN1/*ACTB*	Standard Deviation	DAPT/DMSO ratio	p-value
p-value				
Untreated	1.52	0.15		
DMSO	2.08	0.15		
DAPT 0.5mM	1.38	0.28	0.66	<0.05
DAPT 5mM	1.21	0.38	0.58	<0.01

Repeat 2

	PSEN1/*ACTB*	Standard Deviation	DAPT/DMSO ratio	p-value
Untreated	3.17	0.28		
DMSO	5.63	0.27		
DAPT 0.5mM	4.70	0.59	0.83	<0.3
DAPT 5mM	10.76	0.62	1.91	<0.1

Repeat 3

	PSEN1/*ACTB*	Standard Deviation	DAPT/DMSO ratio	p-value
Untreated	2.12	0.28		
DMSO	3.12	0.13		
DAPT 0.5mM	3.62	0.71	1.16	<0.4
DAPT 5mM	1.37	0.57	0.44	<0.03

Supplementary Data 3: Initial titration data for all morpholino antisense oligonucleotides used

Morpholinos acting on *psen1* mixed with MoCont to a total concentration of 1 mM	embryos with hydrocephalus	embryos without hydrocephalus	% of embryos with hydrocephalus
MoTln 0.5mM	48	2	96
MoTln 0.2mM	39	15	72.2
MoTln 0.1mM	3	65	4.4
MoTln 0.05mM	0	75	0
MoTln 0.001mM	0	99	0
Mo7Ac 0.5mM	70	2	97.2
Mo7Ac 0.2mM	86	3	96.6
Mo7Ac 0.1mM	55	26	67.9
Mo7Ac 0.05mM	4	103	3.7
Mo7Ac 0.001mM	0	71	0
Mo8Ac 0.5mM	75	7	91.5
Mo8Ac 0.2mM	41	11	78.8
Mo8Ac 0.1mM	2	34	5.5
Mo6Do 0.5mM	25	12	67.6
Mo6Do 0.2mM	20	28	41.7
Mo6Do 0.1mM	1	34	2.9

Notes:
Mo9Ac did not produce hydrocephalus at 0.5mM.
MoPS2Tln was only tested at 0.5mM for its effect on Psen2 NTF production as seen by western blotting.

Supplementary Data 4: Data for *neurog1* expression comparisons and mRNA injection experiments in Table 1

neurog1 expression as revealed by whole mount *in situ* transcript hybridisation on morpholino- and/or mRNA-injected embryos.

***neurog1* expression comparison experiments**

Experimental *psen1* morpholinos injected at 0.5mM (together with 0.5mM control morpholino MoCont to give a total morpholino concentration of 1mM). When injected alone, MoCont is injected at 1mM. Embryos were classed as having higher *neurog1* expression ("darker") or equivalent/less expression ("same/lighter")

	darker	same/lighter	Chi Sq.
MoTln	25	8	10.39
MoCont only	4	11	**p< 0.001**

	darker	same/lighter	Chi Sq.
Mo7Ac	34	7	29.1
MoCont only	0	13	**p<< 0.001**

	darker	same/lighter	Chi Sq.
Mo8Ac	33	11	33
MoCont only	0	22	**p<< 0.001**

	darker	same/lighter	Chi Sq.
Mo9Ac	0	33	0
MoCont only	0	16	**not significant**

	darker	same/lighter	Chi Sq.
Mo6Do	0	31	0
MoCont only	0	20	**not significant**

An mRNA encoding a truncated Psen1 protein possessing amino acid residues coded by ORF sequence only up to the end of exon 6 "mRNAΔexon7+" causes stronger expression of *neurog1* than in embryos injected with a functionless RNA "mRNAcont" at the same concentration (200ng/μL);

	darker	same/lighter	Chi Sq.
mRNAΔexon7+	69	152	20.88
mRNAcont	24	169	**p<<0.001**

"Rescue" experiments

MoTln or Mo8Ac injected at 0.5mM (together with 0.5mM control morpholino MoCont to give a total morpholino concentration of 1mM). Embryos were classed as having higher or equivalent *neurog1* expression ("darker/same") or less expression ("lighter"). mRNA was injected at 200ng/μL. Rescue was attempted by a subsequent injection (still during the 1-cell stage) of *psen1* full-length mRNA "mRNAfulllength" at 200ng/μL

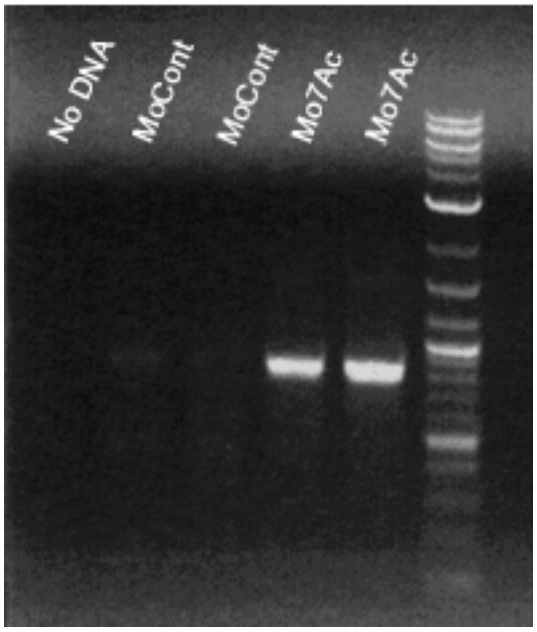
psen1 mRNA injection can rescue MoTln;

	darker/same	lighter	Chi Square
MoTln + mRNAfulllength	20	53	14.9
MoTln	28	16	**p< 0.001**

psen1 mRNA injection cannot rescue Mo8Ac;

	darker/same	lighter	Chi Square
Mo8Ac + mRNAfulllength	20	2	0.28
Mo8Ac	18	3	**not significant**

Supplementary Data 5: Gel electrophoresis image below shows products from RT-PCR using primers *1F* and *4R* on cDNA from whole cell RNA from embryos injected with either MoCont alone (at 1mM) or a 1:1 mixture of MoCont and Mo7Ac (at a final total morpholino injection concentration of 1mM). Each injection and PCR experiment was replicated twice. DNA size marker is 2-Log Ladder (New England BioLabs, Ipswich, Massachusetts). RT-PCR product size is 800bp as predicted. "No DNA" indicates a PCR with no DNA substrate added.



Supplementary Data 6: Severity of yolk extension and hydrocephalus phenotypes in embryos injected with MoTln, Mo7Ac and Mo8Ac

Phenotype severity classifications:

Yolk extension phenotype

normal - 1/4 reduced: yolk extension similar to that in normal embryos
1/4 - 1/2 reduced: yolk extension reduced 1/4 - 1/2 of that seen in normal embryos
1/2 - 3/4 reduced: yolk extension reduced 1/2 - 3/4 of that seen in normal embryos
3/4 – absent : yolk extension reduced 3/4 the thickness of that seen in normal embryos to totally absent

Hydrocephalus phenotype

normal: no expanded brain ventricles
mild: mildly expanded brain ventricles
moderate: moderately expanded brain ventricles
severe: severely expanded brain ventricles

Head-trunk angle - the intersection of the eye-to-otic vesicle axis with the trunk axis expressed as for an analogue clock-face
(Head axis: line through the middle of the ear and eye. Trunk axis: line along the notochord. The trunk axis points toward 6 o'clock. The head axis changes with developmental time and is affected by hydrocephalus – i.e. see Figure 2A.)

At 48hpf the head axis in the control embryos points toward 10.15.
At 48hpf the head axis in the experimental embryos points closest towards 9.30, 10.00 or 10.15.

Yolk extension

Numbers denote embryos at 30 hpf in each class

	normal - 1/4 reduced	1/4 - 1/2 reduced	1/2 -3/4 reduced	3/4 reduced - absent
MoTln	4	28	44	8
Mo7Ac	0	8	53	18

Contingency Chi-Square test. $\chi^2 = 17.55$. Therefore phenotype from injection of Mo7Ac is significantly (**p<0.001**) more severe than from injection of MoTln

	normal - 1/4 reduced	1/4 - 1/2 reduced	1/2 -3/4 reduced	3/4 reduced - absent
MoTln	4	28	44	8
Mo8Ac	0	3	57	11

Contingency Chi-Square test. $\chi^2 = 23.56$. Therefore phenotype from injection of Mo8Ac is significantly (**p<0.001**) more severe than from injection of MoTln

Hydrocephalus

Numbers denote embryos at 48 hpf in each class

	normal	mild	moderate	severe
MoTln	4	28	32	20
Mo7Ac	12	11	25	21

Contingency Chi-Square test $\chi^2 = 10.92$. Therefore no significant difference from MoTln.

	normal	mild	moderate	severe
MoTln	4	28	32	20
Mo8Ac	10	23	15	23

Contingency Chi-Square test. $\chi^2 = 9.44$. Therefore no significant difference from MoTln.

Head-trunk angle

Numbers denote embryos at 48 hpf in each class. Angles are given as analogue clock-face "times". See above for explanation.

	Closest to 10 15	Closest to 10 00	Closest to 9 30

MoTln	47	14	23
Mo7Ac	30	24	15

Contingency Chi-Square test. $\chi^2 = 6.67$. Therefore no significant difference of Mo7Ac from MoTln.

	Closest to 10.15	Closest to 10 00	Closest to 9 30
MoTln	47	14	23
Mo8Ac	51	13	7

Contingency Chi-Squared test. $\chi^2 = 7.69$. Therefore no significant difference of Mo8Ac from MoTln.

Supplementary Data 7: Data used to draw Figure 4

DoLA cell numbers at 30 hpf as revealed by *tbx16 in situ* transcript hybridisation. All Morpholinos were injected at 0.5mM (plus 0.5 mM MoCont)

MoCont	MoTln (Psen1)	MoPS2Tln	ex7 Mo	ex8 Mo
Number of embryos examined				
60	64	63	60	52
Means				
24.18333	23.46875	29.33333333	25.95	26.86538
Standard Deviation				
3.212748	2.713685	3.121207376	3.614589	4.392636
Value of p from two-tailed t-test				
	0.184936	3.80923E-15	0.005489	0.000451

Supplementary Data 8: Western blot (below) shows reduction of Psen2 NTF in zebrafish at 24 hpf after injection at the 1-cell stage with MoPS2TIn that inhibits *psen2* mRNA translation. The blot was stripped and reprobed for β-tubulin as a loading control. Morpholinos were injected at a concentration of 1 mM. For MoPS2TIn injection this was 0.5 mM MoPS2TIn with 0.5 mM MoCont.

